

12-2011

## REGULATION OF HGF EXPRESSION BY $\Delta$ EGFR-MEDIATED C-MET ACTIVATION IN GLIOBLASTOMA CELLS

Jeannine Garnett

Follow this and additional works at: [https://digitalcommons.library.tmc.edu/utgsbs\\_dissertations](https://digitalcommons.library.tmc.edu/utgsbs_dissertations)



Part of the [Cancer Biology Commons](#)

### Recommended Citation

Garnett, Jeannine, "REGULATION OF HGF EXPRESSION BY  $\Delta$ EGFR-MEDIATED C-MET ACTIVATION IN GLIOBLASTOMA CELLS" (2011). *The University of Texas MD Anderson Cancer Center UTHealth Graduate School of Biomedical Sciences Dissertations and Theses (Open Access)*. 192.  
[https://digitalcommons.library.tmc.edu/utgsbs\\_dissertations/192](https://digitalcommons.library.tmc.edu/utgsbs_dissertations/192)

This Dissertation (PhD) is brought to you for free and open access by the The University of Texas MD Anderson Cancer Center UTHealth Graduate School of Biomedical Sciences at DigitalCommons@TMC. It has been accepted for inclusion in The University of Texas MD Anderson Cancer Center UTHealth Graduate School of Biomedical Sciences Dissertations and Theses (Open Access) by an authorized administrator of DigitalCommons@TMC. For more information, please contact [digitalcommons@library.tmc.edu](mailto:digitalcommons@library.tmc.edu).

**REGULATION OF HGF EXPRESSION BY  $\Delta$ EGFR-MEDIATED  
C-MET ACTIVATION IN GLIOBLASTOMA CELLS**

By

Jeannine Garnett

APPROVED:

---

Oliver Bögler, Ph.D., Supervisory Professor

---

Michelle C. Barton, Ph.D.

---

Howard Colman, M.D., Ph.D.

---

Lisa A. Elferink, Ph.D.

---

Zhimin Lu, M.D., Ph.D.

---

Dihua Yu, M.D., Ph.D.

APPROVED:

---

Dean, The University of Texas

Health Science Center at Houston

Graduate School of Biomedical Sciences

**REGULATION OF HGF EXPRESSION BY  $\Delta$ EGFR-MEDIATED  
C-MET ACTIVATION IN GLIOBLASTOMA CELLS**

A

DISSERTATION

Presented to the Faculty of  
The University of Texas  
Health Science Center at Houston  
and  
The University of Texas  
M.D. Anderson Cancer Center  
Graduate School of Biomedical Sciences  
in Partial Fulfillment of the Requirements  
for the Degree of

DOCTOR OF PHILOSOPHY

By

Jeannine Garnett

Houston, Texas

December, 2011

## **DEDICATION**

This research dissertation is dedicated to my daughter, Jessica Monique Garnett. Jessica has taught me more about life, love, happiness, courage, strength, and perseverance, than anyone else ever could. I want to thank her for giving up so much of her childhood for this doctoral degree. Even though she doesn't realize it yet, she has been my greatest motivation and inspiration to complete graduate school.

Jessica, my precious daughter, I love you with all my heart.

## **ACKNOWLEDGEMENTS**

Firstly, I would like to thank my mentor, Dr. Oliver Bögler, for his continuous support, training, and guidance throughout my time in his laboratory. I am extremely proud and honored to have been mentored by him. Not only did he encourage me to sharpen my critical thinking abilities, and to improve on my writing skills, but he was also an exceptional example of the type of mentor / boss that I will aspire to become in the future. At times the long road to graduate school completion seemed unconquerable with many obstacles in my path, but through his temperate encouragement, advice, and understanding, I find that I'm on the brink of entering an exciting new world filled with so many opportunities that are there for the taking. I sincerely thank him for believing in me, and for leading me to this junction in my career; it will simply never be forgotten, and will always be sincerely appreciated.

I am also sincerely appreciative of my supervisory committee members' time, guidance, and for shaping me into a better scientist: Dr. Michelle Barton, Dr. Howard Colman, Dr. Lisa Elferink, Dr. Zhimin Lu, and Dr. Dihua Yu. Their positive influences and pivotal roles in my graduate school career have meant a great deal to me. These members have taken a great deal of time from their busy schedules to offer insightful and helpful advice on my scientific achievements, for which I am extremely grateful. I thank members of my advisory and examination committees for their time and guidance; Dr. Hope Northrup, Dr. Andreas Bergman, Dr. Pierre McCrea and Dr. Janet Price.

Deserving of a big thank you are all members of Dr. Oliver Bögl's laboratory, and of Dr. Ganesh Rao's laboratory, for all their scientific advice, help with methodology, assistance with tasks, and selfless cooperation. Specifically, I would like to thank Dr. Anupama Gururaj for being my technical supervisor; her time, training, assistance, and scientific advice has been invaluable. I would also like to thank Dr. Vaibhav Chumbalkar for performing all mass spectrometry experiments related to this research, and for his assistance with analyzing this large dataset; it was a pleasure to work with him. I would also like to thank Dr. Khatri Latha and Dr. Takashi Shingu for all their kind assistance and support of my thesis project. I am grateful to Laura Gibson for her continuous assistance and support, and for DNA fingerprinting the cell lines that I used in this research.

I have been very fortunate to have collaborated with exceptional scientists during my graduate school career. Specifically, I would like to thank our collaborators, Dr. Lisa Elferink, and her former graduate student, Dr. Kristen Hill, for their time and support of this research. Kristen analyzed conditioned media samples for their HGF content by ELISA for us during times when she had so many of her own deadlines and pressures to meet. I would like to thank Dr. Brian Vaillant, Dr. Howard Colman's former post-doctoral fellow, for performing the bioinformatic analysis of TCGA expression data for us. I really appreciated his meticulous and diligent pursuit of answering our translational questions. It was a pleasure collaborating with him. I would also like to thank Dr. Jun Yao, another collaborator, for his assistance with TCGA analysis. I thank Dr. Waldemar Priebe for collaborating with us and providing us with his STAT3 phosphorylation inhibitor compound, WP1193.

I am grateful that Dr. Wai-Kwan Alfred Yung was my mentor in years 2006 through 2008, and for supporting my studies for two and a half years. I learned a great deal from him over the years.

I thank all members of the Brain Tumor Center at MD Anderson Cancer Center for their assistance over the years. Particularly, I would like to thank the dedicated support staff of the Brain Tumor Center, because none of our research would have been possible without you. I thank Verlène Henry and Lindsay Holmes for performing all animal experiments.

I would like to thank the GSBS Cancer Biology Program, and especially Dr. Yu for all her efforts in making it one of the best training programs nationwide; I'm proud to be a member.

I would also like to thank Dr. Robert Arceci for providing me with the constitutively active STAT3 construct that was used to conduct a portion of this research, Dr. Anwar Hossain for providing me with a scrambled pLK0.1 shRNA virus, Dr. Zhimin Lu for providing me with MDCK cells, and Dr. Howard Colman for his gift of Human Embryonic Kidney 293FT cells. I would also like to thank Dr. Ta-Jen Liu for his kind gift of pCMV-dR8.2 dvpr and pCMV-VSVG constructs, Dr. Suyun Huang for her kind gift of a pcDNA3.1/Hygro(+) empty vector, and Dr. H-J Huang for kindly providing our lab with the pLRNL- $\Delta$ EGFR construct. I thank Dr. Mikio Tomida, Dr. Ramin Massoumi, and Dr. Rajeswara for the human HGF pGL2-HGF-1029 promoter construct. I would also like to thank Dr. Sonali Panchabhai for teaching me how to use the Gelcount colony counter.

I would like to thank my friends and family for giving me the encouragement and support that was needed in order for me to succeed. None of this would have

been possible without your love. Friends that I would like to make special mention of are Troy Hill and Karen and David Buchanan. They have always been there for me, not only during the fun times but also during the challenging times; I really value our friendship.

I would like to thank my mother, Heila Reyneke, deeply for everything that she's done for me. Through her love all of this has been possible. I would like to thank my daughter (Jessica Garnett), my mother (Heila Reyneke), my father (Johan Zwart), and my grandparents (John and Joey Zwart), for teaching me to follow my dreams and for helping me realize that just about anything in life can be achieved with due effort.



# **REGULATION OF HGF EXPRESSION BY $\Delta$ EGFR-MEDIATED C-MET ACTIVATION IN GLIOBLASTOMA CELLS**

Publication No. \_\_\_\_\_

Jeannine Garnett

Supervisory Professor: Oliver Bögl, Ph.D.

## **Abstract**

Overexpression of the hepatocyte growth factor receptor (c-Met) and its ligand, the hepatocyte growth factor (HGF), and a constitutively active mutant of the epidermal growth factor receptor ( $\Delta$ EGFR/EGFRvIII), occur frequently in glioblastoma. c-Met is activated in a ligand-dependent manner by HGF or in a ligand-independent manner by  $\Delta$ EGFR. Dysregulated c-Met signaling contributes to the aggressive phenotype of glioblastoma, yet the mechanisms underlying the production of HGF in glioblastoma are poorly understood. We found a positive correlation between HGF and c-Met expression in glioblastoma, suggesting that they are coregulated. This is supported by the finding that in a c-Met/HGF axis-dependent glioblastoma cell line, shRNA-mediated silencing of c-Met, or treatment with the c-Met inhibitor SU11274, attenuated HGF expression. Biologically, c-Met knockdown decreased anchorage-independent colony formation and the tumorigenicity of intracranial xenografts. Building on prior findings that  $\Delta$ EGFR

enhanced c-Met activation, we found that  $\Delta$ EGFR also led to increased HGF expression, which was reversed upon  $\Delta$ EGFR inhibition with AG1478.  $\Delta$ EGFR required c-Met to maintain elevated HGF expression, colony formation of glioblastoma cells, and the tumorigenicity of orthotopic xenografts. An unbiased mass spectrometry-based approach identified phosphotyrosine-related signaling changes that occurred with c-Met knockdown in a glioblastoma cell line expressing  $\Delta$ EGFR and in parental cells. Notably, phosphorylation of STAT3, a master regulator of the mesenchymal GBM subtype and a known target of  $\Delta$ EGFR, also decreased when c-Met was silenced in these cells, suggesting that the signals from these receptors converge on STAT3. Using a STAT3 inhibitor, WP1193, we showed that STAT3 inhibition decreased HGF mRNA expression in  $\Delta$ EGFR-expressing glioblastoma cells. Consistent with these findings, constitutively active STAT3 partially restored HGF expression and anchorage-independent growth of c-Met knockdown glioblastoma cells that overexpressed  $\Delta$ EGFR. We found that higher levels of HGF and c-Met expression associated with the mesenchymal GBM subtype. Taken together, these results suggest that the activity of c-Met regulates the expression of HGF in glioblastoma cells, that  $\Delta$ EGFR feeds positively into this autocrine loop, that signaling of the two receptors together modulate HGF expression via STAT3, and that the HGF/c-Met axis may therefore be a good additional target for therapy of mesenchymal GBM tumors.

## TABLE OF CONTENTS

<b>APPROVAL SHEET</b> .....	i
<b>TITLE PAGE</b> .....	ii
<b>DEDICATION</b> .....	iii
<b>ACKNOWLEDGEMENTS</b> .....	iv
<b>ABSTRACT</b> .....	viii
<b>TABLE OF CONTENTS</b> .....	x
<b>LIST OF FIGURES</b> .....	xiv
<b>LIST OF TABLES</b> .....	xx
<b>LIST OF ABBREVIATIONS</b> .....	xxi
<b><u>CHAPTER 1: INTRODUCTION</u></b> .....	1
Glioma .....	2
Glioblastoma .....	3
GBM Treatment .....	4
Genetic Aberrations of Primary and Secondary GBM .....	6
GBM Subtypes .....	8
Dysregulated Receptor Tyrosine Kinases in GBM .....	10
EGFR .....	11
EGFR Alterations in GBM .....	12
$\Delta$ EGFR .....	13
$\Delta$ EGFR in GBM .....	15

Targeting EGFR / $\Delta$ EGFR in GBM.....	15
c-Met.....	16
Amplification of the c-Met Signal.....	19
The c-Met / HGF Axis in GBM.....	20
Cross-talk between the EGFR / $\Delta$ EGFR and c-Met Pathways.....	22
Regulation of c-Met and HGF Expression.....	24
 <b><u>CHAPTER 2: MATERIALS AND METHODS</u></b> .....	 27
Cell Culture.....	28
Antibodies.....	29
Reagents.....	29
shRNA Infection of GBM Cells.....	30
Generation of Kinase-deficient c-Met Plasmids.....	31
Transfection and Retroviral Infection.....	32
Cell Lysate Preparation and Western Blotting.....	33
Immunoprecipitation Assays.....	34
RNA Extraction and Quantitative Real-time PCR.....	34
ELISA.....	35
Luciferase Assays.....	37
Anchorage-independent Growth Assays.....	38
WST-1 Assays.....	38
Intracranial Xenograft Studies.....	39
Mass Spectrometry.....	39
Peptide Identification and Quantification.....	41

TCGA Analysis.....	41
Statistical Analysis.....	43
 <b><u>CHAPTER 3: RESULTS: C-MET MODULATES HGF EXPRESSION, COLONY FORMATION, AND TUMORIGENICITY OF GBM CELLS</u>.....</b>	
Coexpression of c-Met and HGF in GBM.....	44
c-Met Modulates HGF Expression.....	45
c-Met is Required for Anchorage-independent Growth of U87 Cells....	46
Silencing c-Met Suppresses the Tumorigenicity of Intracranial GBM Xenografts.....	58
	61
 <b><u>CHAPTER 4: RESULTS: <math>\Delta</math>EGFR REGULATES HGF EXPRESSION VIA C-MET, AND REQUIRES C-MET FOR ONCOGENICITY</u>.....</b>	
$\Delta$ EGFR Induces the Expression of HGF via c-Met Activation.....	63
Inhibition of $\Delta$ EGFR Suppresses HGF expression.....	64
c-Met is Required by $\Delta$ EGFR for HGF Production, Anchorage- independent Growth, and Tumorigenicity of GBM Cells.....	67
	69
 <b><u>CHAPTER 5: RESULTS: STAT3 PARTIALLY MODULATES HGF EXPRESSION IN RESPONSE TO THE C-MET SIGNAL IN <math>\Delta</math>EGFR-EXPRESSING GBM CELLS</u>.....</b>	
STAT3 is a Key Node Regulating HGF Expression in Response to the c-Met Signal.....	75
	76

STAT3 Partially Rescues Attenuated HGF and Anchorage-independent Growth of c-Met Silenced U87 $\Delta$ EGFR Cells.....	96
<b><u>CHAPTER 6: RESULTS: THE C-MET / HGF AXIS IS</u></b>	
<b>UPREGULATED IN MESENCHYMAL GBM TUMORS.....</b>	<b>104</b>
<b><u>CHAPTER 7: DISCUSSION</u>.....</b>	<b>114</b>
<b>BIBLIOGRAPHY.....</b>	<b>124</b>
<b>VITA.....</b>	<b>149</b>

## LIST OF FIGURES

### **CHAPTER 1: INTRODUCTION**

<b>Figure 1.</b> Genetic aberrations associated with the development of primary and secondary GBM.....	7
<b>Figure 2.</b> Biological responses of PI3K and MAPK pathway dysregulation...	11
<b>Figure 3.</b> c-Met structural domains, major phosphorylation sites, and binding partners.....	17

### **CHAPTER 3: RESULTS: C-MET MODULATES HGF EXPRESSION, COLONY FORMATION, AND TUMORIGENICITY OF GBM CELLS**

<b>Figure 4.</b> HGF and c-Met mRNA expression correlates in GBM.....	46
<b>Figure 5.</b> c-Met is acutely activated by HGF in U87 cells.....	48
<b>Figure 6.</b> HGF is secreted by U87 cells.....	49
<b>Figure 7.</b> HGF mRNA expression is dependent on c-Met expression.....	50
<b>Figure 8.</b> HGF protein expression is dependent on c-Met expression.....	51
<b>Figure 9.</b> HGF secretion decreases with c-Met knockdown in U87 cells.....	52
<b>Figure 10.</b> Cellular morphology changes with c-Met knockdown in U87 cells..	53
<b>Figure 11.</b> Cellular morphology alters with overexpression of kinase-impaired c-Met mutants in U87 cells.....	55
<b>Figure 12.</b> c-Met inhibition reduces HGF mRNA and protein amounts in U87 cells.....	56

<b>Figure 13.</b> HGF mRNA expression and protein levels decrease with c-Met knockdown in LN18 cells.....	57
<b>Figure 14.</b> Anchorage-independent growth of U87 cells with c-Met knockdown.....	59
<b>Figure 15.</b> c-Met suppression alters biological characteristics of U87 cells...	60
<b>Figure 16.</b> c-Met silencing decreases the tumorigenicity of U87 xenografts..	61

#### **CHAPTER 4: RESULTS: $\Delta$ EGFR REGULATES HGF EXPRESSION VIA**

##### **C-MET ACTIVATION AND REQUIRES C-MET FOR ONCOGENICITY**

<b>Figure 17.</b> $\Delta$ EGFR increases the mRNA expression of HGF.....	64
<b>Figure 18.</b> $\Delta$ EGFR increases the protein expression of HGF.....	65
<b>Figure 19.</b> Functional HGF is secreted by $\Delta$ EGFR-expressing GBM cells...	66
<b>Figure 20.</b> HGF mRNA expression decreases with inhibition of $\Delta$ EGFR.....	68
<b>Figure 21.</b> HGF protein expression is attenuated with inhibition of $\Delta$ EGFR..	69
<b>Figure 22.</b> c-Met is required by $\Delta$ EGFR to maintain HGF expression.....	70
<b>Figure 23.</b> <i>In vitro</i> colony formation of U87 $\Delta$ EGFR-expressing cells with c-Met knockdown.....	71
<b>Figure 24.</b> Biological properties of U87 $\Delta$ EGFR cells are altered with c-Met knockdown.....	72
<b>Figure 25.</b> c-Met is required by $\Delta$ EGFR to enhance the tumorigenicity of U87 cells.....	73



**CHAPTER 5: RESULTS: STAT3 PARTIALLY MODULATES HGF  
EXPRESSION IN RESPONSE TO THE C-MET SIGNAL IN  $\Delta$ EGFR-  
EXPRESSING GBM CELLS**

<b>Figure 26.</b> Schematic of mass spectrometry experiments.....	77
<b>Figure 27.</b> Confirmation of sample identities that were processed for PhosphoScan analysis.....	78
<b>Figure 28-1.</b> Mass spectrum of the abl interactor 1 (ABI1) Y198 peptide.....	85
<b>Figure 28-2.</b> Mass spectrum of the abl interactor 1 (ABI1) Y213 peptide.....	85
<b>Figure 28-3.</b> Mass spectrum of the annexin A2 (ANXA2) Y238 peptide.....	86
<b>Figure 28-4.</b> Mass spectrum of the mitogen-activated protein kinase 14 (MK14) (MAPK14) Y182 peptide.....	86
<b>Figure 28-5.</b> Mass spectrum of the L-lactate dehydrogenase A (LDHA) Y247 S249 peptide.....	86
<b>Figure 28-6.</b> Mass spectrum of the glycogen synthase kinase 3 $\alpha/\beta$ (GSK3A/B) Y279 S282 peptide.....	87
<b>Figure 28-7.</b> Mass spectrum of the enolase A (ENOA) (ENO1) Y44 peptide.	87
<b>Figure 28-8.</b> Mass spectrum of the glycogen synthase kinase 3 $\alpha/\beta$ (GSK3A/B) Y279 peptide.....	87
<b>Figure 28-9.</b> Mass spectrum of the src homology 2 domain-containing adapter protein B (SHB) Y268 peptide.....	88
<b>Figure 28-10.</b> Mass spectrum of the serine/threonine-protein kinase PRP4 homolog (PRP4B) Y849 peptide.....	88
<b>Figure 28-11.</b> Mass spectrum of the StAR-related lipid transfer protein 13 (STA13) (STARD13) Y39 peptide.....	89

<b>Figure 28-12.</b> Mass spectrum of the Rho-GTPase-activating protein 42 (RHG42) Y792 peptide.....	89
<b>Figure 28-13.</b> Mass spectrum of the paxillin (PAXI) (PXN) Y88 peptide.....	90
<b>Figure 28-14.</b> Mass spectrum of the glucocorticoid receptor DNA binding factor 1 (GRLF1) Y1105 peptide.....	90
<b>Figure 28-15.</b> Mass spectrum of activated CDC42 kinase (ACK1) (TNK2) Y518 peptide.....	90
<b>Figure 28-16.</b> Mass spectrum of the mitogen-activated protein kinase 1 (MK01) (MAPK1) Y185 peptide.....	91
<b>Figure 28-17.</b> Mass spectrum of the vinculin (VINC) Y822 peptide.....	91
<b>Figure 28-18.</b> Mass spectrum of the glucocorticoid receptor DNA-binding factor 1 (GRLF1) Y1087 peptide.....	91
<b>Figure 28-19.</b> Mass spectrum of the vimentin (VIME) (VIM) Y61 peptide.....	92
<b>Figure 28-20.</b> Mass spectrum of the Vimentin (VIME) (VIM) Y150 peptide....	92
<b>Figure 29.</b> Ingenuity pathway analysis of c-Met-dependent phosphopeptides identified by mass spectrometry that may modulate HGF expression.....	93
<b>Figure 30.</b> Mass spectrum of the signal transducer and activator of transcription 3 (STAT3) Y705 peptide.....	94
<b>Figure 31.</b> STAT3 Y705 phosphorylation decreases with c-Met knockdown in U87 and U87 $\Delta$ EGFR cells.....	95
<b>Figure 32.</b> STAT3 activity decreases with c-Met and $\Delta$ EGFR inhibition in U87 $\Delta$ EGFR cells.....	96
<b>Figure 33.</b> STAT3 Y705 inhibition attenuates HGF mRNA expression in U87 $\Delta$ EGFR cells.....	97

<b>Figure 34.</b> Constitutively active STAT3 partially rescues HGF expression in c-Met silenced U87 $\Delta$ EGFR cells.....	98
<b>Figure 35.</b> HGF promoter activity is unresponsive to c-Met knockdown in U87 cells.....	100
<b>Figure 36.</b> c-Met knockdown does not affect HGF mRNA stability.....	101
<b>Figure 37.</b> STAT3 partially rescues colony formation associated with c-Met knockdown in U87 $\Delta$ EGFR cells.....	102
<b>Figure 38.</b> Proposed model of enhanced HGF expression via c-Met activation in GBM cells.....	103

## **CHAPTER 6: RESULTS: THE C-MET / HGF AXIS IS UPREGULATED**

### **IN MESENCHYMAL GBM TUMORS**

<b>Figure 39.</b> c-Met mRNA expression is upregulated in the mesenchymal GBM subtype (Verhaak determined).....	106
<b>Figure 40.</b> Enhanced HGF mRNA expression associates with the mesenchymal GBM subtype (Verhaak determined).....	107
<b>Figure 41.</b> c-Met mRNA expression is elevated in mesenchymal GBM tumors (Verhaak calculated).....	108
<b>Figure 42.</b> Mesenchymal GBM tumors express increased levels of HGF mRNA (Verhaak calculated).....	109
<b>Figure 43.</b> Mesenchymal and proliferative GBM tumors express elevated c-Met mRNA levels (Phillips calculated).....	110
<b>Figure 44.</b> Increased HGF mRNA expression associates most with the mesenchymal and proliferative GBM subtypes (Phillips calculated).....	111

<b>Figure 45.</b> Validation that higher c-Met expression levels associates with the mesenchymal GBM subtype in an independent sample set (Verhaak calculated).....	112
<b>Figure 46.</b> Independent dataset validation that elevated HGF expression levels associate with the mesenchymal GBM subtype (Verhaak calculated)..	113

## LIST OF TABLES

### **CHAPTER 2: MATERIALS AND METHODS**

<b>Table 1.</b> Short tandem repeat fingerprinting of GBM cells.....	28
<b>Table 2.</b> pLKO.1 c-Met shRNA targeting constructs.....	31
<b>Table 3.</b> Primers used to generate kinase-deficient c-Met mutants.....	32
<b>Table 4.</b> qRT-PCR primer sequences.....	35

### **CHAPTER 5: RESULTS: STAT3 PARTIALLY MODULATES $\Delta$ EGFR-MEDIATED C-MET ACTIVATION AND HGF EXPRESSION**

<b>Table 5.</b> List of peptides with a phosphotyrosine modification identified by mass spectrometry.....	81
<b>Table 6.</b> Mean abundance of all tyrosine-phosphorylated peptides that were identified by mass spectrometry.....	83
<b>Table 7.</b> Peptides showing a significant decrease in tyrosine phosphorylation with c-Met knockdown.....	84

## LIST OF ABBREVIATIONS

<b>C/EBP</b>	CCAAT/ enhancer-binding protein
<b>c-Met</b>	hepatocyte growth factor receptor
<b>CM</b>	conditioned media
<b>DMEM</b>	Dulbecco's modified Eagle's medium
<b>EGF</b>	epidermal growth factor
<b>EGFR</b>	epidermal growth factor receptor
<b>ETD</b>	electron transfer dissociation
<b>FBS</b>	fetal bovine serum
<b>GBM</b>	glioblastoma
<b>HB-EGF</b>	heparin-binding EGF-like growth factor
<b>HGF</b>	hepatocyte growth factor
<b>IDH1</b>	isocitrate dehydrogenase 1
<b>IDH2</b>	isocitrate dehydrogenase 2
<b>LOH</b>	loss of heterozygosity
<b>MAPK</b>	mitogen-activated protein kinase
<b>MDCK</b>	Madin-Darby Canine Kidney
<b>MGMT</b>	O <sup>6</sup> -methylguanine- DNA-methyltransferase
<b>mRNA</b>	messenger ribonucleic acid
<b>NSCLC</b>	non-small cell lung cancer
<b>NF1</b>	neurofibromatosis-1
<b>PBS</b>	phosphate buffered saline

<b>PBST</b>	PBS containing 0.05% tween 20
<b>PCR</b>	polymerase chain reaction
<b>PI3K</b>	phosphatidylinositol 3-kinase
<b>PTEN</b>	phosphatase and tensin homolog
<b>qRT-PCR</b>	quantitative reverse transcriptase PCR
<b>REMBRANDT</b>	REpository for Molecular BRAin Neoplasia DaTa
<b>rhHGF</b>	recombinant human HGF
<b>RTK</b>	receptor tyrosine kinase
<b>RIPA</b>	radioimmunoprecipitation assay
<b>RNA</b>	ribonucleic acid
<b>shRNA</b>	short hairpin RNA
<b>STAT</b>	signal transducer and activator of transcription
<b>STAT3-CA</b>	constitutively active STAT3
<b>TCGA</b>	The Cancer Genome Atlas
<b>TGF-<math>\alpha</math></b>	transforming growth factor- $\alpha$
<b>TFA</b>	trifluoroacetic acid
<b>TKI</b>	tyrosine kinase inhibitor
<b>TMZ</b>	temozolomide
<b>TP53</b>	tumor protein 53
<b>WB</b>	western blot
<b>WHO</b>	World Health Organization
<b>WT</b>	wild type

# **CHAPTER 1**

## **INTRODUCTION**



## **Glioma**

Gliomas account for the majority of primary brain malignancies found in adults (Sathornsumetee et al., 2007). The main glioma subtypes include astrocytomas, oligodendrogliomas, and ependymomas (Yan et al., 2009). The most common group of gliomas are the astrocytomas, and are otherwise known as glial tumors (Gonzalez and Gilbert, 2005). On the basis of pathology and clinical criteria, the World Health Organization (WHO) classifies astrocytomas into one of four grades; grades I through IV (Yan et al., 2009). Grade I astrocytic tumors may be either pilocytic astrocytomas or subependymal giant cell astrocytomas (Louis et al., 2007). These low-grade lesions are not aggressive, are generally benign, and are typically cured by surgical resection (Yan et al., 2009). Grade II astrocytic tumors include pilomyxoid astrocytomas, diffuse astrocytomas, and pleomorphic xanthoastrocytomas, and grade III astrocytic tumors are called anaplastic astrocytomas (Louis et al., 2007). Grade II and Grade III astrocytic lesions are infiltratively aggressive, may progress to a higher grade lesion, and are associated with a poor clinical outcome (Yan et al., 2009). Glioblastomas, gliosarcomas, and giant cell glioblastomas are characterized as WHO grade IV tumors (Louis et al., 2007). These high grade gliomas are highly invasive and are associated with an extremely poor clinical prognosis (Yan et al., 2009). The clinical prognosis of glioma patients depends on several criteria, amongst them are age of the patient, performance status (Karnofsky Performance Scale Score), and grade of the lesion (Görke et al., 2010).

## **Glioblastoma**

Glioblastoma (GBM) may arise *de novo* (primary GBM; represents about 90% of cases) or from less malignant precursor lesions (secondary GBM) (Ohgaki and Kleihues, 2011). Primary GBM typically affects people that are older than 45 years of age, while secondary GBM occurs more frequently in individuals that are younger than that (Furnari et al, 2007). As our understanding of the molecular pathogenesis of GBM has evolved, it has become clearer that primary and secondary GBM have very different genetic profiles, even though they appear indistinguishable by histology (Ohgaki and Kleihues, 2011).

Approximately 9000 people in the United States are diagnosed with GBM per annum (Reardon and Wen, 2006). Of all human tumors, GBM is the most difficult neoplasm to treat (Chakravarti et al., 2001). Even with the refinement of conventional treatment options for GBM patients, outcomes have only slightly improved over the past few decades (Sathornsumetee et al., 2007). The overall five year survival rate for GBM patients is 3.4% (Gonzalez and Gilbert, 2005), with most patients succumbing to the disease within 14 months (Görke et al., 2010). However, as we understand more about the molecular pathogenesis of GBM, targeted therapies will likely revolutionize their treatment (Sathornsumetee et al., 2007).

## **GBM Treatment**

The current standard of care for newly diagnosed GBM patients is to surgically remove as much of the lesion/lesions as possible, followed by fractionated radiotherapy along with concurrent and adjuvant treatment with temozolomide (TMZ) (Colman, et al., 2010; Stupp et al., 2005). TMZ is a DNA alkylating agent that methylates DNA at the O<sup>6</sup> position of guanine (Lassman and Holland, 2007). This results in several nucleotide mismatches in complementary DNA, leading to many unsuccessful post-replicative attempts at mismatch repair, ultimately leading to apoptosis (D'Atri et al., 1998). One significant prognostic indicator of a favorable response to TMZ treatment is the degree of methylation, or epigenetic silencing, of the O<sup>6</sup>-methylguanine-DNA-methyltransferase (MGMT) gene promoter (Colman et al., 2010; Weller et al., 2010). MGMT promoter methylation is commonly found (40–57%) in GBM (Ohgaki and Kleihues, 2009). MGMT is a DNA repair protein that restores O<sup>6</sup>-alkylated bases caused by chemotherapy, thereby counteracting the effect of TMZ treatment (Krakstad and Chekenya, 2010). In a large multi-center phase III trial that evaluated the use of TMZ for the treatment of primary GBM with different MGMT promoter methylation statuses, improved survival was reported for those patients whose tumors had methylation of the MGMT promoter (Sulman and Aldape, 2011).

Over the past few decades we have only seen a marginal improvement in progression-free and overall survival, and therefore pre-clinical researchers have focused their attention on being able to understand the genetic pathobiology of these tumors (Gonzalez and Gilbert, 2005). Even though targeted

chemotherapeutic approaches are still in their infancy, they hold a promise of being able to alter the course of this relentless disease (Furnari et al., 2007).

Currently there are many challenges that hinder the responsiveness of GBMs to targeted and non-targeted chemotherapy. One of the major obstacles limiting treatment effectiveness is that perhaps not all of the neoplastic cells are completely removed during resection, which invariably results in tumor recurrence. Additionally, progenitor cells present in the bulk of the tumor are inherently resistant to radiotherapy, and go on to form recurrent lesions that resist further treatment (Phillips et al., 2006). Adding to this complication, the brain is enveloped in a protective blood brain barrier that limits the delivery of polar compounds to the central nervous system that have large molecular weights, such as proteins (Reardon and Wen, 2006). Additionally, chemotherapeutic agents are often actively pumped out of the brain by efflux pumps (Fletcher et al., 2010). Even when chemotherapeutic agents reach the lesion, the highly heterogenous genetic profile of these neoplasms ensures that not all cells are effectively treated (Reardon and Wen, 2006). With all these challenges, patient outcomes remain highly variable (Sulman and Aldape, 2011). It is therefore clear that new agents that more closely target the biology of the disease need to be developed in order to improve on treatment options for this lethal disease.

## **Genetic Aberrations of Primary and Secondary GBM**

Although it is still unclear what the cell of origin is for primary and secondary GBM (Furnari et al., 2007), it has been proposed that primary GBM arises from glial progenitor cells that have accumulated distinct genetic alterations (Ohgaki and Kleihues, 2011). These include epidermal growth factor receptor (EGFR) amplification / mutations / rearrangement, tumor protein 53 (TP53) mutations, phosphatase and tensin homolog (PTEN) mutations, neurofibromatosis-1 (NF1) alterations, and loss of heterozygosity (LOH) of 10p and 10q (Ohgaki and Kleihues, 2011). Other genetic alterations that occur in primary GBM are INK4a/ARF mutations, Cyclin D1/3 amplification or overexpression, murine double minute 2/4 amplification or overexpression, and B-Cell CLL/Lymphoma 2 Like Protein overexpression (Furnari et al., 2007).

There is evidence to suggest that secondary GBM originates from progenitor cells that acquire an isocitrate dehydrogenase 1/2 (IDH1/IDH2) mutation (Yan et al., 2009). IDH1/2 mutations occur in the majority of WHO Grade II diffuse astrocytomas, and the frequency of mutation does not increase with tumor grade (Ohgaki and Kleihues, 2011). The mutation status of IDH1/2 correlates favorably with a better prognosis for GBM patients. Patients are predicted to survive as long as 31 months if their tumors have an IDH1/2 mutation, versus half that survival time for patients whose tumors do not have an IDH1/2 mutation (Yan et al., 2009). Later, it was also shown that an IDH1 mutation status held a lot of predictive power in assessing improved patient survival after surgical resection and radiotherapy, with the mean survival being 27.1 months versus 11.3

months for those patients whose tumors did not have an IDH1 mutation (Nobusawa et al. 2009). Additionally, diffuse astrocytomas have mutations in TP53, and anaplastic astrocytomas acquire LOH of 10q (Ohgaki and Kleihues, 2011).

Key genetic alterations that play important roles in the development of primary and secondary GBM are represented in Figure 1.

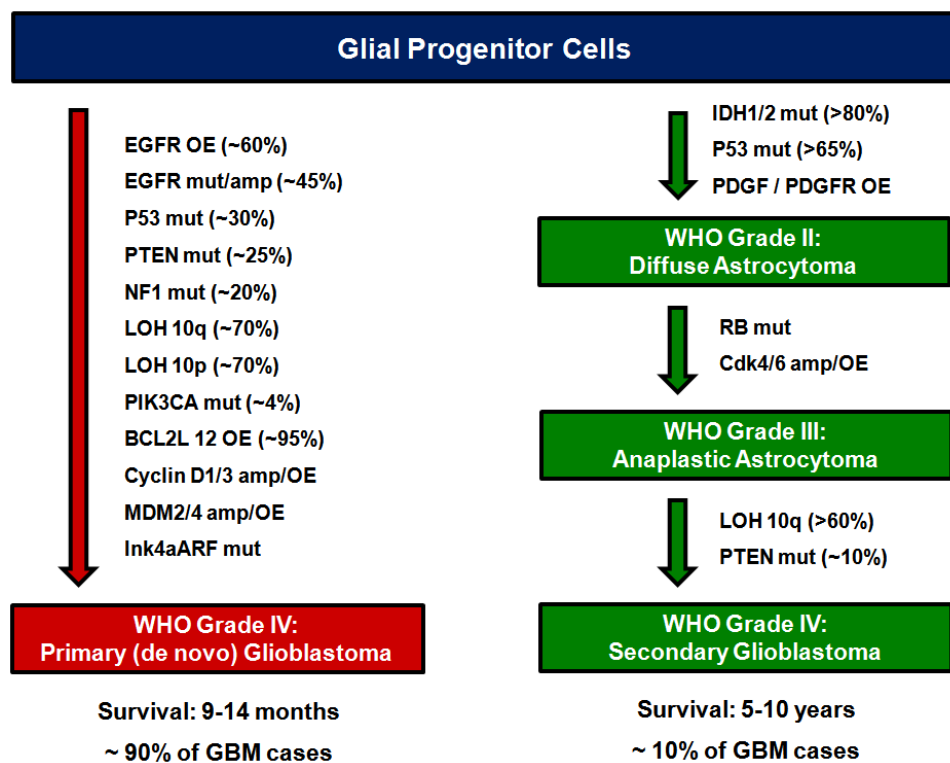


**Figure 1.** Genetic aberrations associated with the development of primary and secondary GBM. [mutation (mut), overexpression (OE); loss of heterozygosity (LOH)].

## **GBM Subtypes**

Using high-throughput expression profiling techniques, GBM has been further classified into various subtypes based on their gene expression profiles (Phillips et al., 2006; Verhaak et al., 2010). The first of these studies by Phillips and colleagues (2006) identified three GBM subclasses, with those being mesenchymal, proneural, and proliferative. They reported that the proneural subclass had a gene expression signature that displayed neuronal lineage markers. Patients with these tumors tended to live longer than patients with tumors expressing mesenchymal (angiogenic) or proliferative markers. Analysis using array comparative genomic hybridization methodologies identified that both the poor prognostic groups had gains or amplification of the EGFR, which was not seen in the proneural GBM subtype. Remarkably, the two poor prognosis subtypes also expressed elevated levels of neural stem cell markers compared with proneural tumors. Their results also showed that if a patient's initial lesion displayed proneural or proliferative markers, then the recurrent tumors would shift their gene expression signature to represent that of the mesenchymal subtype. The recurrent tumors were frequently upregulated in YKL-40, CD44, STAT3 and vimentin; all markers of the mesenchymal-angiogenic phenotype (Phillips et al., 2006). Importantly, these studies have led to the identification of a set of genes, representing both the proneural and mesenchymal GBM subtypes, which has been developed into a clinical test, compatible with how samples are processed following resection, which predicts patient outcome (Colman et al., 2010). Furthermore, these multigenes are currently being used to stratify patients in a

large multi-center Phase III clinical trial (RTOG 0825) that determines whether the addition of bevacizumab (Avastin; anti-VEGF; anti-angiogenic) to standard care regimens improves survival (<http://clinicaltrials.gov>; Sulman and Aldape, 2011).

The second high-throughput profiling study that I would like to mention stratified GBM molecularly in terms of gene expression signatures into four major subtypes; proneural, neural, classic, and mesenchymal, (Verhaak et al., 2010). Patterns of mutation and DNA copy number alterations were also integrated into their analyses. They reported that the proneural signature had PDGFRA/IDH1 genetic aberrations, while the classic and mesenchymal GBM subtypes contained mainly EGFR and NF1 aberrations, respectively. EGFR amplification was found in as many as 95% of classic GBM tumors, and in at least 29% of those classified as being mesenchymal. Increased copy numbers for both the hepatocyte growth factor receptor (c-Met) and EGFR were seen in >86% of all GBM subclasses, except for those tumors classified as being proneural.

These groundbreaking reports may lead to the identification of prognostic and predictive markers that correlate with treatment response. Better therapies could then be explored, with the ultimate goal of eventually being able to personalize medicine (Sulman and Aldape, 2011).



## **Dysregulated Receptor Tyrosine Kinases in GBM**

The Cancer Genome Atlas (TCGA) Network (The Cancer Genome Atlas Research Network, 2008) performed a comprehensive analysis of aberrations that occur in GBM. They reported that there are three major pathways with components that have significant alterations, with those being the receptor driven RAS / phosphatidylinositol 3-kinase (PI3K) (88%), the NF1 (87%), and the p53 (78%) pathways.

Receptor tyrosine kinases (RTKs) are often aberrantly overexpressed and overactive in human cancer, including GBM, and therefore targeting RTK dysregulation has become a key strategy for targeted therapy (Krakstad and Chekenya, 2010). The increased activation of RTKs occurs through ligand-dependent and ligand-independent mechanisms (Li et al., 2007; Pillay et al., 2009; Shinomiya et al., 2004). These include, amplification of RTK signaling by their ligands (Shinomiya et al., 2004), constitutive activation of receptors by missense mutations or multiple exon deletion (Pillay et al., 2009), and receptor crosstalk with resultant activation (Eder et al., 2009). Increased RTK expression and activation in cancer cells contributes significantly to hallmark malignancy phenotypes, such as increased proliferation, survival, invasion, glycolysis, cell growth, and angiogenesis (Figure 2; Bertotti et al., 2009; Frederick et al., 2000; Pillay et al., 2009; Wong et al., 1992). Although Figure 2 provides an incomplete picture of all possible cellular events that may occur in response to RTK dysregulation, the main molecular players involved in PI3K and mitogen activated protein kinase (MAPK) pathway activation are shown.

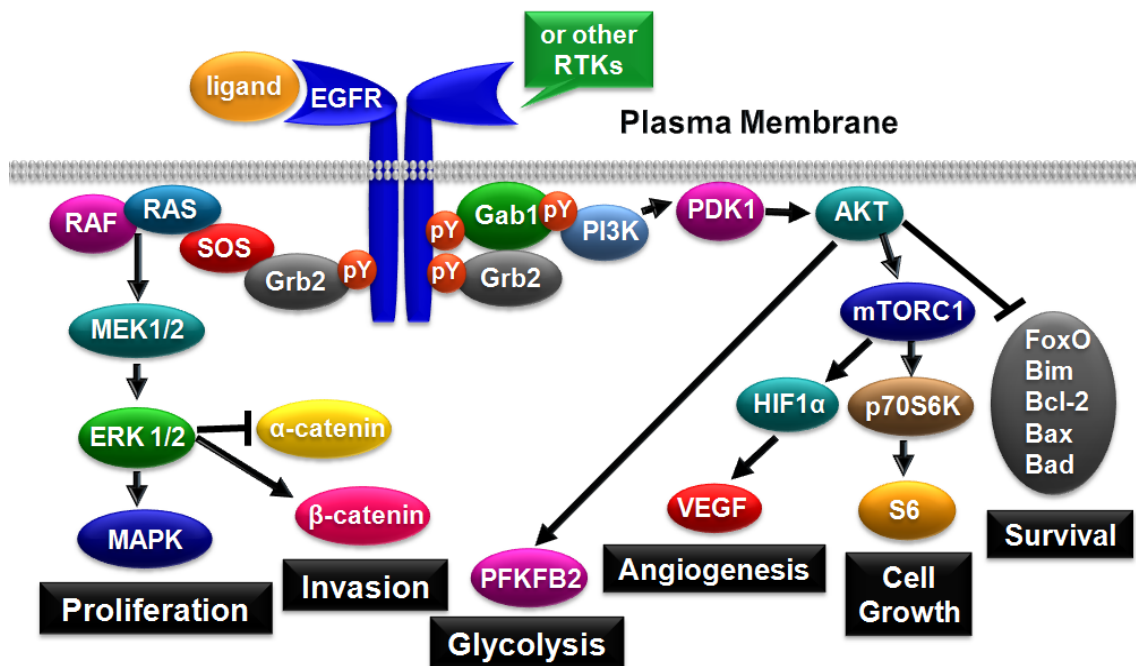


**Figure 2.** Biological responses of PI3K and MAPK pathway dysregulation.

## EGFR

The EGFR (also known as HER1 / ErbB1) belongs to a larger family of ErbB receptors with tyrosine kinase activity (Ymer et al., 2011). Other members of this commonly linked ancestral family include ErbB2 (HER2/neu), ErbB3 (HER3) and ErbB4 (HER4) (Huang et al., 2009). These EGFR family members regulate diverse cellular processes, such as proliferation, migration, survival, adhesion, and differentiation, which are important in normal development, and if dysregulated may contribute to the development of cancer (Yarden and Slivkowski, 2001). EGFR family members share common domain organization, with those being an extracellular ligand binding domain, a transmembrane

domain, and an intracellular domain. The intracellular domain consists of a tyrosine kinase domain and a c-terminal tail with multiple tyrosine residues that can be autophosphorylated following receptor dimerization and activation (Huang et al., 2009). Canonically, the wild type (WT) EGFR may be activated by seven different ligands (Schneider and Wolf, 2009); epidermal growth factor (EGF), transforming growth factor- $\alpha$  (TGF- $\alpha$ ), heparin-binding EGF-like growth factor (HB-EGF), amphiregulin, betacellulin, epiregulin, and epigen (Villares et al., 2007). Ligand binding is crucial for the EGFR to homodimerize, or to heterodimerize with other ErbB family receptors, so that activation and autophosphorylation can occur (Ymer et al., 2011). The preferred autophosphorylation site of the WT EGFR is Y1173 (Schmidt et al., 2003), however others such as Y1068 and Y1148 are also indicative of its tyrosine kinase activity (Huang et al., 2009). The tyrosine residue, Y1045, is a c-Cbl binding site that serves to downregulate the receptor after it has been stimulated with ligand and ubiquitinated (Grovdal et al., 2004). The Y845 site of EGFR is phosphorylated by Src family non-receptor protein tyrosine kinases following their activation by the EGFR (Yamamoto et al., 2006).

## **EGFR Alterations in GBM**

EGFR is overexpressed in approximately 60% of primary GBM cases and in less than 10% of patients with secondary GBMs (Ohgaki and Kleihues, 2007), indicating that EGFR alterations occur predominantly in aggressive cases. Several mechanisms may additionally account for aberrant EGFR signaling in GBM, with

one being the upregulated autocrine expression of its ligands (Huang et al., 2009; Ramnarain et al., 2006; Singh and Harris, 2005). Enhanced EGFR activation in GBM may also be caused by amplification or mutation, which taken together is found in as many as 45% of all GBMs (The Cancer Genome Atlas Research Network, 2008). Almost every classic GBM has focal amplification of the EGFR, with the mesenchymal, neural, and proneural tumors amplifying the EGFR at 29%, 67%, and 17%, respectively (Verhaak et al., 2010). EGFR mutations are also a frequent occurrence in GBM and are found in about a third of all tumors belonging to the classic GBM subclass, and in many of the proneural, neural and mesenchymal tumors (Verhaak et al., 2010). Various point mutations in the extracellular domain of the EGFR account for some of these aberrations (Lee et al., 2006). During the amplification process, the EGFR gene is often rearranged, which may also result in transcripts with large deletions (Cavenee, 2002). The most common rearrangement of the EGFR gene is an in-frame 2-7 exon deletion within the extracellular domain, and is known as  $\Delta$ EGFR (de2–7 EGFR, EGFRvIII, or EGFR\*) (Ohgaki and Kleihues, 2007).

## **$\Delta$ EGFR**

The in-frame 801bp deletion of the  $\Delta$ EGFR gene results in a truncated protein unable to bind its cognate ligands (Schmidt et al., 2003). Despite this, the  $\Delta$ EGFR signals constitutively at a low-level, thereby successfully allowing it to evade signals regulating internalization and downregulation (Huang et al., 1997;

Hwang et al., 2011). This is in contrast with ligand-stimulated WT EGFR that is rapidly attenuated following acute stimulation with ligand (Schmidt et al., 2003). One of the primary reasons for the low signal intensity of the  $\Delta$ EGFR is due to inefficient dimerization (Hwang et al., 2011; Ymer et al., 2011). However, its constitutive signal leads to increased survival of GBM cells *in vivo*, by augmenting mitogenic effects and reducing apoptotic rates (Nagane et al., 1996). Interestingly, when  $\Delta$ EGFR is used to transform INK4A/Arf depleted astrocytes and neural stem cells, high grade lesions are orthotopically and subcutaneously produced when injected into nude mice (Bachoo et al., 2002), raising the possibility that it may be one important initiating event in tumor development. Not only is  $\Delta$ EGFR most likely an important factor in gliomagenesis, but the tumorigenic potential of glioma cells *in vivo* are significantly enhanced by  $\Delta$ EGFR expression when compared with those xenografts expressing the WT EGFR (Cavenee, 2002; Huang et al., 1997; Nishikawa et al., 1994). It has also been shown that cells expressing  $\Delta$ EGFR are inherently recalcitrant to both radiation (Lammering et al., 2004) and chemotherapy (Nagane et al., 1998).  $\Delta$ EGFR also activates the PI3K-Akt-mTOR pathway to a greater degree than the Ras-Raf-MEK cascade, and recruits the activity of STATs (STAT3 and STAT5b) for enhanced cellular proliferation, viability, and transformation (Chumbalkar et al., 2011; de la Iglesia et al., 2008; Huang et al., 2009). Not surprisingly,  $\Delta$ EGFR expression has been strongly associated with a poor survival prognosis for patients whose tumors amplify EGFR (Heimberger et al., 2005; Shinjima et al., 2003), or express YKL-40 (Pelloski et al., 2007).

## **$\Delta$ EGFR in GBM**

The  $\Delta$ EGFR is not detected in normal tissues, and is therefore a cancer specific mutant of the EGFR (Wikstrand et al., 1998). Several studies have shown that the  $\Delta$ EGFR is expressed in about 45-50% of GBMs that amplify the WT EGFR (Pedersen et al., 2001; Shinojima et al., 2003; Wikstrand et al., 1998). In a more recent study performed by the TCGA Network, the  $\Delta$ EGFR deletion is mostly found in the classic GBM subclass (23%), a subclass amplifying EGFR the most compared with other GBM subclasses, and in 3% of proneural and mesenchymal GBMs (Verhaak et al., 2010). However, the 200 GBMs analyzed in this study may have had a negative selection bias towards the  $\Delta$ EGFR, as necrotic tissue, which is frequently found in high grade GBM (Li et al., 2009), was limited to 40% of each sample (Verhaak et al., 2010). Most likely the  $\Delta$ EGFR was not detected in as many GBMs as previously reported, due to the patchy expression of  $\Delta$ EGFR (Wiesner et al., 2009) in only a small percentage of the total number of cells in a GBM (Jungbluth et al., 2003).

## **Targeting EGFR / $\Delta$ EGFR in GBM**

Given that the EGFR is highly dysregulated in GBM, it is surprising that EGFR inhibitors, including tyrosine kinase inhibitors (TKIs) that also target the  $\Delta$ EGFR, have not lived up to their clinical promise (Halatsch et al., 2006). Resistance to anti-EGFR therapy has been partly attributed to signal

compensation by other RTKs, or via their transactivation by EGFR and  $\Delta$ EGFR, leading to the persistent activation of redundant signaling pathways (Camp et al., 2005; Pillay et al., 2009). It has therefore become critically important to identify key players that mediate their signal and maintain their biological characteristics.

## **c-Met**

c-Met is a RTK essential for normal physiological and developmental programs, such as branching morphogenesis, wound repair, organ patterning, and organ homeostasis (Birchmeier et al., 2003; Trusolino et al., 2010). It is also a protein highly active in most cancers, regulating processes such as metastasis, angiogenesis, proliferation, survival, and invasion (Bardelli et al., 1997; Birchmeier et al., 2003; Sheth et al., 2008). c-Met is produced as a glycosylated 170 kDa precursor protein that is cleaved by proteases into a 50 kDa  $\alpha$ -chain and a 145 kDa  $\beta$ -chain, which are linked by disulphide bridges (Crepaldi et al., 1994). The  $\beta$ -chain spans the membrane, having an intracellular tyrosine kinase domain and a large extracellular domain, and the  $\alpha$ -chain is located extracellularly (Ma et al., 2003; Figure 3).

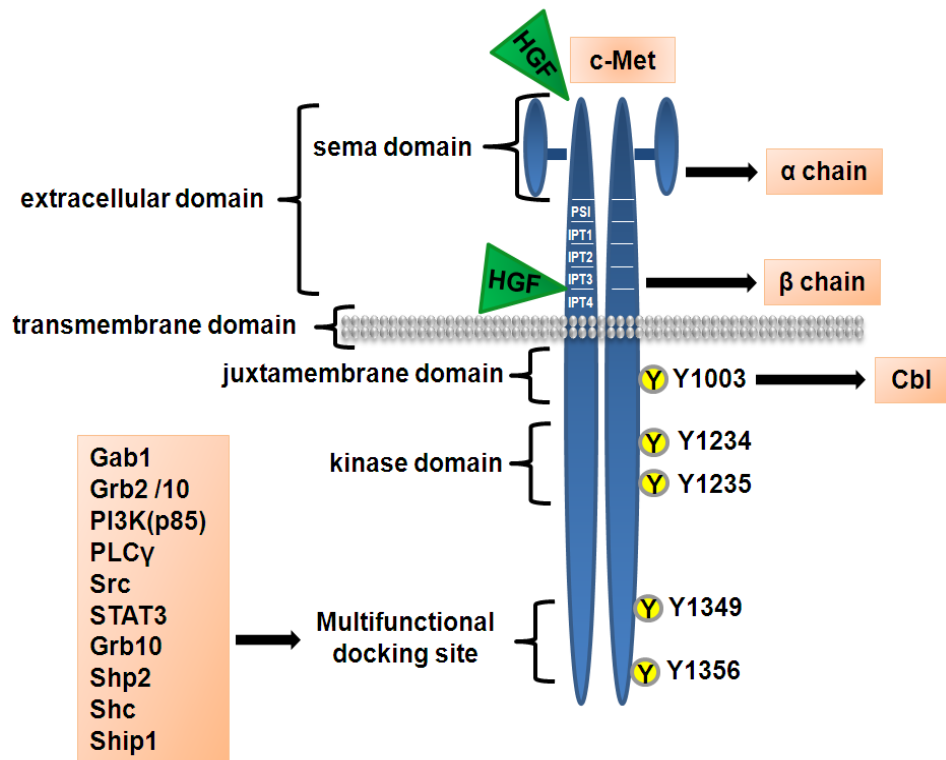


**Figure 3.** c-Met structural domains, major tyrosine phosphorylation sites, and binding partners.

The hepatocyte growth factor (HGF), c-Met's only known activating physiological ligand, binds c-Met in the sema (Gherardi et al., 2003) and IP3/IP4 domains (Trusolino et al., 2010). The sema domain, also found in semaphorins and plexins (Trusolino et al., 2010), is equally important for receptor dimerization (Kong-Beltran et al., 2004). c-Met's intracellular region contains a juxtamembrane domain, tyrosine kinase catalytic domain, and a multi-functional docking site. All three intracellular domains contain tyrosine residues that are phosphorylated upon ligand binding (Hov et al., 2004).

Phosphorylation of c-Met Y1003 has been shown to be important for Cbl-mediated ubiquitination and degradation following receptor internalization (Abella



et al., 2005; Li et al., 2007). The c-Met signal may also be downregulated by decorin, an extracellular small leucine-rich proteoglycan, within first few minutes of their association (Goldoni et al., 2009). Attenuation of c-Met signaling by disintegrin and metalloprotease-mediated extracellular domain cleavage, produces a soluble N-terminal fragment that is capable of sequestering HGF present in the extracellular environment; a process known as shedding. This 'decoy' fragment may also interfere with c-Met dimerization, ultimately leading to signal attenuation. The membrane-anchored cytoplasmic tail is proteolytically cleaved by  $\gamma$ -secretase and then degraded (Foveau et al., 2009). Phosphorylation of Y1234 and Y1235 of c-Met, which are located in the kinase domain, are required for full receptor activation (Bardelli et al., 1997). In the absence of activating mutations, Y1235 is the first tyrosine residue in the autophosphorylation (kinase) domain to be phosphorylated, which is then followed by Y1234 phosphorylation (Chiara et al., 2003). Once this occurs, phosphorylation at Y1349 and Y1356 in the COOH terminus links Src homology 2 domain containing signaling adapters and transducers to the receptor for initiation of signal transduction (Peruzzi and Bottaro, 2006). These adapter proteins and signaling effectors (listed in Figure 2) signal primarily through the PI3K signaling cascade, signal transducer and activator of transcription proteins (STATs), MAPK pathways, and the nuclear factor- $\kappa$ B inhibitor- $\alpha$  – nuclear factor- $\kappa$ B complex (Birchmeier et al., 2003; Trusolino et al., 2010).

## Amplification of the c-Met Signal

c-Met signal amplification may occur via its interaction with the  $\alpha 6\beta 4$  integrin at the plasma membrane, which acts as an additional docking platform for signaling adapters and transducers (Bertotti et al., 2006). Another protein that intensifies the c-Met signal at the cell surface is the v6 splice variant of CD44, which is a cell adhesion molecule connecting the extracellular matrix to the cellular actin cytoskeleton. The ternary structure produced by the interaction of c-Met, CD44v6 and HGF activates c-Met, which in turn results in the activation of Ras, a MAPK pathway signaling effector (Trusolino et al., 2010). Ligand-independent strengthening of the c-Met signal may also occur through interactions with semaphorin receptors at the plasma membrane, such as is the case with class B plexins and neuropilin (Knutsen and Vande Woude, 2008). Recently it was shown that in non-small cell lung cancer (NSCLC) cases that acquired resistance to EGFR inhibitors, c-Met became amplified and its signal transduced via ERBB3 activation (Engelman et al., 2007). Additionally, c-Met interacts with the RON receptor tyrosine kinase, which it shares a great deal of sequence homology with, and with the EGFR (Gentile et al., 2008), which will be expanded upon later.

The compartmentalization of c-Met signaling on endosomes has gained a lot of attention lately. After c-Met is stimulated by ligand and internalized by clathrin-mediated endocytosis, the c-Met signal sustains ERK activation at peripheral early endosomes. Activated ERK then translocates to cell adhesion sites at the plasma membrane, which is mediated by protein kinase C $\epsilon$ , where cell

migration is initiated (Kermorgant et al., 2004). The delivery of c-Met along microtubules to the perinuclear compartment allows for the rapid activation and translocation of STAT3 into the nucleus (Kermorgant and Parker, 2008), which most likely shields STAT3 from phosphatases that may attenuate its signal (Trusolino et al., 2010). Recently, Joffre and colleagues (2011) showed that active, cancer-specific, c-Met mutants accumulate on endosomes due to enhanced rates of endocytosis and reduced receptor degradation. Additionally, they showed that c-Met aggregation on endosomes activates Rac1, which ultimately leads to increased cell migration. When they blocked endocytosis, which did not affect c-Met activity, tumorigenicity and metastasis were reduced *in vivo*. Therefore, compartmentalization of the c-Met signal may serve to enhance tumorigenicity by temporally spacing preferential signaling partners.

## **The c-Met / HGF axis in GBM**

In normal tissues, HGF that is secreted by mesenchymal cells activates c-Met on epithelial cells in a paracrine manner (Gentile et al., 2008; Moriyama et al., 1998; Wojcik et al., 2006). In cancer (Hung and Elliott, 2001; Hov et al., 2004; Rahimi et al., 1996), including GBM, both receptor and ligand pair are often coexpressed, which establishes a permissive microenvironment for sustained oncogenic signaling through c-Met (Abounader et al., 2005).

In 1997, Nabeshima and colleagues used immunohistochemistry to examine the expression of c-Met across increasing grades of astrocytic tumors.

They found that c-Met protein expression was enhanced in GBM compared with tumors that represented lower grades of glioma. Similarly, HGF protein expression increases with glioma grade (Kunkel et al., 2001).

In total, there have been three studies published that have examined the coexpression of c-Met and HGF in GBM. The first study by George F. Vande Woude's research group (Koochekpour et al., 1997) used double immunofluorescence staining to show that HGF and c-Met expression increased with glioma grade. These authors also found that costaining of c-Met and HGF was present in 13 out of 15 GBMs. Soon after their discovery, Moriyama and colleagues (1998) analyzed HGF and c-Met messenger ribonucleic acid (mRNA) expression in GBMs. They found that their mRNA expression increased with astrocytic tumor grade, and that both c-Met and HGF were coexpressed in 6 of 15 GBMs. A subsequent study analyzed the mRNA expression of HGF and c-Met in a subset of 43 GBM tumors using Affymetrix U133 arrays (Beroukhim et al., 2007). They showed that c-Met and HGF, which are located on chromosome 7 (Beau-Faller et al., 2008), were mostly coexpressed in GBM samples with broad gains of chromosome 7 ( $P < 0.06$ ). Trisomy of chromosome 7 is frequently found (70%) in GBMs (Piccirillo et al., 2009), indicating that this signaling axis plays a pivotal role in this tumor.

Not surprisingly, tumorigenicity was significantly enhanced upon the intracranial implantation of HGF-overexpressing GBM cells into mice (Lattera et al., 1997). This degree of tumorigenicity was reversed through the use of U1snRNA/ribozymes that targeted c-Met or HGF in established GBM xenografts (Abounader et al., 1999; Abounader et al., 2002). Further, other investigators

have shown that inhibition of c-Met's activity in intracranial GBM xenografts impairs tumor growth (Buchanan et al., 2009; Tseng et al., 2008). However, GBM tumors that are not addicted to the c-Met / HGF axis, meaning that these molecules are not highly expressed and signaling, are unresponsive to c-Met inhibition (Martens et al., 2006). These studies have been further expanded to provide evidence that high-level expression of c-Met correlates with a worse survival prognosis for GBM patients, when compared with those GBM patients whose tumors did not express c-Met (Kong et al., 2009).

### **Cross-talk between the EGFR / $\Delta$ EGFR and c-Met Pathways**

A complex relationship exists between EGFR and c-Met signaling, where HGF-mediated c-Met activation increases EGFR ligand expression (TGF- $\alpha$  and HB-EGF), thereby aiding in EGFR dysregulation (Reznik et al., 2008). Once EGFR is activated by TGF- $\alpha$  and HB-EGF, c-Met expression may be stimulated in a HIF-1 $\alpha$  hypoxia-independent manner (Xu et al., 2010).

Although c-Met is primarily activated by its ligand, HGF, the ligand-independent activation of c-Met is emerging as an important contributing factor to aberrant c-Met signaling (Yamamoto et al., 2006). Transactivation of c-Met by the EGFR in cancer cells was first described by Jo and colleagues (2000). They showed that upon EGFR stimulation by TGF- $\alpha$  that c-Met was activated, which could be reversed with TGF- $\alpha$  and EGFR antagonists. Since then, c-Met activation by EGFR has been confirmed in various cancer cell lines (Bergström et

al., 2000; Bonine-Summers et al., 2007; Fischer et al., 2004; Pai et al., 2003), suggesting that the EGFR signals through c-Met. This interaction has been reported to be by direct association (Agarwal et al., 2009), and potentially unidirectional, until a recent study showed that amplified c-Met is capable of transactivating the EGFR (Bachleitner-Hofmann et al., 2008).

By enriching for phosphotyrosine peptides, Huang and colleagues (2007) used mass spectrometry to examine preferential signaling of  $\Delta$ EGFR in U87 GBM cells. They overexpressed titrated levels of  $\Delta$ EGFR in U87, and asked which specific signaling events were most strengthened by the  $\Delta$ EGFR signal. They discovered that Y1234 of c-Met, which is a good indicator of its overall activation (Chiara et al., 2003), was steadily activated with increased expression of  $\Delta$ EGFR. This indicated that c-Met activation was downstream of  $\Delta$ EGFR signaling, and that c-Met activity could be regulated by  $\Delta$ EGFR in GBM cells. Additionally, they found that c-Met inhibition could circumvent  $\Delta$ EGFR-mediated chemoresistance in U87 cells.

Recently, our laboratory examined signaling differences in GBM cells by mass spectrometry after tyrosine enrichment when  $\Delta$ EGFR, kinase-inactive  $\Delta$ EGFR ( $\Delta$ EGFR-ki), or WT EGFR was expressed, and when WT EGFR was stimulated with EGF, which showed that c-Met is a preferential target of the  $\Delta$ EGFR even when compared with EGF-stimulated EGFR (Chumbalkar et al., 2011). c-Met activation was also examined in U87 xenografts expressing either WT EGFR,  $\Delta$ EGFR, or  $\Delta$ EGFR-ki, where it was found that c-Met activation was enhanced in those tumors expressing  $\Delta$ EGFR (Chumbalkar et al., 2011). Another group suggested that the kinase activity of  $\Delta$ EGFR, and not autophosphorylation,

is necessary to coactivate c-Met in a ligand-independent manner in GBM cells (Pillay et al., 2009). Furthermore, their finding that when using EGFR and HGF antagonists in combination to treat  $\Delta$ EGFR-expressing c-Met-/HGF-dependent GBM xenografts that a significant reduction in tumor growth would occur compared with either agent alone, suggests the clinical potential of combination therapy (Pillay et al., 2009).

## **Regulation of c-Met and HGF Expression**

Aside from chromosome 7 trisomy (Beroukhi et al., 2007), mechanisms governing aberrant HGF regulation in GBM have not yet been identified. Functional studies in other cancer cell lines have highlighted the importance of the transcriptional induction of the HGF gene as a major cause of dysregulated autocrine HGF circuitry (Hung and Elliott, 2001; Wojcik et al., 2006). HGF gene transcription in human cells has been shown to be regulated in the proximal promoter at a Stat3-binding element (-99/-91; TTACCGTAA) (Tomida and Saito, 2004). Similarly, in mouse mammary carcinoma cells a -95 STAT3 consensus site in the HGF gene was linked to aberrant HGF expression, which promoted transformation (Wojcik et al., 2006). STAT3 signaling is required for the maintenance of the aggressive mesenchymal phenotype in GBM, and its expression (Carro et al., 2010) or activity (Birner et al., 2010) is a negative prognostic factor for GBM patients. More than 90% of GBM tumors have elevated STAT3 activity (Rahaman et al., 2002), which has been found to be imperative for

c-Met / HGF-mediated anchorage-independent growth and tumorigenicity *in vivo* (Zhang et al., 2002). c-Met is capable of activating STAT3 directly or indirectly (Birchmeier et al., 2003), and once activated, it homodimerizes, or heterodimerizes with other STAT family members, and translocates to the nucleus where it controls gene expression by binding to promoter elements (Song et al., 2003).

In the 5' flanking region of the mouse HGF promoter, a Sp1 binding site (-318 to -303) binds Sp1 and Sp3 transcription factors to regulate HGF expression (Jiang et al., 1997). Later, p53 was also found to regulate the mouse HGF promoter (Seol et al., 1999). HGF may also be regulated in the basal promoter region (-4 to +3 from the transcription start site) by CCAAT/ enhancer-binding protein  $\beta$  (C/EBP $\beta$ ) / C/EBP $\zeta$ . Binding of C/EBP $\beta$  to the HGF promoter could be induced by the action of several cytokines, such as IL6, IL-1, TNF- $\alpha$ , and TGF- $\alpha$ . Later, Jiang and colleagues (2001) also found that the mouse HGF promoter bound ligand-activated peroxisome proliferator-activated receptor  $\gamma$  at -246 to -233 bp upstream from the HGF gene's transcription start site.

c-Met overexpression in GBM occurs through amplification (4-20%; Mueller et al., 1997; The Cancer Genome Atlas Research Network, 2008), rare missense mutations (Moon et al., 2000), upregulation of its transcriptional activity (Abounader and Lattera, 2009; Kong et al., 2009), chromosome 7 trisomy (Beroukhi et al., 2007), and through HGF-mediated activation of the c-Met receptor (Abounader et al., 2001). c-Met stimulation by HGF not only induces the expression of c-Met in GBM cells, but it also does so in lung adenocarcinoma cells (Boccaccio et al., 1994). Since positive regulatory loops have also been described



for other receptors and their ligands (Caolo et al., 2010; Chen et al., 2010; Clark et al., 1985; Reem et al., 1984), we hypothesized that the enhanced levels of autocrine HGF expression in GBM may additionally hinge on the action of c-Met.

## **CHAPTER 2**

### **MATERIALS AND METHODS**

## Cell Culture

The U87MG and LN18 human GBM cells were originally obtained from the American Type Culture Collection, and cultured in Dulbecco's modified Eagle's medium (DMEM) supplemented with 10% fetal bovine serum (FBS), 2 mM glutamine, 100 U/mL penicillin, and 100 mg/mL streptomycin. GBM cell lines were cultured under normal growth conditions; 7% CO<sub>2</sub> and 37°C in a humidified incubator. Dr. Zhimin Lu (The University of Texas M. D. Anderson Cancer Center) generously provided us with Madin-Darby Canine Kidney (MDCK) cells. Human Embryonic Kidney 293FT cells were a kind gift from Dr. Howard Colman (The University of Utah). These cells were cultured under normal conditions in a humidified chamber that delivered 5% CO<sub>2</sub> at 37°C. To establish identity, U87 and LN18 GBM cells were DNA fingerprinted using a polymerase chain reaction (PCR)-based approach (GenomeLab Human Short Tandem Repeat Primer set from Beckman Coulter) (Table 1).

Locus	U87		LN18	
	1	2	1	2
AMEL	105.92	0	110.96	105.81
D3s 1358	134.41	130.52	130.80	126.97
TH01	177.34	0	174.95	0
D13s 317	188.58	176.81	197.34	193.23
D8s 1179	217.23	213.18	230.40	222.22
D7s 820	225.18	221.12	222.03	0
TPOX	268.73	0	269.68	0
D16s 539	294.75	0	300.33	291.74
D18s 51	306.12	0	330.76	322.77
CSF1PO	341.37	337.10	346.35	0

**Table 1.** Short tandem repeat fingerprinting of GBM cells. U87 and LN18 cells were analyzed for their specific marker allele content for comparative purposes and identification.

## **Antibodies**

The following primary antibodies were purchased from Cell Signaling and used at the indicated final concentration: anti-c-Met (1:1000), anti-pc-Met (Y1234/Y1235) (1:1000); anti-EGFR (1:1250), anti-pEGFR (Y1173) (1:1000), anti-STAT3 (1:1000), and anti-pSTAT3 (Y705) (1:1000). We obtained the anti-HGF primary antibody from R&D Systems; it was diluted to a final concentration of 1:1000 for western blot (WB) analysis. For actin detection on western blots, we used an anti- $\beta$ -actin conjugated to horseradish peroxidase (1:50000) that was purchased from Sigma. Secondary antibodies that were used were as follows: anti-mouse secondary antibody (1:3000; Fisher Scientific); anti-rabbit secondary antibody (1:20000; Jackson ImmunoResearch Laboratories); and an anti-goat secondary antibody (1:3000; Santa Cruz). For HGF neutralization experiments, we used the HGF primary antibody at a final concentration of 0.6  $\mu$ g/ml.

## **Reagents**

The recombinant human HGF that was used in our studies was obtained from Chemicon. The c-Met kinase inhibitor, SU11274, and the EGFR kinase inhibitor, AG1478, were purchased from Calbiochem. Actinomycin D was obtained from Sigma-Aldrich. Hygromycin B, G418, and puromycin were obtained from Fischer Scientific. WP1193 was a generous gift from Dr. Waldemar Priebe (The University of Texas M. D. Anderson Cancer Center).

## **shRNA Infection of GBM Cells**

HEK 293FT cells were cultured to 50% confluence in 10 cm plates and transfected with short hairpin ribonucleic acids (shRNAs) targeting c-Met (1  $\mu$ g; pLKO.1 backbone; Open Biosystems) or a non-targeting scrambled shRNA (1  $\mu$ g; pLKO.1 backbone, Addgene number 1864), and pCMV-dR8.2 dvpr (0.9  $\mu$ g; Addgene number 8455), and pCMV-VSVG (0.1  $\mu$ g; (Addgene number 8454) (kindly shared by Dr. Ta-Jen Liu, U.T. MD Anderson Cancer Center), with 6  $\mu$ L Eugene HD (Roche), according to the manufacturer's instructions. After 48 h, the viral supernatant was filter sterilized through a 0.45  $\mu$ m syringe filter, and either stored at -80° or applied to 50% confluent U87 GBM cells after the addition of hexadimethrine bromide (8  $\mu$ g/mL). After 3 h of infection, viral supernatant was removed and fresh media added to the cells. After 48 h, cells were split and selected with puromycin (1  $\mu$ g/mL) for 6 days. Cloning by limiting dilution was performed to obtain clonal populations of U87 sh-c-Met clones. Details of the c-Met shRNA pLKO.1 hairpin sequences may be found in Table 2.

<i>Open Biosystems # Label</i>	<i>Strand</i>	<i>Sequence</i>	<i>Accession#</i>
TRCN0000009850	sense	5'-CAGAATGTCATTCTACATGAG-3'	NM_001127500.1
sh-c-Met #A	antisense	5'-CTCATGTAGAATGACATTCTG-3'	NM_001127500.1
TRCN0000040047	sense	5'-GCCAGCCTGAATGATGACATT-3'	NM_001127500.1
Sh-c-Met #B	antisense	5'-AATGTCATCATTGAGGCTGGC-3'	NM_001127500.1

**Table 2.** pLKO.1 c-Met shRNA targeting constructs. Sequence and sequence identifying information of the c-Met shRNA targeting sequences.

## Generation of Kinase-deficient c-Met Plasmids

An internal 2kb fragment was restricted out of pMSCV-wt c-Met (a generous gift from Dr. Lisa Elferink, UTMB) with Apa1, and the Apa1 ends of the pMSCV-wt c-Met plasmid ligated to generate a pMSCV-wt c-Met ( $\Delta$ Apa1) plasmid. QuickChange site-directed mutagenesis (Stratagene) was performed to create the pMSCV-c-Met Y1234 ( $\Delta$ Apa1) and pMSCV-c-Met Y1235 ( $\Delta$ Apa1) mutants; primers that were used are listed in Table 3. Next, the gel-purified internal 2kb fragment (generated as previously described) was ligated into the pMSCV-c-Met Y1234 ( $\Delta$ Apa1) and pMSCV-c-Met Y1235 ( $\Delta$ Apa1) mutant expression vectors that had been restricted with Apa1 to generate the pMSCV-c-Met Y1234 and pMSCV-c-Met Y1235 plasmids.

<i>Mutation</i>	<i>Strand</i>	<i>Sequence</i>	<i>Accession#</i>
<b>c-Met Y1234F</b>	sense	5'-GAGACATGTATGATAAAGAATTCTAT AGTGTACACAACAAAAC-3'	NM_001127500.1
	antisense	5'-GTTTTGTTGTGTACACTATAGAATTC TTTATCATACATGTCTC-3'	NM_001127500.1
<b>c-Met Y1235F</b>	sense	5'- CATGTATGATAAAGAATACTTTAGTGT ACACAACAAAACAGG-3'	NM_001127500.1
	antisense	5'- CCTGTTTTGTTGTGTACACTAAAGTAT TCTTTATCATACATG-3'	NM_001127500.1

**Table 3.** Primers used to generate kinase-deficient c-Met mutants.

## Transfection and Retroviral Infection

A constitutively active STAT3 (STAT3-CA) in a pcDNA3.1/Hygro(+) vector was kindly provided by Dr. Robert Arceci (Johns Hopkins, Baltimore, MD, USA) (Ning et al., 2001). The constitutively active STAT3 contains Cys substitutions at Ala662 and Asn664 (Bromberg et al., 1999). The pcDNA3.1/Hygro(+) empty vector was a generous gift from Dr. Suyun Huang (MD Anderson Cancer Center). STAT3-CA and empty vector were transfected into 50% confluent U87-ΔEGFR cells using Fugene HD (Roche), according to the manufacturer's instructions. After 48 h, the cells were split and selected using 50 µg/mL Hygromycin B.

10 µg pLRNL-ΔEGFR (a generous gift from Dr. H-J Huang, UCSD), pMSCV-puro empty vector, pMSCV-wt c-Met, pMSCV-c-Met P991S, pMSCV-c-Met Y1003 (c-Met plasmids were kind gifts from Dr. Lisa Elferink, UTMB), pMSCV-c-Met Y1234, and pMSCV-c-Met Y1235 was packaged into viral particles

using 50% confluent GP2 cells, pCMV-VSVG (10 µg) and Lipofectamine 2000, according to the manufacturer's instructions (Invitrogen). After 48 hrs, viral supernatant was collected and sterilized through a 0.45 µm filter syringe. Viral supernatant was stored at -80°C for future use, or used to infect either 50% confluent U87 or U87  $\Delta$ EGFR GBM cells in T25 flasks using 0.8 µg/mL hexadimethrine bromide. After 3 h, the viral supernatant was removed and complete media added to the cells. When the dishes were confluent, the cells were split and selected using G418 (200 µg/mL) or puromycin (1 µg/mL) according to the selection marker present on the expression plasmid.

## **Cell Lysate Preparation and Western Blotting**

For most western blot analyses, cells were cultured in 10% serum prior to collection. For all immunoprecipitation experiments, cells were cultured in serum-free conditions for 20 h. Cells were then either collected, washed with phosphate buffered saline (PBS), and then scraped into ice-cold PBS. Pellets were gently resuspended in RadiolImmunoPrecipitation (RIPA) lysis buffer (50mM Tris HCl pH 7.4, 150 mM NaCl, 1% NP-40, 0.5% sodium Deoxycholate, 0.1% SDS) that contained phosphatase inhibitors (Sigma-Aldrich Cocktail Inhibitors I and II) and SigmaFAST protease inhibitor cocktail (Sigma-Aldrich), and then passed through a 21-gauge needle 10 times. Lysis proceeded on ice for 30 min before the supernatant was clarified from the cellular debris by centrifugation. Protein concentration was estimated colorimetrically using the Pierce BCA Protein Assay



Kit (Thermo Scientific), and lysates were stored at -20°C until further analysis. For western blot analysis, 20/30 µg protein was separated on 4-12% Bis-Tris NuPage gels (Invitrogen), except for HGF analysis where 150 µg of protein lysate was used.

## **Immunoprecipitation Assays**

Total lysates were incubated with primary antibodies overnight with gentle rocking at 4°C. For the c-Met immunoprecipitation assay, an anti-c-Met antibody from R&D Systems was used. Subsequently, Protein G PLUS-Agarose beads from Santa Cruz bound the complexes. The beads were washed thrice using RIPA buffer, and then washed twice with ice-cold PBS. Immunoprecipitated proteins (500 µg) were resolved on 4-12% Bis-Tris NuPage gels, and analyzed using immunoblotting/western techniques that have been described.

## **RNA Extraction and Quantitative Real-time PCR**

All cells were cultured in complete media in 10-cm diameter dishes until they reached 80% confluence. All cells were cultured under normal conditions. Cells were washed twice with PBS and scraped into ice-cold PBS. mRNA was extracted from the cell pellets using Qiagen's RNeasy Mini Kit, and quantified using a NanoDrop 2000 instrument. Reverse transcription was performed with

Bio-Rad's iScript cDNA Synthesis Kit. For the quantitative detection of transcripts, quantitative real-time PCR (qRT-PCR) was performed using FastStart SYBR Green Master reagent (Roche) with the primers that are detailed in Table 4. Samples were analyzed in duplicate/triplicate and normalized to an internal  $\beta$ -2-microglobulin control. All experiments were repeated three times.

<i>Primer</i>	<i>Strand</i>	<i>Sequence</i>	<i>Accession#</i>
<b>HGF</b>	sense	5'-CTCACACCCGCTGGGAGTAC-3'	NM_000601.4
	antisense	5'-TCCTTGACCTTGGATGCATTC-3'	NM_000601.4
<b>BCL-XL</b>	sense	5'-GATCCCCATGGCAGCAGTAAAGCAAG-3'	NM_138578.1
	antisense	5'-CCCCATCCCGGAAGAGTTCATTCAC-3'	NM_138578.1
<b><math>\beta</math>-2-Microglobulin</b>	sense	5'-ATCCATCCGACATTGAAGTT-3'	NM_004048.2
	antisense	5'-GGCAGGCATACTCATCTTTT-3'	NM_004048.2

**Table 4.** qRT-PCR primer sequences. Sequence of primers used in qRT-PCR experiments.

## ELISA

Cells were cultured in T225 flasks until they reached 80% confluence, washed twice in PBS, and cultured for 24 h in 40 mLs of serum-free media. Conditioned media (CM) from duplicate samples were pooled, centrifuged for

debris removal, and stored at -80°C until further analysis. Samples were concentrated using an Amicon concentrator using a regenerated cellulose ultrafiltration membrane with a 30,000 molecular weight cut off (Millipore). A 96-well Nunc MaxiSorp plate was coated with 0.5 µg/mL mouse anti-human HGF monoclonal antibody (R&D Systems) or isotype control antibody diluted in PBS. Following an overnight incubation at room temperature (RT), wells were washed in PBS containing 0.05% Tween 20 (PBST), blocked for 1 hour at RT in 50mM Tris pH 8.0 containing 0.14 M NaCl, 1% BSA, and 0.05% Tween 20, and then washed with PBST. The concentrated samples, and a HGF standard, were serially diluted in Tris-buffered saline containing 0.1% BSA and 0.05% Tween 20 (pH 7.3), and then 100µL of each sample was applied to wells of the plate. Additionally, in order to control for background noise of the assay, a media only control was added to three wells of the plate. Following an overnight incubation at 4°C, wells were washed with PBST, and incubated for 2 hr at room temperature with 100 µL goat anti-human HGF polyclonal antibody (0.5 µg/mL; R&D Systems). After washing with PBST, 100 µL of HRP-conjugated bovine anti-goat IgG (40 ng/mL; Jackson ImmunoResearch Laboratories Inc.) was added per well, and incubated for 1 hr at RT. Non-bound antibody was removed by washing with PBST. For the detection of HGF, QuantaBlu™ Fluorogenic Peroxidase Substrate (Thermo Fisher Scientific) was prepared according to the manufacturer's instructions, and 100 µL added per well. The reaction was terminated after 30 min using QuantaBlu™ Stop Solution (Thermo Fisher Scientific), and the fluorescence (Ex325/Em420) measured using a SpectraMax Gemini (Molecular Probes)

fluorescent plate reader having SOFTmax Pro (v. 3.0) software. HGF ELISAs were performed twice.

## **Luciferase Assays**

The human HGF promoter construct pGL2-HGF-1029 was a kind gift from Dr. Tomida, Saitama Cancer Center, Japan (Tomida and Saito, 2004). The 1029bp sequence of the 5'-flanking region of the HGF gene was cloned into XhoI/HindIII sites of the luciferase reporter plasmid pGL2-basic (Promega).

Cells were plated in six-well plates ( $1 \times 10^5$ ) the day before transfection. Fugene HD was used to transfect the HGF luciferase promoter constructs (1  $\mu$ g/well), or the pGL2 empty vector (1  $\mu$ g/well), along with the pSV- $\beta$ -Galactosidase Control Vector (10 ng), using 3  $\mu$ L Fugene HD (Roche) per well. After 48 h, lysates were prepared with the lysis buffer present in the Dual-Glo Luciferase Assay System (Promega) and analyzed for their luciferase activity according to the manufacturer's instructions.  $\beta$ -galactosidase activity (Beta-Glo Assay System; Promega) was also measured in the lysates with a luminometer according to the manufacturer's instructions. Transfection efficiency for each sample was normalized by calculating the luciferase activity to that of  $\beta$ -galactosidase activity. A mean relative value was then calculated.

## **Anchorage-independent Growth Assays**

For colony formation, U87, U87 sh-c-Met #A2, U87 sh-c-Met #B2, U87 sh-control  $\Delta$ EGFR, U87 sh-c-Met #A2  $\Delta$ EGFR, and U87 sh-c-Met #B2  $\Delta$ EGFR cells were seeded at  $7.5 \times 10^2$  cells / well in media containing 0.5% low-melting Agarose on a 0.7% low-melting agarose base in 24-well plates. U87 sh-control pcDNA3.1, U87 sh-control STAT3-CA, U87 sh-c-Met #B2 pcDNA3.1, and U87 sh-c-Met #B2 STAT3-CA cells were plated at  $1.5 \times 10^3$  cells / well in 12-well plates. After 1 h, 0.25 mL of media was added to wells of the 24-well plates, and 0.5 mL of media was added per well to the 12-well plates. Another aliquot of media was added to wells of the plates after 7 days in culture. Cells were cultured at 37°C in a humidified chamber receiving 7% CO<sub>2</sub>. Colony numbers were counted after 14 days in culture using GelCount's software and scanner. Additional experimental details have been previously described (Kajiwara et al., 2008).

## **WST-1 Assays**

$7.5 \times 10^2$  cells were plated per well of a 96-well plate in triplicate and cultured for 72 h at 37°C in a humidified chamber set to deliver 7% CO<sub>2</sub>. The WST-1 assay was performed according to the manufacturer's specifications (Roche).

## **Intracranial Xenograft Studies**

8-12 wk old nude (nu/nu) mice were stereotactically injected with  $2 \times 10^5$  cells in 5  $\mu$ L PBS into the right frontal lobe. Mice were maintained at The University of Texas MD Anderson Cancer Center's Isolation Facility. Mice were euthanized when they started to show symptoms of neurological damage from the tumor burden, including but not limited to seizures, lethargy and paralysis. All animal experiments were performed on the same day. The maintenance and care of mice were conducted in accordance with Laboratory Animal Resources Commission standards under an approved protocol (100712131).

## **Mass Spectrometry**

Cells were grown in large 15cm-diameter cell culture dishes to 80% confluence and then serum-starved for 24 h. Proteins from two biological replicates were extracted from the cells using urea lysis buffer (20 mM HEPES pH 8.0, 9 M urea, 1 mM sodium orthovanadate, 2.5 mM sodium pyrophosphate, 1 mM  $\beta$ -glycerophosphate). After 10 minutes on ice, cells were sonicated using 3 pulses at 30 seconds each, with 2 minutes incubation on ice between pulses. After centrifugation at 20 000g for 20 min, lysates were reduced with 4.5mM dithiothreitol for 20 min at 60°C. Samples were then alkylated in the dark at room temperature for 15 min using carboxo-amidomethylation that contained 10 mM iodoacetamide. Lysates were tryptically digested overnight at room temperature in

a solution of HEPES and trypsin TPCK solution (Worthington Biochemical) to final concentrations of 20 mM and 10 µg/mL, respectively. Peptides were then desalted with Sep-Pak C18 columns (Waters Corp) and freeze-dried. Peptides were resuspended in an Immunnoaffinity Purification (IAP) buffer (50mM MOPS, pH 7.2, 10 mM sodium phosphate, 50 mM NaCl), prior to the addition of P-Tyr-100 mouse monoclonal antibody beads (Cell Signaling). Samples were rotated at 4°C overnight, and the beads washed thrice with IAP buffer and water. Trifluoroacetic acid (0.15%; TFA) was used to elute the bound peptides, which were then further purified using ZipTip C18 (Millipore Corp).

After the peptides had been resuspended in acetonitrile (3%) containing 0.1% TFA, they were loaded onto Protein ID #2 chip (Agilent; 40 nL enrichment column, 75 µm x 150 mm analytical column). LC-MS/MS analysis was performed in duplicate with Agilent's 6340 Ion trap System with electron transfer dissociation (ETD) capability, where fragmentation alternated between collision induced dissociation and ETD modes. Four peptides were chosen per scan that had at least a double charge. Two biological repeats were performed. For specific run conditions, we followed the protocol of Chumbalkar et al., 2011.

## **Peptide Identification and Quantification**

Initially the MS/MS spectra were extracted using Bruker CompassXport (<http://www.bruker.com>) which created \*.mzxml files, which were later converted

to \*.mgf files using Trans-Proteomic Pipeline (Seattle Proteome Center; <http://www.proteomecenter.org/software.php>). Database searches of the human subset of Swiss-Prot database's proteins was performed using Mascot search engine version 2.3.02 (<http://www.matrixscience.com>). Manual inspection of the spectra was performed to assign phosphorylation sites. Based on retention time, Ideal-Q (Tsou et al., 2010) software aligned the runs. Next, the peak areas were calculated manually for all identified phosphopeptides, and the data normalized to the run's total ion current. Then we calculated individual mean peak areas for the phosphopeptides. For more detailed information, we followed the protocol of Chumbalkar et al., 2011.

## **TCGA Analysis**

Level 3 gene expression data (Agilent 244K Custom Gene Expression chip platform; AgilentG4502A\_07) was downloaded from the TCGA Data Portal (<http://tcga-data.nci.nih.gov/tcga/tcgaHome2.jsp>) on 07/15/11 to examine HGF and c-Met mRNA expression in 495 GBMs. The downloaded data was represented as  $\log_{10}$  ratios to Universal Human Reference RNA (Stratagene). Spearman correlation (two-tailed, 95% CI) calculated the Spearman correlation coefficient between c-Met and HGF expression in GBM. For GBM subtype determination, 'Verhaak determined' data made use of the subtype calls that can be found in the supplementary data from Verhaak et al., 2010. For 'Calculated Verhaak' or 'Calculated Phillips' datasets, we downloaded the gene lists that were



defined by the authors for the various GBM subtypes (Phillips et al., 2006; Verhaak et al., 2010). For each tumor, expression values for genes that defined each GBM subclass were averaged to derive a metagene score per each of the four Verhaak GBM subtypes (mesenchymal, proneural, neural, and classical), and for each of the three Phillips GBM subtypes (mesenchymal, proliferative, and proneural). Metagene scores were converted to z-scores (assume metagene score normal distribution, and set all scores to mean = 0 and standard deviation = 1) so that metagene scores could be compared. A GBM subtype was then assigned to a tumor based on the metagene score with the highest value. The use of metagenes in statistics has previously been described by Colman et al., 2010.

Data validity was verified in an independent gene expression data set (n=180) from the REpository for Molecular BRAin Neoplasia DaTa (REMBRANDT; <http://caintegrator-info.nci.nih.gov/rembrandt>) that used the Human Genome U133 Plus 2.0 Array; gene expression data normalized to pooled normal brain expression. Data were processed using a robust multiarray average (RMA) algorithm with quantile normalization, using R (R Development Core Team, 2009) and Bioconductor (Gentleman et al., 2004) and a custom CDF (Sandberg and Larsson, 2007). GBM subtype calls were performed as was previously described in the 'Calculated Verhaak' method.

## **Statistical Analysis**

GraphPad Prism 5.03 software was used to determine significance of most experiments. Specific statistical tests are described in the figure legends. All t-tests and the Spearman correlation test were two-tailed.

## **CHAPTER 3**

### **RESULTS**

#### **C-MET MODULATES HGF EXPRESSION, COLONY FORMATION, AND TUMORIGENICITY OF GBM CELLS**

## **Coexpression of c-Met and HGF in GBM**

There have been reports that c-Met and HGF mRNA are often coexpressed in GBM (Beroukhim et al., 2007; Moriyama et al., 1998), prompting us to analyze the wealth of new data now available in the TCGA database. The TCGA database (<http://tcga-data.nci.nih.gov/tcga/findArchives.htm>) was established to generate a comprehensive archive of various genetic aberrations that occur in cancer, with their initial focus on GBM (Verhaak et al., 2010). The TCGA database catalogs DNA, mRNA, microRNA and DNA methylation profiles of GBM tumors (Sulman and Aldape, 2011; The Cancer Genome Atlas Research Network, 2008). We analyzed the coexpression of c-Met and HGF in the TCGA expression data using the Agilent (level 3; processed) platform. In total 495 GBM tumors were analyzed for their c-Met and HGF expression. We found that c-Met and HGF mRNA expression correlated significantly in GBM (Figure 4; Spearman correlation;  $r = 0.5199$ ,  $P < 0.0001$ ), suggesting that the two proteins are coregulated.

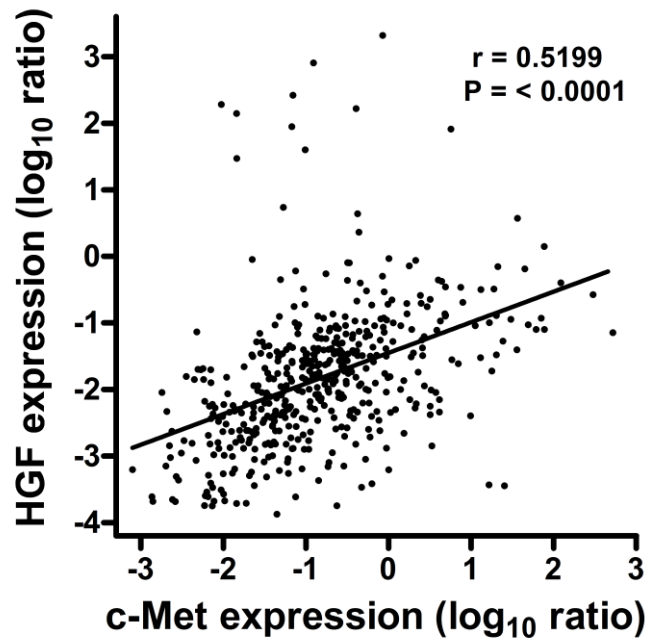


**Figure 4.** HGF and c-Met mRNA expression correlates in GBM. TCGA mRNA expression data for HGF and c-Met were correlated in 495 GBM tumors using Spearman correlation ( $r = 0.5199$ ;  $P < 0.0001$ ; linear regression is shown; TCGA level 3 expression data for the Agilent platform was downloaded as log<sub>10</sub> ratios to Universal Human Reference RNA; Dr. Brian Vaillant, Dr. Howard Colman's former post-doctoral fellow, performed this analysis).

### **c-Met Modulates HGF Expression**

c-Met and HGF are both located on the same arm of chromosome 7 (7q31 and 7q21, respectively; Beau-Faller et al., 2008). Even though trisomy of chromosome 7 is a frequent occurrence in GBM (Lopez-Gines et al., 2005; Piccirillo et al., 2009), our data shows a broad dynamic range of expression for HGF and c-Met that is not easily accounted for by the addition of a single gene copy. One possible mechanism that may explain their coordinated regulation may

be due to the formation of a positive regulatory loop. It has been shown previously that c-Met's expression can be induced by HGF stimulation (8 h) in GBM cells (Abounader et al., 2001). We therefore hypothesized that HGF expression may positively be modulated by its own receptor.

Immortalized human cancer cells have been used for many decades as useful biological tools with which to expand our knowledge of cancer biology. Certain tumor cells are largely reliant on specific oncogenes that they express for the generation of prosurvival signals (Pillay et al., 2009). Cell lines that coexpress HGF and c-Met are considered c-Met-dependent cell lines (Beroukhim et al., 2007), and are dependent on this signaling axis for proliferation and survival (Martens et al., 2006; Pillay et al., 2009). U87 is one such c-Met-dependent GBM cell line (Pillay et al., 2009). Therefore, we confirmed that c-Met could be acutely activated by recombinant human HGF (rhHGF) in U87 cells (Figure 5), and that HGF was being secreted by this cell line (Figure 6). c-Met was activated (Y1234/Y1235) within 5 minutes of HGF stimulation in U87 cells, with strongest activity seen between 15 and 45 minutes of treatment (Figure 5). AKT phosphorylation at S473 was used to assess PI3K pathway activation, which occurred within 30 minutes of HGF stimulation.

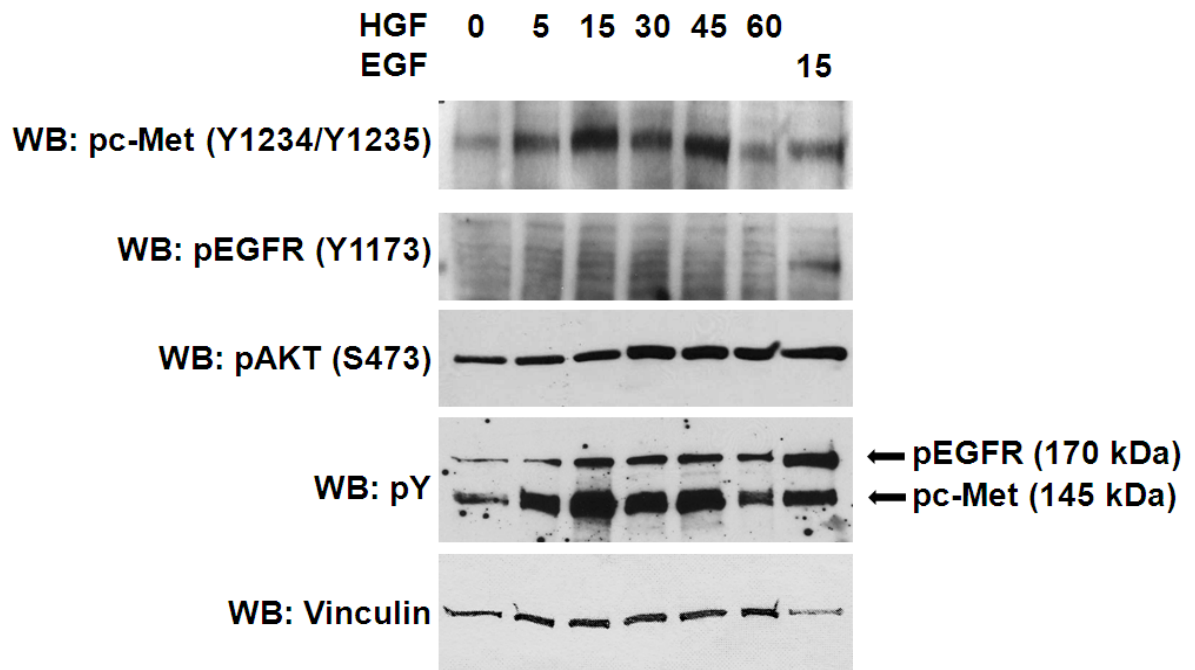


**Figure 5.** c-Met is acutely activated by HGF in U87 cells. Western blots measured c-Met activation (Y1234/Y1235), and p-AKT (S473), via HGF stimulation (50 ng/mL) of U87 cells for the indicated amounts of time. EGF stimulation (10 ng/mL) of U87 cells was used as a positive control. Vinculin was used as a loading control.

Using ELISA, we did not detect HGF secretion from U251, a GBM cell line known not to produce HGF (Beroukhi et al., 2007). Conversely, HGF secretion was detected in conditioned media from U87 cells (Figure 6).

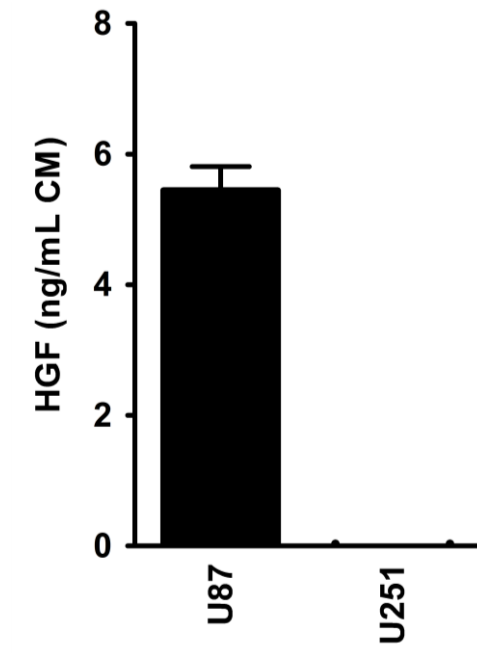


**Figure 6.** HGF is secreted by U87 cells. ELISA quantification of HGF in CM from U87 and U251 GBM cells. Cells were cultured in serum-free conditions for 24 h (triplicate serial dilutions analyzed above background; Dr. Kristen Hill, Dr. Lisa Elferink's former graduate student, UTMB, performed the analysis).

Based on these findings we used the U87 cell line to investigate the effect of c-Met abrogation on the expression of HGF. We stably expressed lentiviral short hairpin RNA (shRNA) constructs that targeted c-Met in U87 cells, and established clonal populations from the two most effective shRNA constructs by limiting dilution (data not shown). As measured by quantitative RT-PCR (qRT-PCR), knockdown of c-Met decreased HGF expression at the mRNA level in U87 cells (Figure 7).



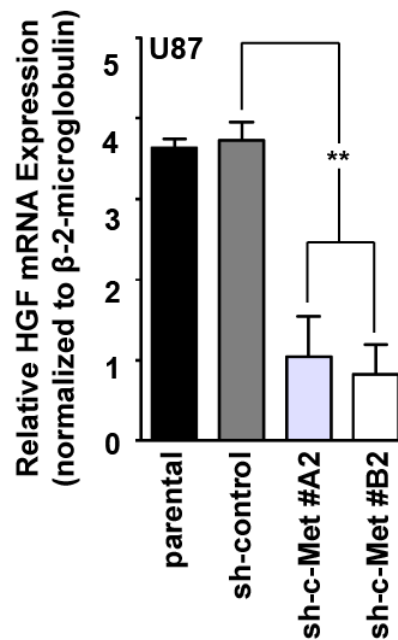


**Figure 7.** HGF mRNA expression is dependent on c-Met expression. qRT-PCR analysis of HGF mRNA expression in clonal populations of U87 cells that expressed different c-Met shRNA targeting constructs. Cells were cultured in media containing 10% FBS (\*\* =  $P < 0.01$ ; Student's t-test compared with sh-control;  $n = 3 \pm \text{SEM}$ ; samples were analyzed at least in duplicate per experiment).

mRNA levels are not necessarily comparable to protein amounts within a cell, therefore it was important for us to investigate what effect c-Met silencing would have on HGF protein levels. We examined U87 c-Met knockdown cells using western blotting techniques and confirmed that HGF protein levels decreased with c-Met knockdown (Figure 8).

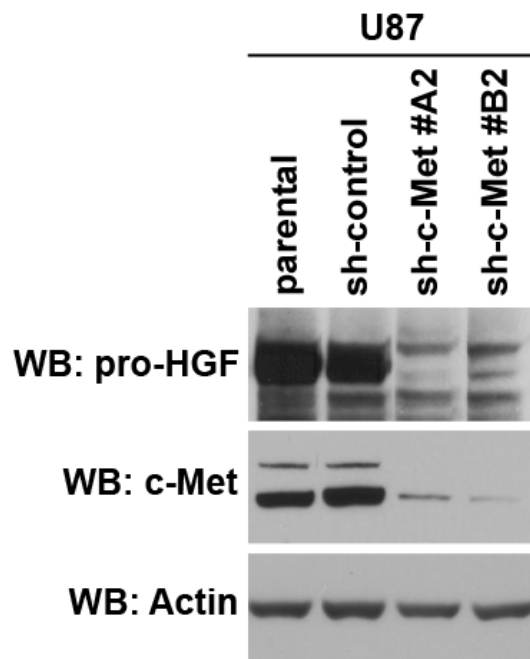


**Figure 8.** HGF protein expression is dependent on c-Met expression. Western blot analysis of HGF protein expression in clonal populations of U87 cells that expressed different c-Met shRNA targeting constructs. Protein lysates were obtained from cells that were cultured in media containing 10% FBS.

Given that HGF is a secreted protein that binds and activates the c-Met receptor at the cell surface, we performed Enzyme-linked Immunosorbent Assays (ELISAs) to analyze HGF amounts that were secreted into the CM from U87 cells with c-Met knockdown. We found that HGF secretion was attenuated by c-Met knockdown in U87 cells (Figure 9A). Western blot analysis revealed that levels of secreted HGF were not proportional to the degree of c-Met knockdown (Figure 9B). This suggested that threshold levels of c-Met expression may modulate the expression of HGF in this cell line. Cumulatively, our data revealed that the

expression of c-Met is an important component necessary for the production and secretion of HGF in U87 GBM cells.

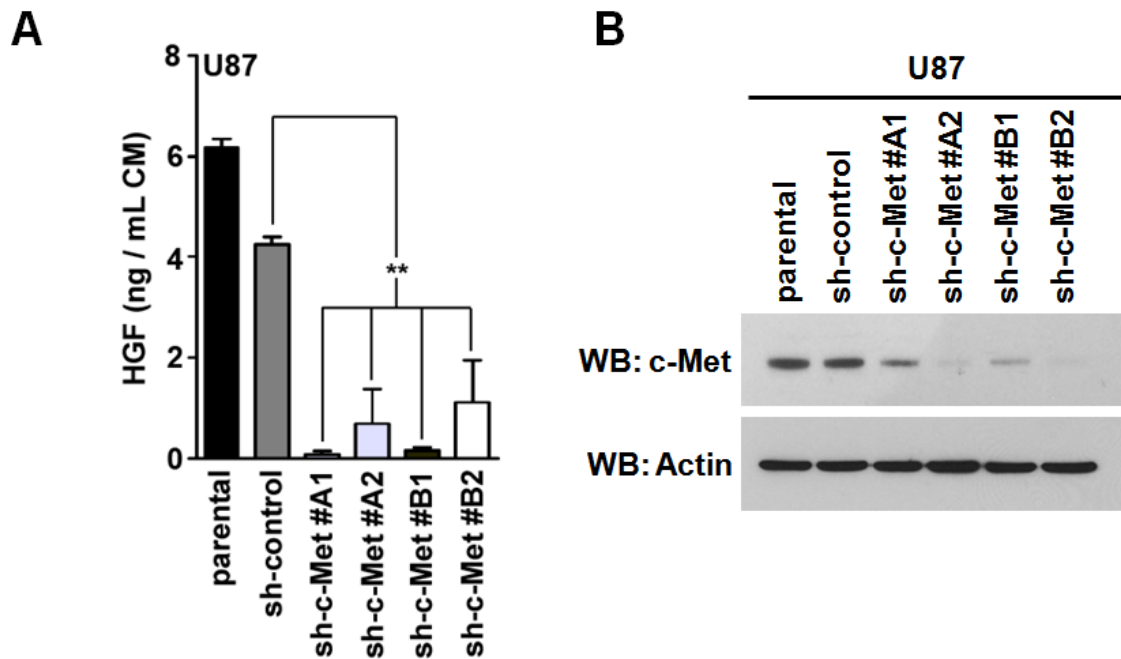


**Figure 9.** HGF secretion decreases with c-Met knockdown in U87 cells. (A) ELISA quantification of HGF in CM from U87 sh-c-Met knockdown clones that represent two different shRNA targeting sequences, A and B (\*\* =  $P < 0.01$ ; one-way ANOVA compared with U87 sh-control cells; Dunnett's multiple comparison test; triplicate serial dilutions above background analyzed per experiment;  $n = 2$ ; Dr. Kristen Hill, Dr. Lisa Elferink's former graduate student, UTMB, performed these analyses). Cells were cultured in serum-free conditions. (B) Western analysis showing c-Met knockdown in cell lines that were represented in A. Cells were cultured in media containing 10% FBS.

Interestingly, using bright field microscopy we observed that the cellular morphology of U87 cells changed with silencing of c-Met (Figure 10). The U87

parental or sh-control cells had the appearance of being scattered, spindle-shaped, mesenchymal-like cells, whereas the U87 cells with c-Met knockdown appeared epithelial-like with loss of the scattering phenotype. HGF, also known as scatter factor (Birchmeier et al., 2003), typically leads to the dissociation and dispersion of epithelial cells (Maulik et al., 2002). Given our data showing that the expression of HGF, or scatter factor, is lost with c-Met knockdown (Figures 7-9), it is tempting to speculate that the altered morphology observed with c-Met knockdown may in part be due to decreased HGF expression in these cells.

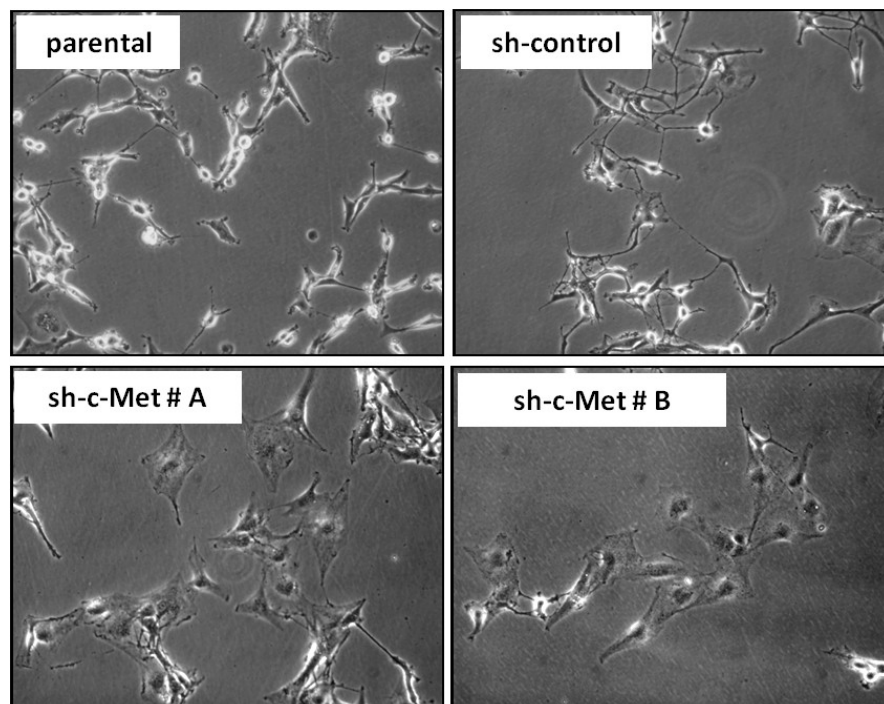
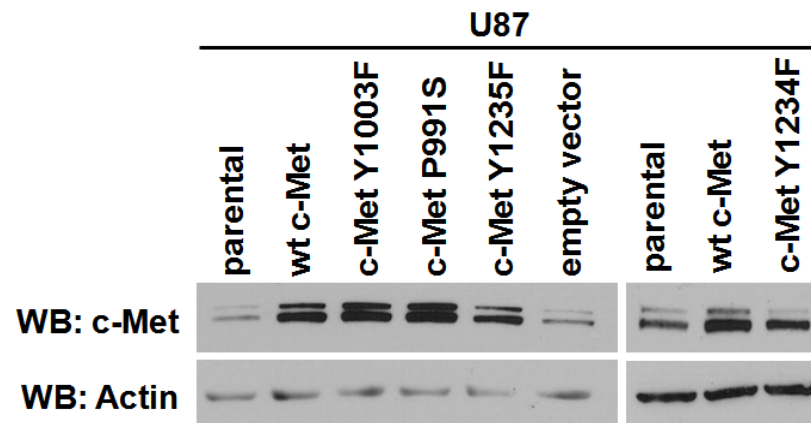


**Figure 10.** Cellular morphology changes with c-Met knockdown in U87 cells. Bright field microscopy of U87, U87 sh-control, U87 sh-c-Met #A and U87 sh-c-Met #B polyclonal populations.

We next examined whether the kinase function of c-Met was important for this phenotypic change. We generated and overexpressed kinase-deficient c-Met mutants (Y1234F and Y1235F), wt-c-Met, and oncogenic c-Met mutants [P991S (Lee et al., 2000); Y1003F (Abella et al., 2005)], in U87 cells (Figure 11A). Bright field microscopy revealed that the U87 cells expressing kinase-deficient mutants lost their spindle, mesenchymal-like, appearance and were transformed into cuboidal, epithelial-like, shaped cells (Figure 11B). These results suggest that Y1234 and Y1235 of c-Met are necessary to maintain the mesenchymal-like morphology of U87 GBM cells.

**A**



**B**

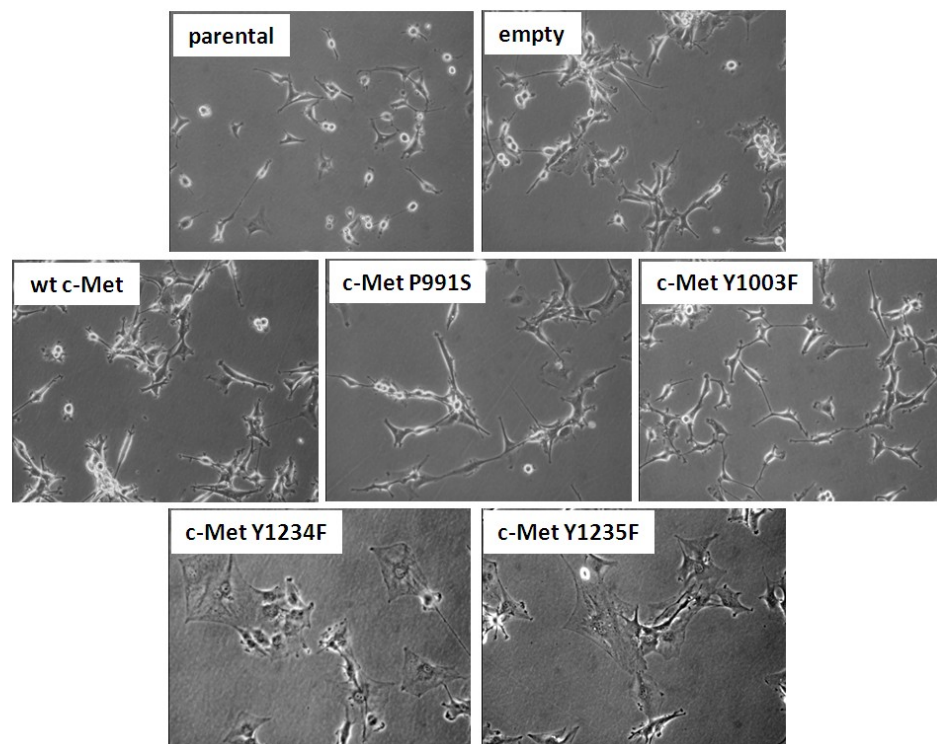


**Figure 11.** Cellular morphology alters with overexpression of kinase-impaired c-Met mutants in U87 cells. (A) Western blot analysis of U87 cells that overexpressed an empty vector control (pMSCV-puro), wt c-Met, c-Met P991S, c-Met Y1003F, c-Met Y1234F, c-Met Y1235F. (B) Bright field microscopy of all cell lines represented in (A).

Next, we asked whether the c-Met signal was required for HGF production. To answer this question, we treated U87 cells with SU11274. This compound selectively targets the c-Met receptor by a factor of 50 when compared with other receptor tyrosine kinases (Peruzzi and Bottaro, 2006). The treatment of U87 GBM cells with SU11274 decreased HGF mRNA (Figure 12A) and protein (Figure 12B) amounts.

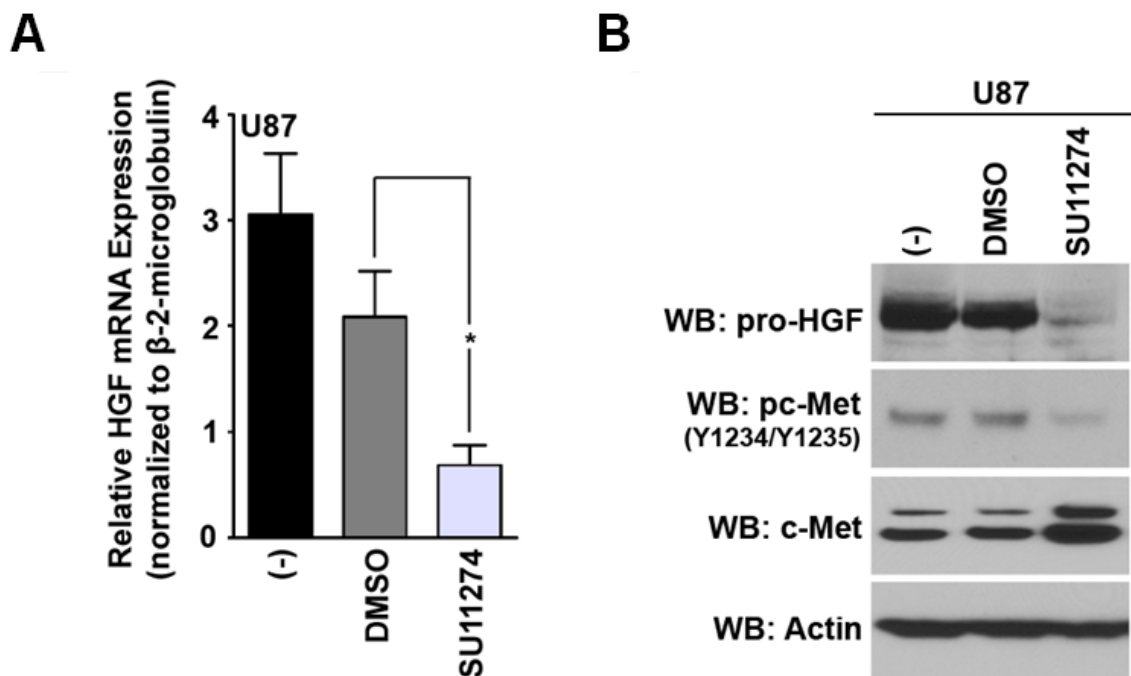


**Figure 12.** c-Met inhibition reduces HGF mRNA and protein amounts in U87 cells. (A) HGF qRT-PCR of U87 cells treated with 10  $\mu$ M SU11274 for 16h; media contained 10% FBS (\* =  $P < 0.05$ ; Student's t-test compared with 0.1% DMSO control;  $n = 4 \pm \text{SEM}$ ; at least duplicate samples per experiment). (B) Western blot analysis of HGF and c-Met activity levels (Y1234/Y1235) in U87 cells after 0.1% DMSO or 10  $\mu$ M SU11274 treatment for 16h; media contained 10% FBS.

We wanted to determine if HGF expression would also be suppressed in a cell line other than U87 when c-Met's tyrosine kinase activity was inhibited. The GBM cell line LN18 produces both c-Met and HGF, and is therefore considered c-Met-dependent (Beroukhi et al., 2007). We treated LN18 cells with SU11274 to inhibit c-Met activity, and analyzed HGF content by qRT-PCR and by western analysis. We found that LN18 cells responded analogously to that of U87 cells, where HGF mRNA (Figure 13A) and protein (Figure 13B) amounts decreased with c-Met inhibition.

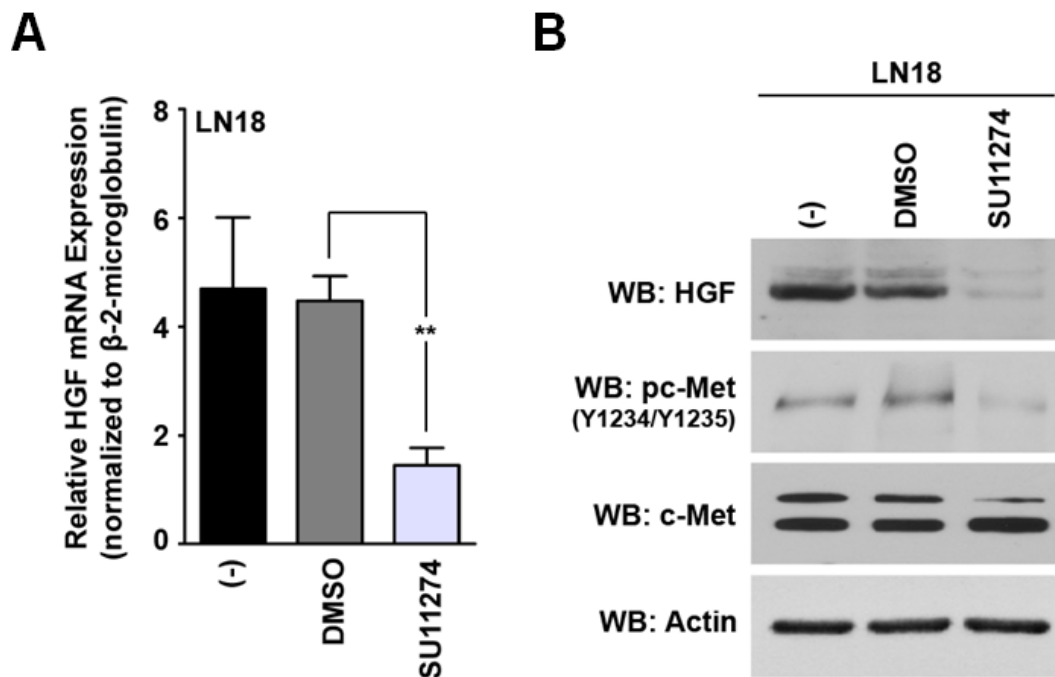


**Figure 13.** HGF mRNA expression and protein levels decrease with c-Met knockdown in LN18 cells. (A) HGF qRT-PCR of LN18 cells treated with 10  $\mu$ M SU11274 for 16h; media contained 10% FBS (\*\* =  $P < 0.01$ ; Student's t-test compared with 0.1% DMSO control;  $n = 4 \pm \text{SEM}$ ; at least duplicate samples per experiment). (B) Western blot analysis of HGF and c-Met activity levels (Y1234/Y1235) in LN18 cells after 0.1% DMSO or 10  $\mu$ M SU11274 treatment for 16h; media contained 10% FBS.



Taken together, our results suggest that the coregulation of HGF and c-Met occurs primarily at the mRNA level, and that the activity of c-Met is required for HGF expression in GBM cells.

### **c-Met is Required for Anchorage-independent Growth of U87 Cells**

Next, we characterized the biological implications of shRNA-mediated silencing of c-Met in U87 cells. Initially, we started our investigations by performing anchorage-independent growth assays, since it is a quick and simple method to perform, yet models some important aspects of tumorigenicity *in vivo*, such as cancer cell proliferation without firm attachment. We found that the number of colonies (Figure 14A), and the size of the colonies (Figure 14B), decreased significantly with reduced c-Met expression in U87 cells.

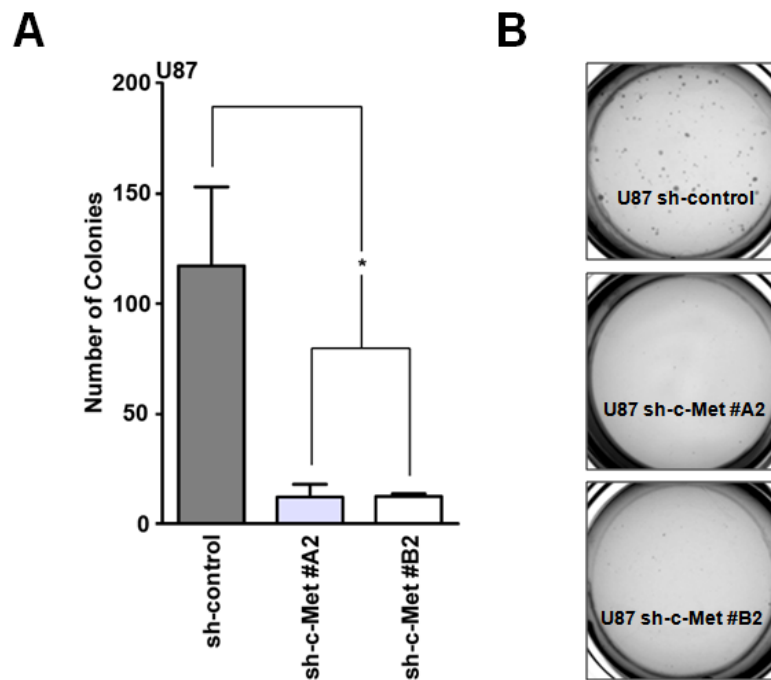


**Figure 14.** Anchorage-independent growth of U87 cells with c-Met knockdown. (A) Colony formation assays determined the number of colonies produced by U87 sh-control cells when compared with U87 shRNA-c-Met clones (different targeting constructs) after growth for 14 days (\* =  $P < 0.05$ ; Student's t-test;  $n = 3 \pm \text{SEM}$ ; at least triplicate samples per experiment). (B) Representative images of colony formation on day 14.

To understand the mechanisms that may contribute to the decreased anchorage-independent growth of U87 sh-c-Met cells, we performed WST-1 assays that measured the metabolic activity of viable cells. Even though all of the cell lines were plated on the same day using equal cell numbers, and grown under the same conditions, the metabolic activities of the U87 sh-c-Met clones were less than that observed in the U87 sh-control cells after 3 days of growth (Figure 15A). Therefore, the total number of viable cells may have decreased over time with c-Met knockdown when compared with the scrambled sh-control cell line.

Although it's not definitive proof of apoptosis, altered BCL-XL expression levels suggest that changes in cell viability have occurred (Boise et al., 1993, Nagane et al., 1996). Using qRT-PCR, we showed that BCL-XL expression decreased with SU11274 treatment of U87 cells (Figure 15B).

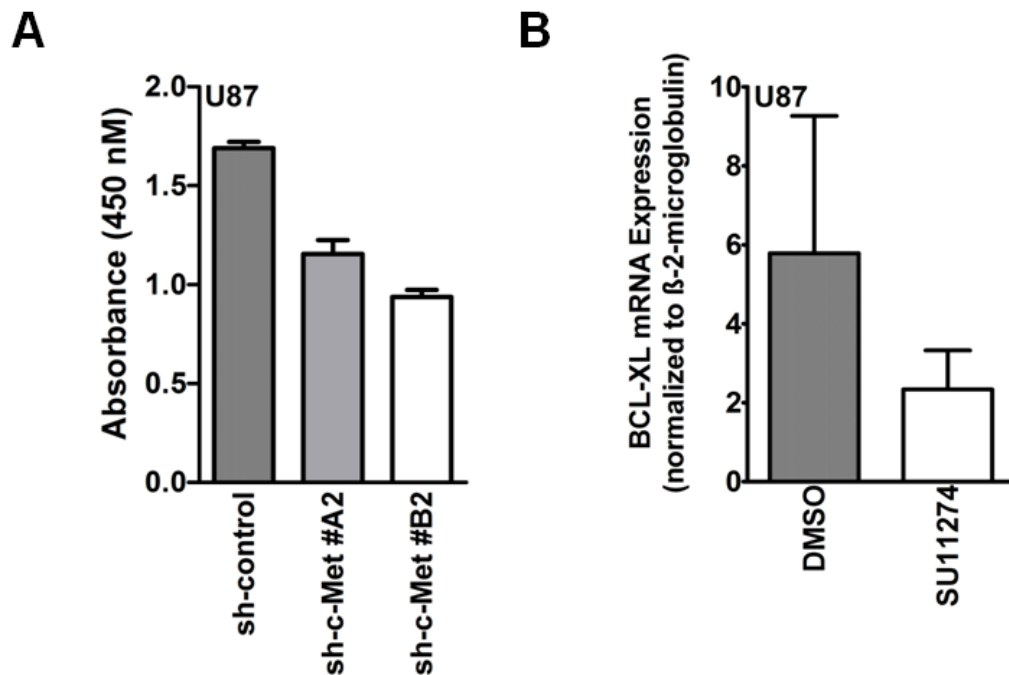


**Figure 15.** c-Met suppression alters biological characteristics of U87 cells. (A) WST-1 assays measured the metabolic activities of U87 sh-control cells, and U87 sh-c-Met clones (different c-Met sh-RNA targeting constructs) after 72 h in culture ( $\pm$  SEM); media contained 10% FBS (B) BCL-XL qRT-PCR of U87 cells treated with 0.1% DMSO or 10  $\mu$ M SU11274 for 16h ( $\pm$  SEM); media contained 10% FBS.

Taken together, the decrease in anchorage-independent growth of U87 sh-c-Met cells may be due to increased cell death. However, in order to support this conclusion, additional experiments should be performed that would measure the degree of apoptosis directly.

## Silencing c-Met Suppresses the Tumorigenicity of Intracranial GBM Xenografts

We examined the tumorigenicity of U87 cells with c-Met knockdown *in vivo* by measuring the survival of nude mice that had been intracranially injected with these cells (Figure 16). The median survival of mice in the U87 sh-control group was 16 days. After 65 days, we sacrificed the mice in the U87 sh-c-Met groups since they did not show any neurological symptoms of tumor burden. We confirmed the absence of tumors in two mouse brains per c-Met knockdown cell line tested by microscopic examination of H&E stained brain sections.

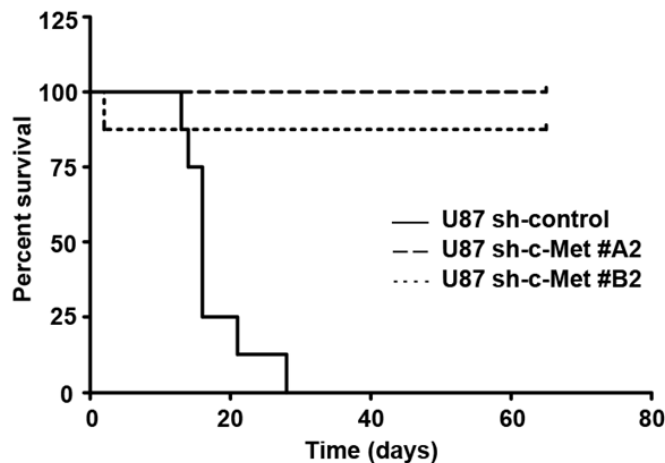


**Figure 16.** c-Met silencing decreases the tumorigenicity of U87 xenografts. Nude mice were injected intracranially with  $2 \times 10^5$  U87 sh-control or  $2 \times 10^5$  U87 sh-c-Met clonal cells and their survival was documented over 65 days. The median survival for each group of mice and the significant differences between them are shown (Log-rank test;  $P < 0.0001$ ; U87 sh-control versus U87 sh-c-Met clones).

Cell line	Median survival (days)	P value
U87 sh-control	16	
U87 sh-c-Met #A2	Undefined >65	< 0.0001
U87 sh-c-Met #B2	Undefined >65	< 0.0001

Taken together, our data suggest that the expression of c-Met is an important component needed to maintain anchorage-independent growth and tumorigenicity of U87 GBM cells.

## **CHAPTER 4**

### **RESULTS**

#### **$\Delta$ EGFR REGULATES HGF EXPRESSION VIA C-MET ACTIVATION AND REQUIRES C-MET FOR ONCOGENICITY**

## **$\Delta$ EGFR Induces the Expression of HGF via c-Met Activation**

Using an open mass spectrometry-based approach to examining the  $\Delta$ EGFR signal in GBM cells, our laboratory (Chumbalkar et al., 2011), and an independent group of investigators (Huang et al., 2007), found that the intensity of the c-Met phosphopeptide Y1234 increased in response to the  $\Delta$ EGFR signal in GBM cells. Since the activity of c-Met is an important component necessary for the production of HGF in c-Met-dependent GBM cells, we asked whether  $\Delta$ EGFR could increase HGF expression via c-Met activation. Using qRT-PCR, we found that HGF mRNA amounts tripled with  $\Delta$ EGFR expression in U87 cells (Figure 17).

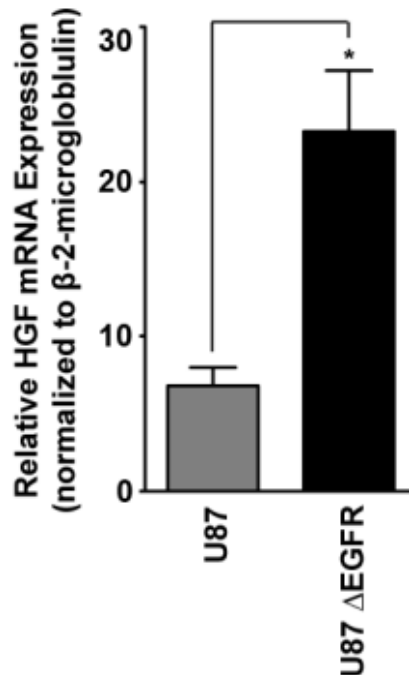


**Figure 17.**  $\Delta$ EGFR increases the mRNA expression of HGF. HGF mRNA amounts were measured by qRT-PCR in U87 cells and in those that overexpressed  $\Delta$ EGFR (cells were cultured in DMEM media containing 10% FBS; \* =  $P < 0.05$ ; Student's t-test;  $n = 3 \pm \text{SEM}$ ; samples were analyzed at least in duplicate per experiment).

We performed western blot analysis to confirm that the protein expression of HGF increased with  $\Delta$ EGFR expression (Figure 18). To confirm that increased HGF expression correlates with enhanced c-Met signaling, we immunoprecipitated c-Met and performed western blot analysis. As shown in Figure 18, c-Met activity was enhanced in the presence of constitutively active  $\Delta$ EGFR. It was necessary to immunoprecipitate c-Met due to a strong cross-reactivity of the pc-Met Y1234/Y1235 antibody with phosphorylated  $\Delta$ EGFR; c-Met and  $\Delta$ EGFR are approximately the same size when analyzed by western blot.

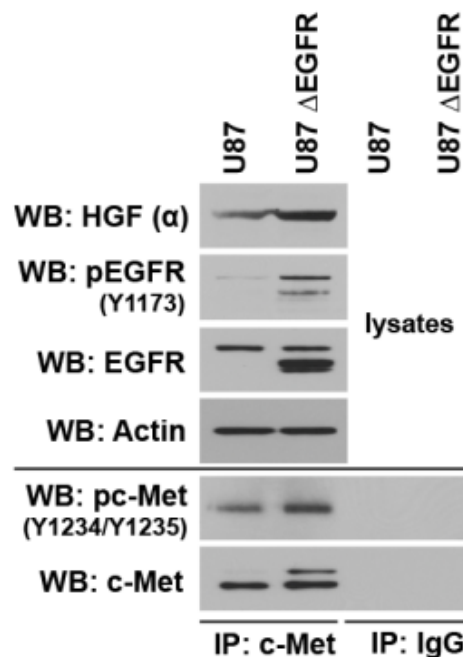


**Figure 18.**  $\Delta$ EGFR increases the protein expression of HGF. Western blots measured HGF protein expression and p-c-Met (Y1234/Y1235) amounts after c-Met was immunoprecipitated from lysates that were prepared from U87 and U87  $\Delta$ EGFR cells. Cells were cultured for 20 h in media containing 1% serum.

Madin-Darby Canine Kidney (MDCK) cells are acutely sensitive to HGF stimulation, and respond rapidly by eliciting c-Met-dependent biological programs



(Cao et al., 2001; Christensen et al., 2003). Therefore, we used MDCK cells to determine if HGF was being secreted from U87 cells that expressed  $\Delta$ EGFR, and if the secreted HGF was functional. Upon stimulation of MDCK cells with CM from U87  $\Delta$ EGFR cells, we found that c-Met was acutely activated (Y1234/Y1235) in a time-dependent manner (Figure 19). This level of c-Met activation was also observed when MDCK cells were acutely stimulated with rhHGF. In order to prove that HGF from U87  $\Delta$ EGFR CM was responsible for c-Met activation in MDCK cells, we pre-neutralized HGF in an aliquot of the CM with an anti-HGF antibody. This resulted in attenuation of the c-Met signal in MDCK cells when compared with the signal generated by rhHGF stimulation or with untreated U87  $\Delta$ EGFR CM. These data suggested that HGF was being secreted by U87  $\Delta$ EGFR cells, and that the secreted HGF was functional.

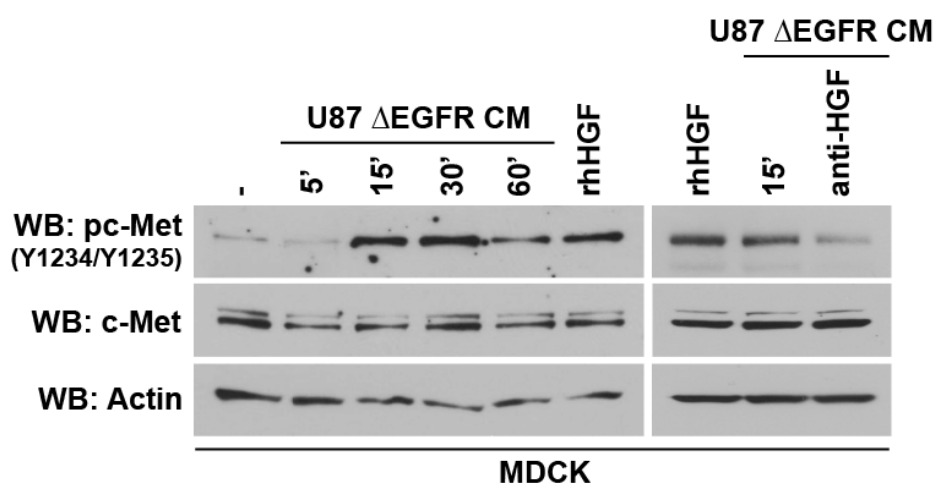


**Figure 19.** Functional HGF is secreted by  $\Delta$ EGFR-expressing GBM cells. CM from U87  $\Delta$ EGFR cells was transferred to MDCK cells for the indicated amounts of time (min). c-Met activation was detected by western blot. MDCK cells were also stimulated for 15 min with rhHGF (50 ng/mL), or media (-), or with CM that had been pre-neutralized for 2 h with an anti-HGF antibody. Cells were cultured in media containing 1% FBS.

## **Inhibition of $\Delta$ EGFR suppresses HGF expression**

The kinase-dependent function of the  $\Delta$ EGFR is responsible for enhanced c-Met activation in GBM cells (Pillay et al., 2009). We have shown that c-Met is responsive to the  $\Delta$ EGFR signal (Figure 18; Chumbalkar et al., 2011), and that HGF production increases with  $\Delta$ EGFR overexpression (Figures 17-18). Therefore, we tested the hypothesis that  $\Delta$ EGFR's kinase activity regulates HGF expression. We inhibited the kinase activity of  $\Delta$ EGFR with AG1478, a specific EGFR TKI that preferentially antagonizes the  $\Delta$ EGFR (Huang et al., 2007), and analyzed HGF mRNA expression by qRT-PCR. This analysis revealed that HGF mRNA amounts decreased with inhibition of the  $\Delta$ EGFR signal (Figure 20). As expected, HGF mRNA expression also decreased with SU11274 treatment of U87  $\Delta$ EGFR cells. Treatment of U87  $\Delta$ EGFR cells with either SU11274 or AG1478 suppressed the expression of HGF to a similar extent. The dual inhibition of U87  $\Delta$ EGFR cells with SU11274 and AG1478 did not result in greater attenuation of HGF mRNA expression to that of either agent alone. These results suggest that c-Met and  $\Delta$ EGFR regulates HGF mRNA expression through the same pathway.

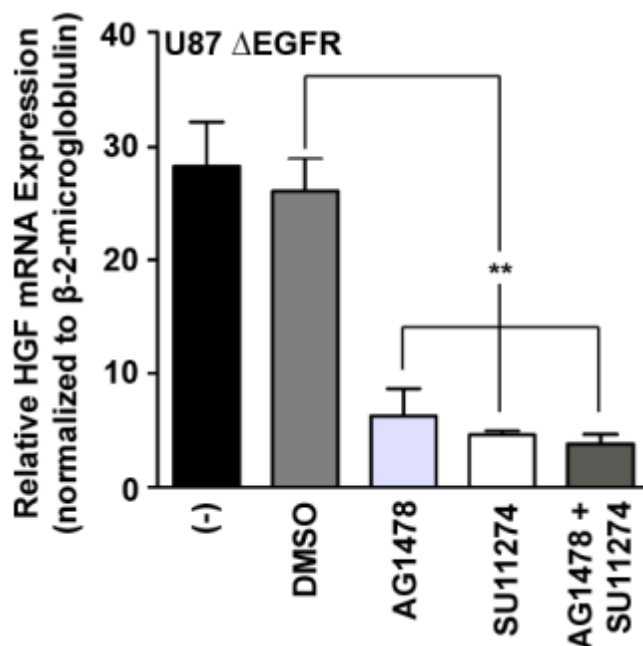


**Figure 20.** HGF mRNA expression decreases with inhibition of  $\Delta$ EGFR. HGF mRNA amounts were measured by qRT-PCR of U87  $\Delta$ EGFR cells that were either untreated, or treated with 0.1% DMSO, 10  $\mu$ M AG1478, 10  $\mu$ M SU11274, or with a combination of 10  $\mu$ M AG1478 and 10  $\mu$ M SU11274. Cells were treated for 16 h in media containing 10% FBS (\*\* =  $P < 0.01$ ; Student's t-test when compared with the DMSO-treated control;  $n = 3 \pm \text{SEM}$ ; samples were analyzed at least in duplicate per experiment).

We performed western blot analysis in order to confirm that the treatment of U87  $\Delta$ EGFR cells with SU11274 and AG1478 effectively inhibited the kinase activities of c-Met and  $\Delta$ EGFR, as well as the protein expression of HGF. Surprisingly, AG1478 treatment of U87  $\Delta$ EGFR cells did not attenuate HGF protein expression and c-Met phosphorylation (Y1234/Y1235) to the same extent as SU11274 (Figure 21). The inhibitor-dependent decrease in c-Met phosphorylation did however correlate with the amount of HGF that was being produced at the protein level. Given that HGF mRNA and protein amounts are not inhibited to the same extent following the treatment of U87  $\Delta$ EGFR cells with

AG1478 (Figure 20 and Figure 21), our results suggest that HGF may also be post-transcriptionally or post-translationally regulated in U87  $\Delta$ EGFR-expressing cells. However, our data provide solid support for the existence of a positive feed-forward relationship between the degree of c-Met activation and the level of HGF protein expression.

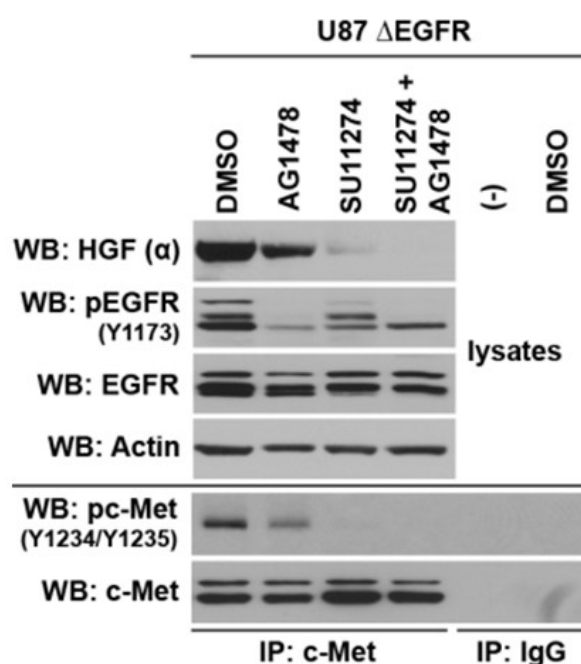


**Figure 21.** HGF protein expression is attenuated with inhibition of  $\Delta$ EGFR. HGF, pc-Met (Y1234/Y1235), and pEGFR (Y1173) levels were detected by western blot analysis of U87  $\Delta$ EGFR cells that were either untreated or were treated with 0.1% DMSO, 10  $\mu$ M AG1478, 10  $\mu$ M SU11274, or a combination of 10  $\mu$ M AG1478 and 10  $\mu$ M SU11274. pc-Met (Y1234/Y1235) amounts were detected by western blot following c-Met immunoprecipitation. Cells were treated for 16 h in media containing 10% FBS.

### c-Met is Required by $\Delta$ EGFR for HGF Production, Anchorage-Independent Growth, and Tumorigenicity of GBM Cells

We then asked whether HGF expression could be maintained by  $\Delta$ EGFR in the absence of c-Met. To answer this question, we overexpressed  $\Delta$ EGFR in U87 sh-c-Met clones and examined HGF mRNA by qRT-PCR. We found that  $\Delta$ EGFR

did not sustain HGF production when c-Met levels were silenced (Figure 22A). HGF protein levels were then evaluated in U87  $\Delta$ EGFR sh-c-Met cells by western blot analysis, and we found that the protein expression of HGF was attenuated with c-Met knockdown in these cells (Figure 22B). As with previous experiments where U87 cells were engineered to overexpress  $\Delta$ EGFR (Figure 20 and Figure 21), there appears to be an uncoupling in regulation of HGF at the mRNA and protein levels. Therefore, these data suggest that HGF may additionally be controlled post-transcriptionally or post-translationally by the  $\Delta$ EGFR signal. Cumulatively, our findings suggest that  $\Delta$ EGFR requires the presence of c-Met to maintain enhanced levels of HGF expression in U87 cells.

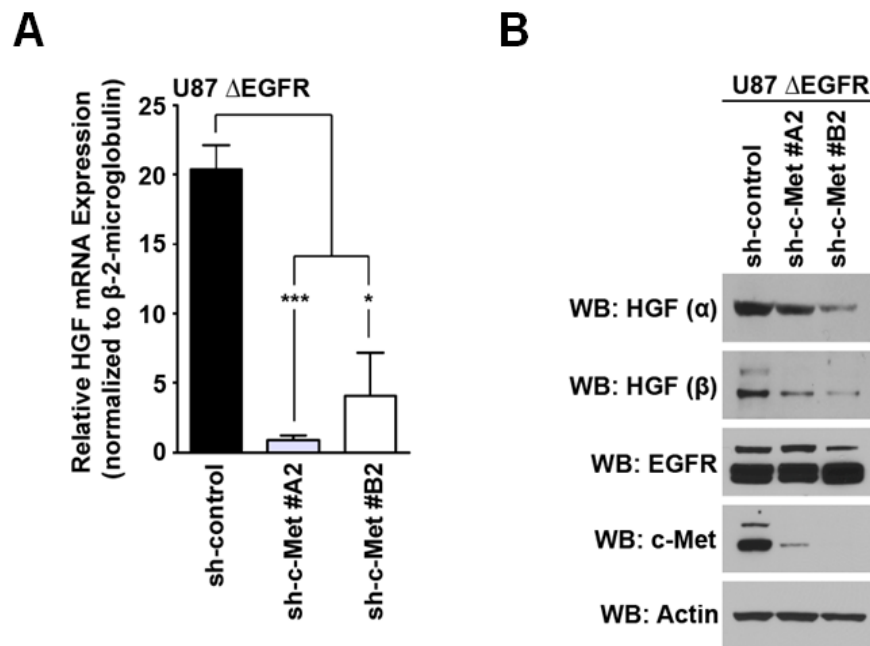


**Figure 22.** c-Met is required by  $\Delta$ EGFR to maintain HGF expression. (A) HGF mRNA amounts were measured by qRT-PCR in U87 sh-c-Met clonal populations (different c-Met shRNAs) that expressed  $\Delta$ EGFR. Cells were cultured in media containing 10% FBS (\* =  $P < 0.05$ ; \*\*\* =  $P < 0.001$ ; Student's t-test;  $n = 3 \pm$  SEM; samples were analyzed at least in duplicate per experiment). (B) HGF protein levels were measured by western blot analysis in all cells detailed in (A). Cells were cultured in media containing 10% FBS.

We determined whether  $\Delta$ EGFR was capable of overcoming the suppression in anchorage-independent growth that we have previously seen with c-Met knockdown in U87 cells (Figure 14). Our results indicated that  $\Delta$ EGFR required c-Met to exert its stimulation of anchorage-independent growth of U87 cells, as it was unable to rescue the loss in colony formation of U87 cells with c-Met knockdown (Figure 23A). Even though the number of colonies for the U87 cell line were comparable to the number of colonies of the U87  $\Delta$ EGFR cell line (Figure 14A and Figure 23A), by visual examination we found that the colonies produced by the latter cell line were far larger in diameter and volume compared with the growth of parental cells (Figure 14B, and Figure 23B).

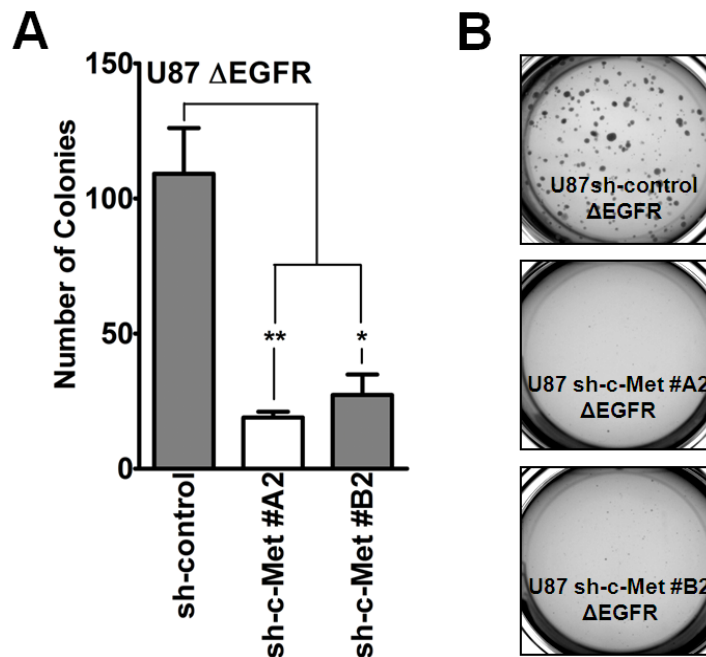


**Figure 23.** *In vitro* colony formation of U87  $\Delta$ EGFR-expressing cells with c-Met knockdown. (A) Anchorage-independent growth assays determined the number of U87 sh-control  $\Delta$ EGFR colonies compared with U87 sh-c-Met #A2  $\Delta$ EGFR and U87 sh-c-Met #B2  $\Delta$ EGFR colonies after 14 days growth (\* =  $P < 0.05$ ; \*\* =  $P < 0.01$ ; Student's t-test;  $n = 3 \pm \text{SEM}$ ; at least triplicate samples per experiment). (B) Representative images of anchorage-independent growth of cell lines described in (A) on day 14.

In order to determine if the diminished anchorage-independent growth of U87 sh-c-Met  $\Delta$ EGFR cells may partly be due to changes in cell viability and BCL-XL expression, we performed WST-1 and qRT-PCR assays, respectively (Figure 24A and Figure 24B). We found that with c-Met knockdown, U87  $\Delta$ EGFR cells were unable to maintain a high level of metabolic activity (Figure 24A), and that BCL-XL expression decreased with c-Met inhibition in these cells (Figure 24B). These results indicated that the total number of cells, and BCL-XL expression, decreased with c-Met suppression in U87  $\Delta$ EGFR cells. These data suggested that c-Met plays an important role in the viability of U87 cells even when  $\Delta$ EGFR is expressed.

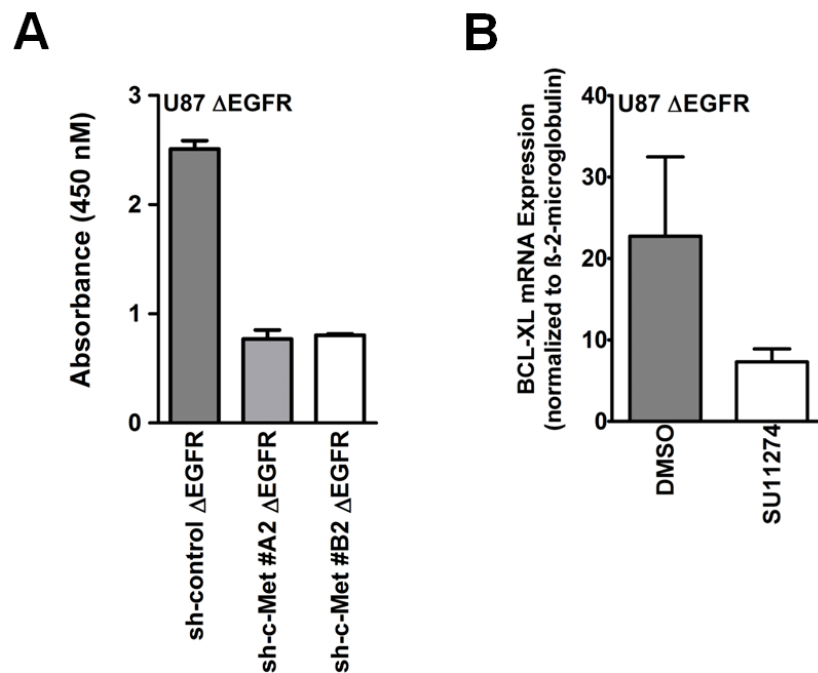
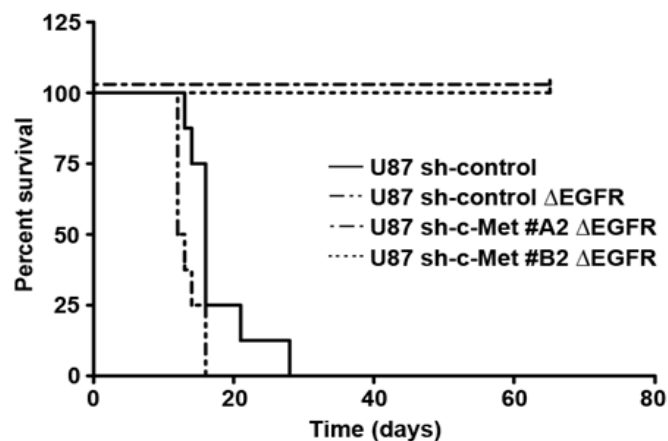


**Figure 24.** Biological properties of U87  $\Delta$ EGFR cells are altered with c-Met knockdown. (A) WST-1 assays measured changes in metabolic activity ( $\pm$  SEM) of U87  $\Delta$ EGFR cells with c-Met knockdown (U87 sh-c-Met #A2  $\Delta$ EGFR cells and U87 sh-c-Met #B2  $\Delta$ EGFR cells) after 72 h growth in media containing 10% FBS (B) qRT-PCR quantified BCL-XL mRNA expression ( $\pm$ SEM) in U87  $\Delta$ EGFR cells that were treated with 0.1% DMSO or 10  $\mu$ M SU11274 for 16h in media containing 10% FBS.

The  $\Delta$ EGFR is a potent oncogene that confers enhanced tumorigenicity to U87 cells *in vivo* (Huang et al., 1997; Nishikawa et al., 1994). Our data therefore raised the question of whether  $\Delta$ EGFR was capable of overcoming the reduced tumorigenicity that we've found to be associated with c-Met knockdown in U87 cells (Figure 16). Hence, we measured the survival of nude mice that had been intracranially injected with either U87 sh-c-Met cells overexpressing  $\Delta$ EGFR, with U87 sh-control cells, or with U87 sh-control cells that overexpressed  $\Delta$ EGFR over a period of 65 days (Figure 25).



Cell line	Median survival (days)	P value
U87 sh-control	16.0	
U87 sh-control $\Delta$ EGFR	12.5	0.0190
U87 sh-c-Met #A2 $\Delta$ EGFR	Undefined >65	<0.0001
U87 sh-c-Met #B2 $\Delta$ EGFR	Undefined >65	<0.0001

**Figure 25.** c-Met is required by  $\Delta$ EGFR to enhance the tumorigenicity of U87 cells. Over a period of 65 days, survival curves were generated from mice that had been intracranially injected with  $2 \times 10^5$  U87 sh-control  $\pm$   $\Delta$ EGFR, U87 sh-c-Met #A2  $\Delta$ EGFR, or with U87 sh-c-Met #B2  $\Delta$ EGFR cells (Log-rank test;  $P < 0.0001$  when compared with the U87 sh-control group; median survival per group of mice was recorded).



Compared with the U87 sh-control group,  $\Delta$ EGFR overexpression significantly augmented the tumorigenicity of U87 cells *in vivo* as expected from many prior studies. Surprisingly, mice that received U87 sh-c-Met (#A2 or #B2 clones) cells that overexpressed  $\Delta$ EGFR did not become moribund within 65 days of intracranial injection. The absence of tumors in these mice was verified in H&E stained serial sections by visual examination under a microscope. Cumulatively, these data suggest that c-Met is an important component necessary for the maintenance of tumorigenicity of c-Met-dependent GBM cells, regardless of the  $\Delta$ EGFR signal.

## **CHAPTER 5**

### **RESULTS**

#### **STAT3 PARTIALLY MODULATES HGF EXPRESSION IN RESPONSE TO THE C-MET SIGNAL IN $\Delta$ EGFR-EXPRESSING GBM CELLS**

## **STAT3 is a Key Node Regulating HGF Expression in Response to the c-Met Signal**

We used an unbiased shotgun phosphoproteomics-based approach to further understand the signaling events that lead to changes in HGF expression upon modification of the c-Met signal in U87 and U87  $\Delta$ EGFR cells. We chose to enrich for phosphotyrosine peptides so as to provide an accurate snapshot of signaling events that were initiated by c-Met and  $\Delta$ EGFR. By doing this, we also increased the probability of being able to detect all phosphotyrosine modifications present on low-abundance proteins, and phosphotyrosine-related signaling events occurring in a milieu of unphosphorylated, serine-phosphorylated, and threonine-phosphorylated proteins (Macek et al., 2009). Specifically, after recovering tyrosine-phosphorylated peptides from tryptically digested lysates of U87 sh-control, U87 sh-control  $\Delta$ EGFR, U87 sh-c-Met #B2, and U87 sh-c-Met #B2  $\Delta$ EGFR cells, we performed LC-MS/MS (see Figure 26 for a schematic of the methodology that was performed).

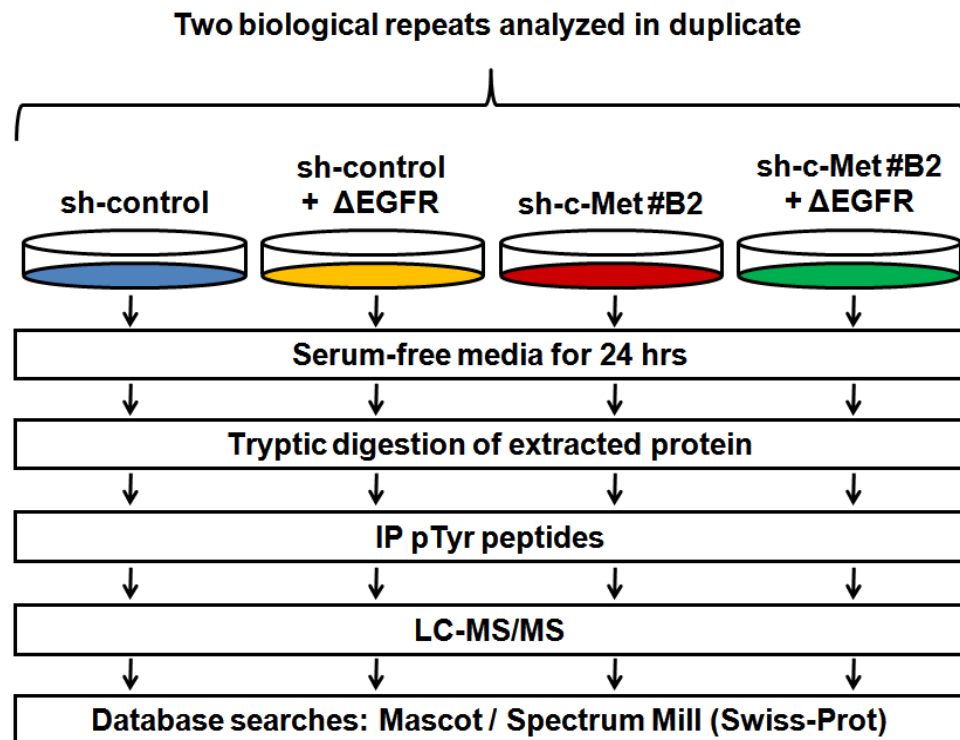


**Figure 26.** Schematic of mass spectrometry experiments. Two biological repeats per cell line (U87 sh-control, U87 sh-control  $\Delta$ EGFR, U87 sh-c-Met #B2, and U87 sh-c-Met #B2  $\Delta$ EGFR) were processed and analyzed in duplicate by mass spectroscopy (Dr. Vaibhav Chumbalkar, Dr. Oliver Bögler's former post-doctoral fellow, performed all mass spectrometry experiments).

An equal volume of lysate from each cell line that was processed for PhosphoScan was analyzed by western to confirm their identity (Figure 27). These data also showed that comparable amounts of protein, as assessed by actin levels, were present in each sample within a biological replicate set.

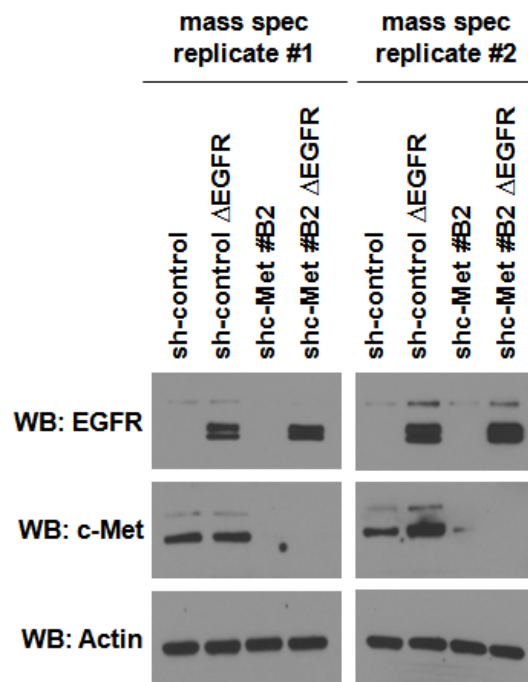


**Figure 27.** Confirmation of sample identities that were processed for PhosphoScan analysis. Western blot analysis of lysates that were used in mass spectrometry experiments.

We identified 112 peptides that were tyrosine-phosphorylated, which corresponded with 82 proteins. Table 5 provides a complete list of all phosphotyrosine-modified peptides that were identified in our screen.

Peptide Index	Swissprot ID (Human)	m/z	Charge	Modification site (s)
1157	ABI1	765.5856	3	TLEPVKPPTVPNDyMTSPAR
1233	ABI1	966.5225	3	NTPyKTLEPVKPPTVPNDYMTSPAR
651	ABL2/ABL1	506.6402	3	LMTGDTyTAHAGAK
1063	ACK1	802.5335	3	KPTyDPVSEDQDPLSSDFKR
1288	ACK1	764.2574	3	VSSTHyYLLPERPSYLER
954	ACTN1	370.8297	3	sIVNyKPK
542	ACTS	802.4712	3	DLYANNVMSGGtTMypGIADR
1764	ANKL2	760.7147	2	yVVDLYLNTPDK
919	ANXA2	963.2993	2	LSLEGDHSTPPSAyGSVK

927	ANXA2	642.7831	3	LSLEGDHSTPPSAyGSVK
1653	ANXA2	771.2139	2	SYSPyDMLESIR
1339	BCAR1	656.7297	3	HLLAPGPQDIyDVPPVR
849	CALR	908.7309	3	GLQTSQDARFyALSAsFEPFSNK
2216	CCNL2	415.302	3	ERSRsyER
883	CDK1	673.6172	2	IGEGtyGVVYK
863	CDK2	633.7101	2	IGEGTyGVVYK
893	CDK3	634.1149	2	IGEGTYGVVyK
1338	CILP2	339.2904	3	VRAYANDK
524	CML1	838.6844	3	LVNALSEDTGHSSyPSHRSFTK
695	COF1	624.6044	3	HELQANCyEEVKDR
1779	CSKI2	817.7112	3	NTyNQ TALDIVNQFTTSQASR
634	CSKP	821.7138	3	GSItFKIVPSyRTQSSSCER
1359	DCBD2	694.248	3	ATGNQPPPLVGTyNTLLSR
1487	DCBD2	977.9353	3	AGKPGLPAPDELVyQVPQSTQEVSGAGR
1942	DCBD2	1012.035	3	EVTTVLQADSAEyAQPLVGGIVGTLHQR
1013	DYH6	690.5724	3	LVMTCAAFITMNPgyAGR
873	DYH7	844.2557	3	NMEKANSLYVIKLsEPDyVR
728	DYR1A	576.1992	2	IYQyIQSR
1372	EF1A1	698.1473	2	EHALLAyTLGVK
678	EGFR	645.9033	2	GSTAENAEyLR
1347	EGFR	773.0428	3	GSHQISLDNPDyQQDFFPK
1605	ENOA	943.5977	2	AAVPSGASTGlyEALELR
1608	ENOA	628.9258	3	AAVPSGASTGlyEALELR
2191	ENOA	1023.007	3	SFIKDyPVVSIEDPFDQDDWGAWQK
1903	ENOG	772.2438	3	AGyTEKIVIGMDVAASEFYR
2304	EVPL	367.7344	3	SQYRDLLK
1548	FKBP4	763.0661	2	EKKLyANMFER
1198	GCYA3	404.0985	3	INVSPtTyJR
1552	GDE	547.7351	3	EAMsAyNSHEEGR
1624	GDE	732.2042	2	FsCDVAEGKyK
770	GRLF1	1014.507	2	NEEENlySVPHDSTQGK
771	GRLF1	676.6196	3	NEEENlySVPHDSTQGK
1890	GRLF1	1086.948	3	SVSSSPWLPQDGFDPsDyAEPMDAVVKPR
808	GSK3A	721.2467	2	GEPNVsyICSR
842	GSK3A	454.7474	3	GEPNVSyICSR
841	GSK3A/GSK3B	681.7287	2	GEPNVSyICSR
681	IMPG1	802.5516	3	LRVCQEAVWEAyRIFLDR
949	ITB1	652.7658	2	WDTGENPlyK
2200	ITIH2	502.407	3	LGfyFQsEDIK
642	ITSN1	423.9775	3	GWFPKsyVK
2048	K2C1B	708.8024	3	GRSGGGYGSGCGGGGGSyGGsGR
1737	LDHA	600.2064	2	DQLIyNLLK
2247	LDHA	885.3657	3	GyTsWAIGLSVADLAESIMKNLR
1046	LRCC1	612.3049	3	RDTDITSESDyGNRK
1960	LY75	730.6363	2	yLNNLYKIIPK
955	M3K8	884.0403	3	ADlySLGATLIHMQTGTPPWVKR
1083	MK01	742.2217	3	VADPDHDHTGFLTEYyVATR
1107	MK01	769.2481	3	VADPDHDHTGFLtEYyVATR

1135	MK03	751.7668	3	IADPEHDHTGFLTEyVATR
1153	MK03	778.1629	3	IADPEHDHTGFLtEyVATR
719	MK14	525.9742	3	HTDDEMTGyVATR
725	MK14	789.0988	2	HTDDEMTGyVATR
2217	MLL3	727.2823	2	KEKLyEsQNR
1534	NP1L2	547.8437	3	yDEPILKLLTDIK
693	ODPAT	585.316	3	YHGHsMSDPGVSyR
1830	OR8J1	867.6084	3	MASVFYtLVIPMLNPLIySLR
1760	OSBL5	760.8906	3	LTRNLLLSGDNELyPLSPGK
704	PAXI	703.5767	3	FIHQPPQSSsPVyGSSAK
736	PAXI	677.1365	3	FIHQPPQSSSPVyGSSAK
802	PAXI	539.0703	3	VGEEHVySFPNK
809	PAXI	808.4905	2	VGEEHVySFPNK
1410	PRP4B	840.0695	3	LCDFGSASHVADNDITPyLVSR
1411	PRP4B	1259.978	2	LCDFGSASHVADNDITPyLVSR
1754	PRRC1	612.3048	3	QMIYsAARAIAGMyK
981	PTN11	908.8163	2	IQNTGDYyDLYGGEK
1666	PTPRA	995.5192	2	VVQEYIDAFSDyANFK
1694	PTPRA	663.9271	3	VVQEYIDAFSDyANFK
819	PTRF	500.7654	3	KSFTPDHVyAR
1629	PUR8	528.9814	3	RAFIITGQtyTR
1365	RGPD3	491.0598	3	MGSGLNSFyDQR
741	RHG42	667.865	3	LDTASSNGyQRPGSVAAK
1002	RIN1	948.6034	3	EKPAQDPLyDVPNASGGQAGGPQRPRGR
1076	S12A5	847.27	3	GLSLSAARyALLRLEEGPPHtK
1328	SETB2	386.8967	3	KLPQFKyR
801	SHB	835.1677	2	GESAGyMEPYEAQR
1097	SHB	627.6371	3	DKVTIADDySDPFDAK
1419	SHC1	988.7607	2	ELFDDPSyVNVQNLDK
730	SMC1B	602.6334	2	yQSLLEELK
1155	SRC8	746.0805	3	GPVSGTEPEPVySMEAADYR
2337	SSH1	915.7318	3	sCPNGMEDDAIFGILNKVKPSyK
895	STA13	502.2786	3	FDQTTRRSPyR
1968	STAR9	754.4364	3	GTVLSyCETLLEPECSsR
2345	STAT3	861.73	3	YCRPESQEHPADPGSAAPyLK
1822	SYNE1	839.7582	2	AQyHLKIGSsEQR
574	TEKT4	363.4678	3	yHQAFAADR
810	TITIN	382.0819	3	VGGGEyIELK
2306	TITIN	404.9394	3	EISTsAKyR
1163	TLN1	563.3869	2	ALDyYMLR
1303	TLN1	639.8245	3	TMQFEPSTMVydACR
1320	TLN1	958.8162	2	TMQFEPSTMVydACR
2183	TLN1	885.3069	3	AVSSAIAQLLGEVAQGNENyAGIAAR
656	TPP2	859.9542	3	IPKGAGPGCyLAGSLTLsKTELGK
975	TYK2	534.3826	3	LLAQAEGEPCyIR
1206	UBP36	993.5783	3	VKCSVCKSVSDtYDPyLDVALEIR
869	VIME	755.2954	2	SLYASSPGGVyATR
906	VIME	754.7248	2	SLYASSPGGVyATR
947	VIME	668.077	2	LGDLYEEEMR

879	VINC	512.7556	2	SFLDSGyR
544	VP13D	428.6271	3	ARDAVSytDK
1325	ZN483	603.4999	2	AFGysASLTK
925	ZNF45	383.5233	3	syLQVHLK
1156	ZO2	639.1482	3	IEIAQKHPDIyAVPIK

**Table 5.** List of peptides with a phosphotyrosine modification identified by mass spectrometry. Peptides identified as being tyrosine phosphorylated by PhosphoScan analysis are listed along with their peptide modification(s), charge-to-mass ratio, charge, and assigned peptide identification number.

The mean abundance (signal intensity) of all phosphotyrosine-modified peptides that were discovered by mass spectrometry in U87-sh-control, U87 sh-c-Met #B2, U87 sh-control  $\Delta$ EGFR, and in U87 sh-c-Met #B2  $\Delta$ EGFR cells are listed in Table 6.

Swissprot ID (Human)	Mean Abundance			
	U87 sh-control	U87 sh-c-Met #B2	U87 sh-control $\Delta$ EGFR	U87 sh-c-Met #B2 $\Delta$ EGFR
ABI1	1390002.36	557123.89	1490703.14	401405.14
ABI1	158052.85	27027.32	182937.34	73016.99
ABL2/ABL1	388297.30	101083.20	493929.28	153875.20
ACK1	922657.35	333189.57	745719.99	715348.00
ACK1	429038.44	144901.52	559607.14	560046.88
ACTN1	128379.18	136078.11	124709.16	168452.27
ACTS	617198.57	369574.73	704295.28	656811.68
ANKL2	1774484.45	2445698.98	1422771.92	2501135.40
ANXA2	711053.25	281965.01	696757.11	476815.75
ANXA2	4590724.40	1656585.32	2190044.66	3652219.54
ANXA2	1218735.63	297124.22	1007833.07	812580.46
BCAR1	338525.72	170291.96	240378.32	457820.48
CALR	856490.77	144311.67	1577667.45	352306.49
CCNL2	98213.39	104840.38	54001.81	114658.33
CDK1	357808.24	955824.69	624606.45	3886702.79
CDK2	3574261.61	8766808.98	6128642.02	18815182.68
CDK3	3396418.72	8328703.27	6794913.38	10262738.33
CILP2	198869.28	104733.45	157605.84	326180.47
CML1	110263.22	94791.65	556951.74	470237.14



COF1	86620.46	48305.97	104066.87	95410.82
CSKI2	721190.38	176123.34	1541311.73	694879.63
CSKP	218776.87	70649.60	216349.67	74970.31
DCBD2	425302.85	367333.51	239285.34	215799.23
DCBD2	401805.37	308981.38	311079.20	620632.76
DCBD2	142033.39	100294.09	175640.41	262152.16
DYH6	560410.51	321770.58	265848.97	212790.97
DYH7	86817.34	62947.91	48393.49	21957.75
DYR1A	8262429.11	2437101.61	9503113.33	7099249.49
EF1A1	419470.06	286270.09	506843.26	515893.50
EGFR	48479.48	31038.18	54539.98	58243.35
EGFR	153667.34	138807.68	1613495.47	2332661.72
ENOA	591440.38	263297.31	539507.44	674096.10
ENOA	813145.43	240266.06	1003193.55	517421.27
ENOA	163483.09	77074.08	184819.13	137985.92
ENOG	163908.51	382148.71	440202.16	370887.04
EVPL	110101.06	17203.91	190048.12	135678.82
FKBP4	186902.72	449656.21	146856.64	414893.25
GCYA3	290009.12	419760.09	318321.48	271937.53
GDE	751602.89	1237566.66	714019.64	1570468.93
GDE	1086822.68	673636.30	403062.21	832924.82
GRLF1	551726.17	127120.43	578900.76	131611.28
GRLF1	3769455.06	735348.48	4058405.24	3251988.54
GRLF1	647273.97	264677.75	531222.95	453676.11
GSK3A	292438.80	116195.30	406780.29	308156.27
GSK3A	1284481.07	361673.58	2258000.97	1052806.79
GSK3A/GSK3B	58973570.27	18487522.61	68422426.76	51875222.35
IMPG1	48187.08	18389.24	54606.81	61369.63
ITB1	414073.39	105515.75	249640.44	253044.23
ITIH2	213895.65	551833.13	168948.65	1180317.74
ITSN1	191846.80	254251.42	144069.95	99209.40
K2C1B	1004608.92	428898.19	819603.07	800675.38
LDHA	178060.84	356635.60	200782.47	276784.13
LDHA	937046.05	246653.48	1004697.90	334786.50
LRCC1	891307.14	1987929.83	510156.21	1177797.79
LY75	951036.24	704593.96	1688136.87	1091289.86
M3K8	222848.73	60605.74	196627.13	92722.08
MK01	6162581.65	3025377.73	8683044.75	4169461.99
MK01	982491.32	2458393.65	6949922.49	4580568.60
MK03	4030442.06	2575478.19	5685960.73	4674193.25
MK03	1556220.89	1093051.82	2897934.66	2900633.59
MK14	460716.59	147457.89	493933.75	243555.30
MK14	421256.65	197804.34	595724.34	152649.85
MLL3	13577863.43	7888312.09	22925084.03	11205540.01
NP1L2	603266.04	1629862.91	569777.91	1653791.99
ODPAT	46419.13	50736.35	260792.17	136124.88
OR8J1	113892.36	96435.46	136819.70	57195.30
OSBL5	217517.75	1057819.60	556028.01	183019.46
PAXI	142911.89	74099.51	128332.51	204732.17

PAXI	3425913.02	717944.37	2163262.61	2984657.09
PAXI	1481296.61	385555.40	986958.93	2019925.20
PAXI	668854.90	170925.79	629594.94	603031.16
PRP4B	62508210.09	10700694.99	38639222.94	42857360.56
PRP4B	970333.54	249949.54	542897.06	933738.06
PRRC1	680073.39	271494.39	690468.92	1118398.09
PTN11	353620.17	484080.79	355906.63	595519.07
PTPRA	180804.24	106987.14	78080.90	205051.99
PTPRA	328479.48	519433.10	363376.01	562648.10
PTRF	265348.74	301795.53	622019.56	614181.95
PUR8	471549.51	112110.67	775696.15	208785.66
RGPD3	268844.55	445067.02	265452.70	446122.77
RHG42	145980.20	26016.70	214772.27	154456.97
RIN1	1361034.49	1129682.34	1106079.43	824274.14
S12A5	68673.86	589706.43	135749.53	132364.21
SETB2	90142.09	200632.22	123086.89	135194.12
SHB	479254.88	137621.34	280839.62	169672.56
SHB	264818.99	149017.29	458824.90	311520.14
SHC1	119915.23	113395.27	449191.18	925914.91
SMC1B	166241.83	65420.99	135669.71	180261.30
SRC8	516368.90	409707.97	503111.45	496457.58
SSH1	162164.28	199662.87	186439.31	237512.98
STA13	362436.22	58877.91	717986.29	222776.68
STAR9	934283.08	389216.91	550970.60	658491.40
STAT3	529238.13	296316.17	668754.82	302675.77
SYNE1	701296.76	431172.62	585429.11	505765.76
TEKT4	155574.86	22708.13	106416.80	49106.18
TITIN	554417.65	135557.02	110192.85	295694.52
TITIN	85602.64	118260.96	234272.73	398067.72
TLN1	411342.53	832645.65	1269804.27	829497.92
TLN1	473842.88	172340.28	340899.78	260559.94
TLN1	267913.94	79250.33	248350.52	248087.55
TLN1	803581.90	206432.88	675670.12	362316.34
TPP2	133942.55	44955.13	429553.76	169451.57
TYK2	234589.59	181405.55	363538.63	340488.76
UBP36	46025.10	426206.40	101046.95	34069.23
VIME	577122.99	338176.91	845643.65	522585.07
VIME	737212.49	165750.07	455206.91	318707.84
VIME	496835.10	360392.85	418098.89	142685.35
VINC	916028.31	237204.26	751924.80	419799.49
VP13D	284079.75	64221.07	234289.97	154684.58
ZN483	329195.30	423184.49	301593.77	537240.64
ZNF45	2017668.03	1894840.99	2362456.32	2744836.59
ZO2	594539.30	241264.93	492106.00	246486.65

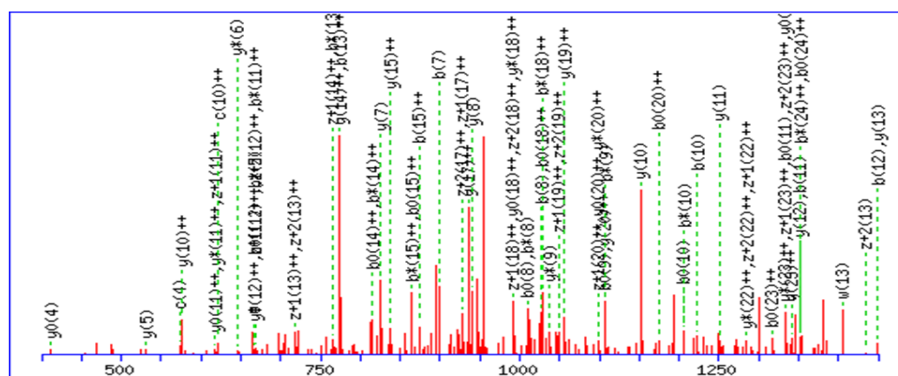
**Table 6.** Mean abundance of all tyrosine-phosphorylated peptides that were identified by mass spectrometry. Listed are average phosphotyrosine intensities that were quantified for each peptide.

Since HGF expression decreases with c-Met knockdown, we were interested in determining which phosphotyrosine peptides changed the most in response to the c-Met signal in U87 and U87  $\Delta$ EGFR cells. Therefore, we determined which peptides showed the most significant decrease in tyrosine phosphorylation with c-Met knockdown in U87 sh-control cells and in U87 sh-control  $\Delta$ EGFR cells (Table 7). Those identified to decrease significantly in their tyrosine phosphorylation status with c-Met knockdown in U87 sh-control  $\Delta$ EGFR cells, also had significantly reduced phosphotyrosine levels with c-Met silenced in U87 sh-control cells.

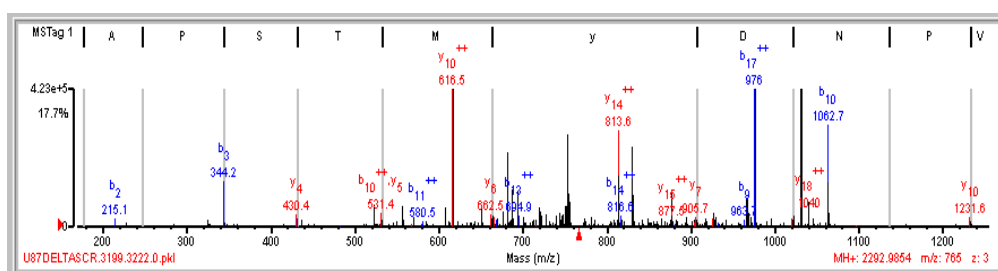
Protein	Peptide Modification	Comparison (P value)	
		U87 sh-control vs U87 sh-c-Met #B2	U87 sh-control $\Delta$ EGFR vs U87 sh-c-Met #B2 $\Delta$ EGFR
Abl interactor 1 (ABI1)	NTPyKTLEPVKPPTVPNDYMTSPAR	0.0001	NS
Abl interactor 1 (ABI1)	TLEPVKPPTVPNDYMTSPAR	NS	0.0000
Annexin A2 (ANXA2)	SYSPyDMLESIR	0.0003	NS
Mitogen-activated protein kinase 14 (MK14) (MAPK14)	HTDDEMTGyVATR	0.0007	NS
L-lactate dehydrogenase A chain (LDHA)	GyTsWAIGLSVADLAESIMKNLR	0.0017	0.0058
Glycogen synthase kinase 3 $\alpha$ /3 (GSK3A / GSK3B)	GEPNVyICsR	0.0029	NS
Enolase A (ENOA) (ENO1)	AAVPSGASTGlyEALRLR	0.0035	0.0423
Glycogen synthase kinase 3 $\alpha$ /3 (GSK3A / GSK3B)	GEPNVyICSR	0.0037	NS
Src homology 2 domain containing adaptor protein B (SHB)	GESAGyMEPYEAQR	0.0045	NS
Serine/threonine-protein kinase PRP4 homolog (PRP4B)	LCDFGSASHVADNDITPyLVSR	0.0053	NS
StAR-related lipid transfer protein 13 (STA13) (STARD13)	FDQTTRRSyR	0.0057	NS
Rho GTPase-activating protein 42 (RHG42)	LDTASSNGyQRPGSVVAAK	0.0071	NS
Paxillin (PAXI) (PXN)	FIHQQPQSSSPVyGSSAK	0.0179	NS
Glucocorticoid receptor DNA binding factor 1 (GRLF1)	NEEENlySVPHDSTQGK	0.0218	0.0004
Activated CDC42 kinase 1 (ACK1) (TNK2)	KPTyDPVSEDQDPLSSDFKR	0.0307	NS
Mitogen-activated protein kinase 1 (MK01) (MAPK1)	VADPDHDTGFLTEyVATR	0.0311	0.0102
Vinculin (VINC)	SFLDSGyR	0.0411	NS
Glucocorticoid receptor DNA binding factor 1 (GRLF1)	SVSSSPWLPQDGFDPsDyAEPMDAVVKPR	0.0424	NS
Vimentin (VIME) (VIM)	SLYASSPGGVyATR	0.0466	NS
Vimentin (VIME) (VIM)	LGDLyEEEMR	NS	0.0200

**Table 7.** Peptides showing a significant decrease in tyrosine phosphorylation with c-Met knockdown. Listed are peptides that showed the most significant decrease in intensity of their phosphotyrosine signal with c-Met knockdown in U87 sh-control and in U87 sh-control  $\Delta$ EGFR cells ( $P < 0.05$  was considered significant; Student's t-test;  $n = 2$ ; duplicate samples per experiment).

Mass spectra [intensity versus  $m/z$  (mass-to-charge ratio) plot] for all phosphotyrosine-modified peptides that were most significantly attenuated in response to c-Met knockdown in U87 sh-control and U87 sh-control  $\Delta$ EGFR cells are provided in Figure 28-1 through Figure 28-20.



**Figure 28-1.** Mass spectrum of the abl interactor 1 (ABI1) Y198 peptide. This spectrum shows Y198 phosphorylation [(R)NTP $\underline{Y}$ KTLEPVKPPTVPNDYMTSPAR(L)]. Peptide Index: 1233.



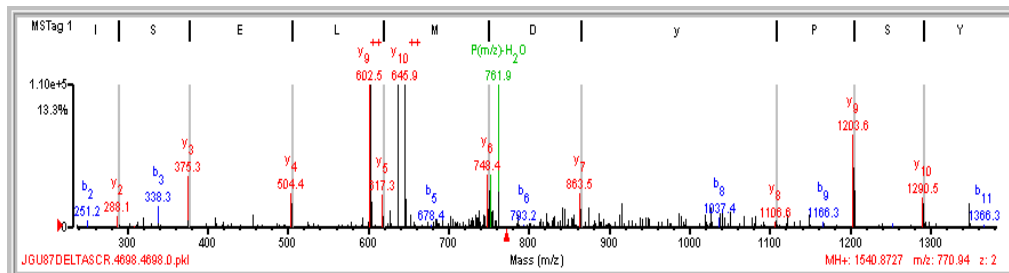


**Figure 28-3.** Mass spectrum of the annexin A2 (ANXA2) Y238 peptide. This spectrum shows Y238 phosphorylation [(K)SYSP<sub>y</sub>DMLESIR(K)]. Peptide Index: 1653.

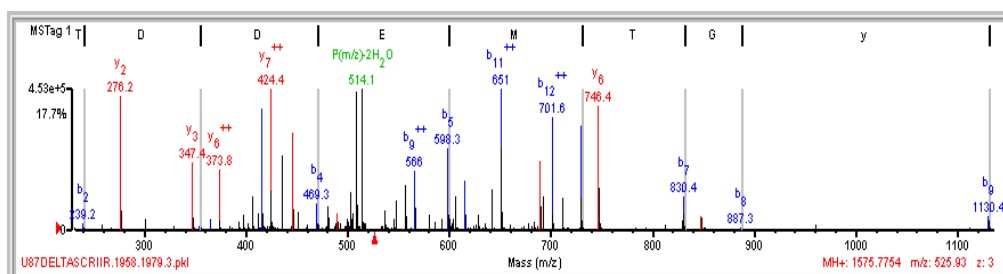


**Figure 28-4.** Mass spectrum of the mitogen-activated protein kinase 14 (MK14) (MAPK14) Y182 peptide. This spectrum shows Y182 phosphorylation [(R)HTDDEMTG<sub>y</sub>VATR(W)]. Peptide Index: 719.

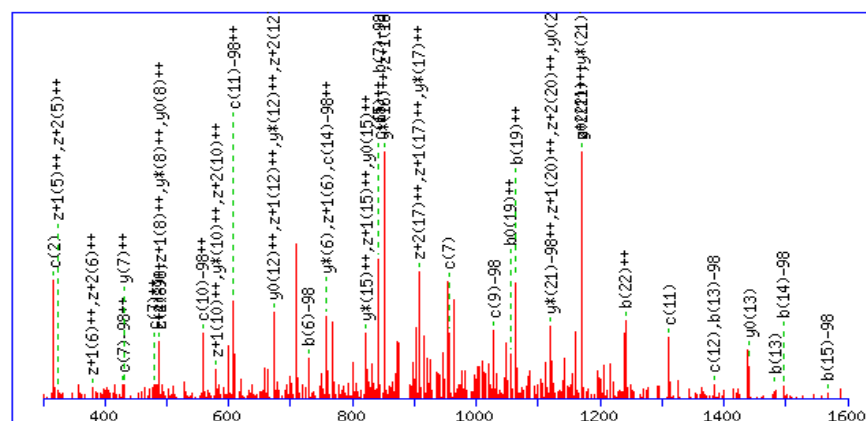


**Figure 28-5.** Mass spectrum of the L-lactate dehydrogenase A (LDHA) Y247 S249 peptide. This spectrum shows Y247 and S249 phosphorylation [(K)G<sub>y</sub>T<sub>s</sub>WAIGLSVADLAESIMKNLR(R)]. Peptide Index: 2247.

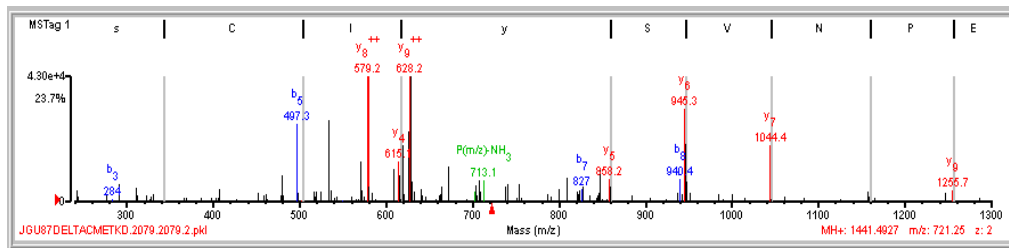


**Figure 28-6.** Mass spectrum of the glycogen synthase kinase 3  $\alpha/\beta$  (GSK3A/B) Y279 S282 peptide. This spectrum shows Y279 and S282 phosphorylation [(R)GEPNVS $\underline{Y}$ ICsR(Y)]. Peptide Index: 808.

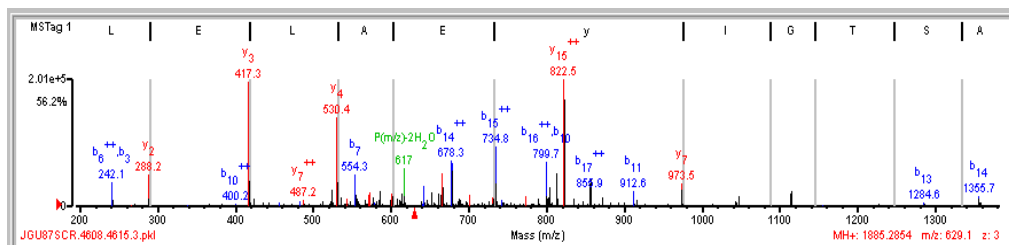


**Figure 28-7.** Mass spectrum of the enolase A (ENOA) (ENO1) Y44 peptide. This spectrum shows Y44 phosphorylation [(R)AAVPSGASTGI $\underline{Y}$ EALRL(D)]. Peptide Index: 1608.

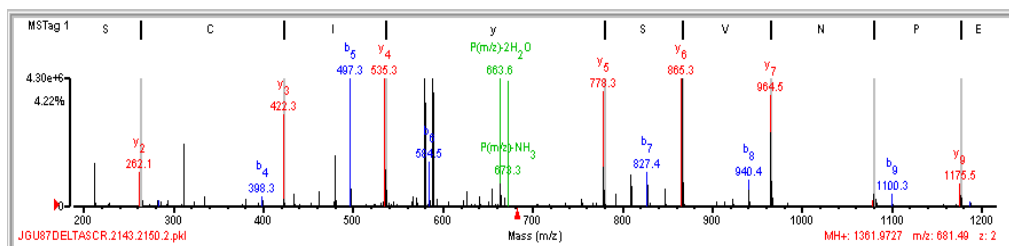


**Figure 28-8.** Mass spectrum of the glycogen synthase kinase 3 $\alpha/\beta$  (GSK3A/B) Y279 peptide. This spectrum shows Y279 phosphorylation [(R)GEPNVS $\underline{Y}$ ICSR(Y)]. Peptide Index: 841.

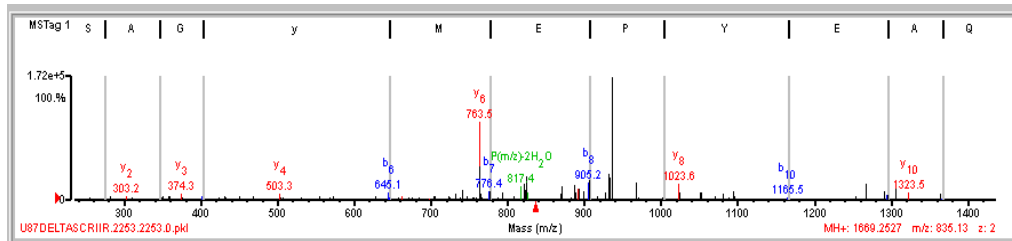


**Figure 28-9.** Mass spectrum of the src homology 2 domain-containing adapter protein B (SHB) Y268 peptide. This spectrum shows Y268 phosphorylation [(K)GESAG $\underline{\text{Y}}$ MEPYEAQR(I)]. Peptide Index: 801.

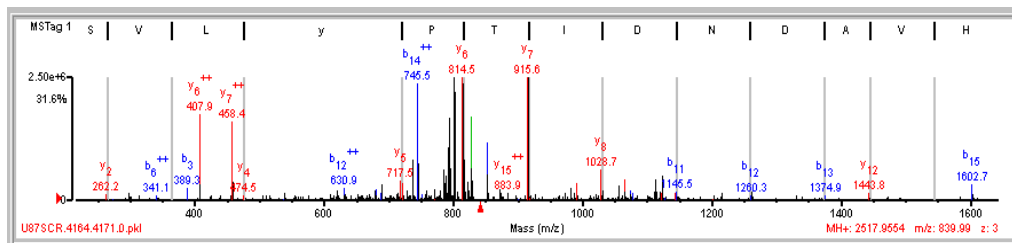


**Figure 28-10.** Mass spectrum of the serine/threonine-protein kinase PRP4 homolog (PRP4B) Y849 peptide. This spectrum shows Y849 phosphorylation [(K)LCDFGSASHVADNDITP $\underline{\text{Y}}$ LVS(R)(F)]. Peptide Index: 1410.

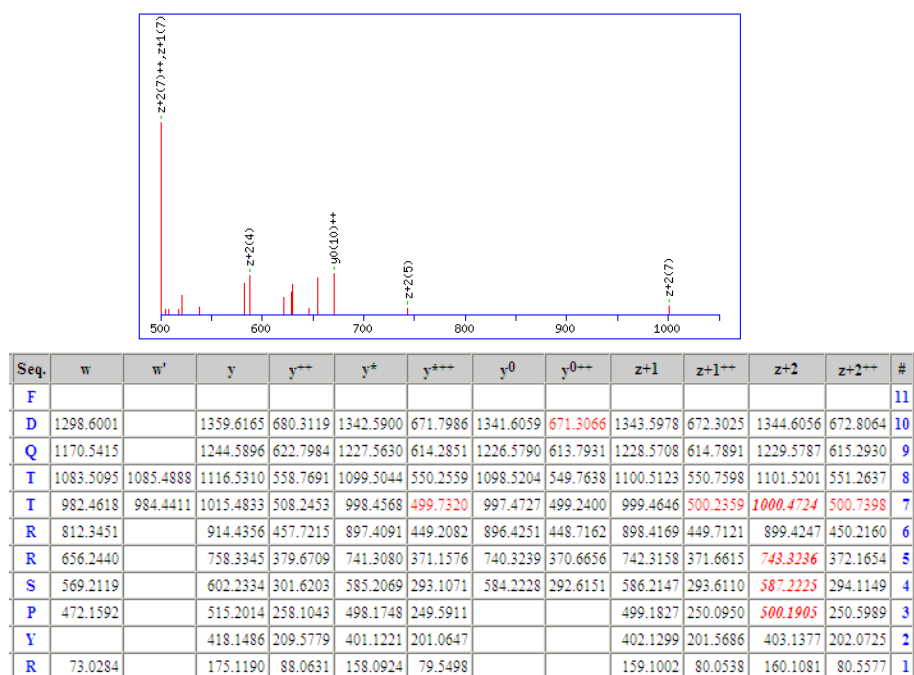


**Figure 28-11.** Mass spectrum of the StAR-related lipid transfer protein 13 (STA13) (STARD13) Y39 peptide. This spectrum and table provides data that indicates Y39 phosphorylation [(R)FDQTTRSPyR(M)]. Peptide Index: 895.

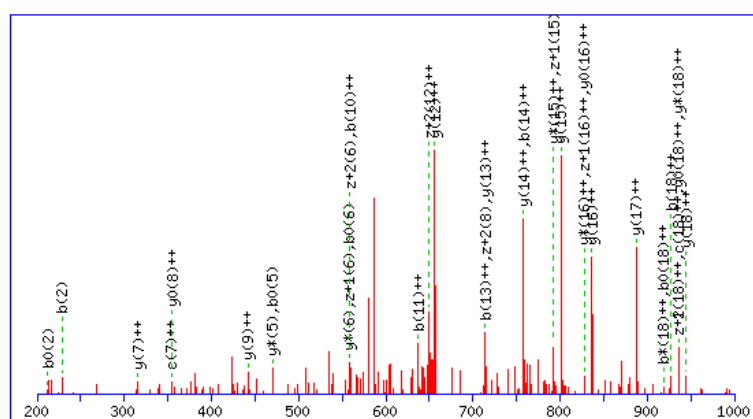


**Figure 28-12.** Mass spectrum of the Rho-GTPase-activating protein 42 (RHG42) Y792 peptide. This spectrum shows Y792 phosphorylation [(R)LDTASSNGyQRPGSVVAAK(A)]. Peptide Index: 741.



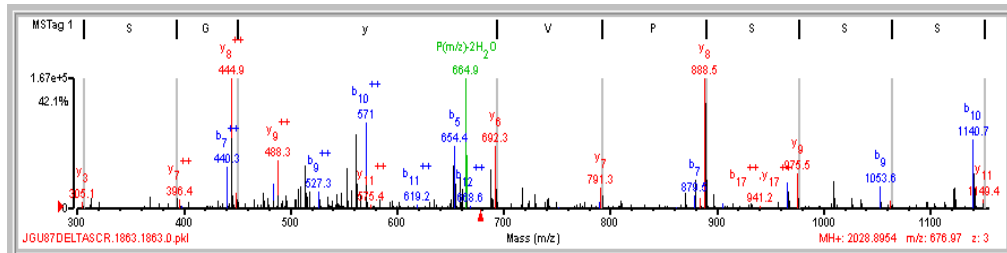


**Figure 28-13.** Mass spectrum of the paxillin (PAXI) (PXN) Y88 peptide. This spectrum shows Y88 phosphorylation [(R)FIHQPPQSSSPV $\mathbf{Y}$ GSSAK(T)]. Peptide Index: 736.

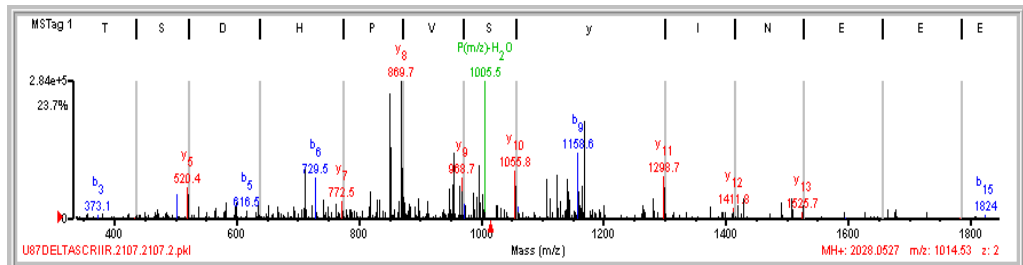


**Figure 28-14.** Mass spectrum of the glucocorticoid receptor DNA binding factor 1 (GRF1) Y1105 peptide. This spectrum shows Y1105 phosphorylation [(R)NEEENI $\mathbf{Y}$ SVPHDSTQGK(I)]. Peptide Index: 770.

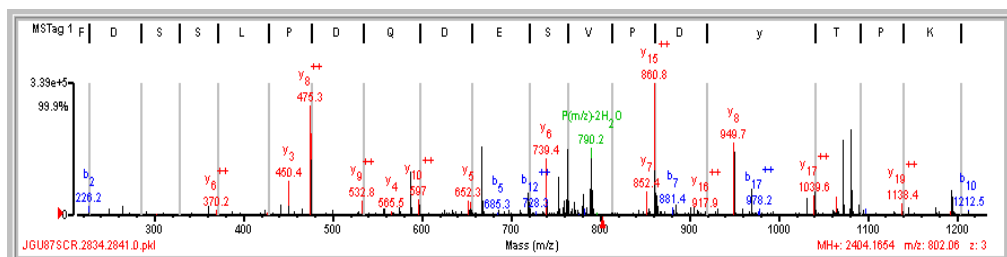


**Figure 28-15.** Mass spectrum of activated CDC42 kinase (ACK1) (TNK2) Y518 peptide. This spectrum shows Y518 phosphorylation [(K)KPT $\mathbf{Y}$ DPVSEDQDPLSSDFKR(L)]. Peptide Index: 1063.

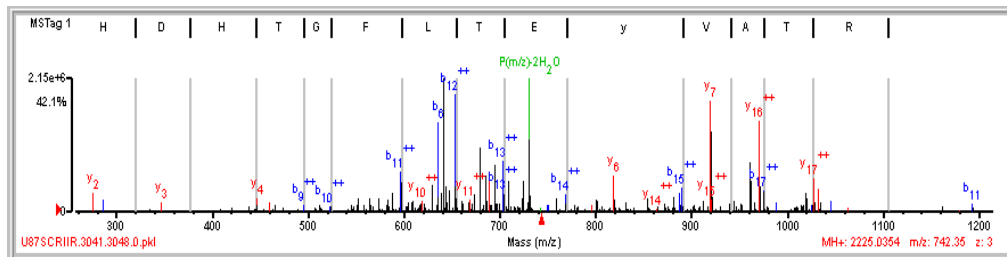


**Figure 28-16.** Mass spectrum of the mitogen-activated protein kinase 1 (MK01) (MAPK1) Y185 peptide. This spectrum shows Y185 phosphorylation [(R)VADPDHDHTGFLTEyVATR(W)]. Peptide Index: 1083.

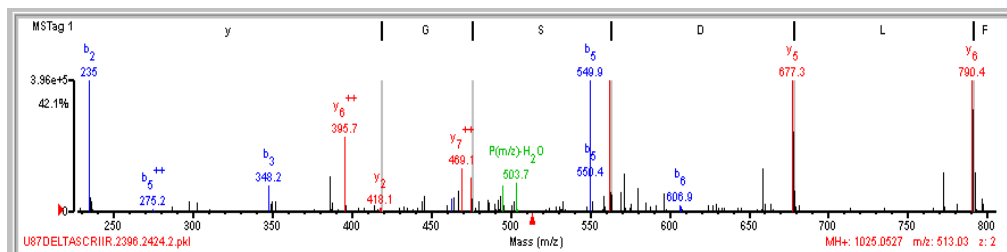


**Figure 28-17.** Mass spectrum of the vinculin (VINC) Y822 peptide. This spectrum shows Y822 phosphorylation [(K)SFLDSGyR(I)]. Peptide Index: 879.

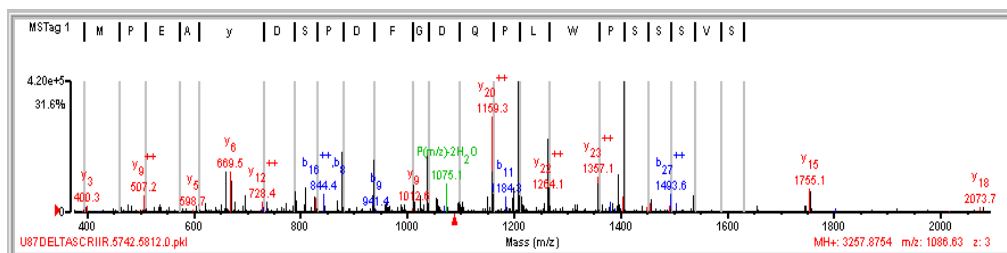


**Figure 28-18.** Mass spectrum of the glucocorticoid receptor DNA-binding factor 1 (GRLF1) Y1087 peptide. This spectrum shows Y1087 phosphorylation [(K)SVSSSPWLPQDGFDPSDAEPMDAVVKPR(N)]. Peptide Index: 1890.

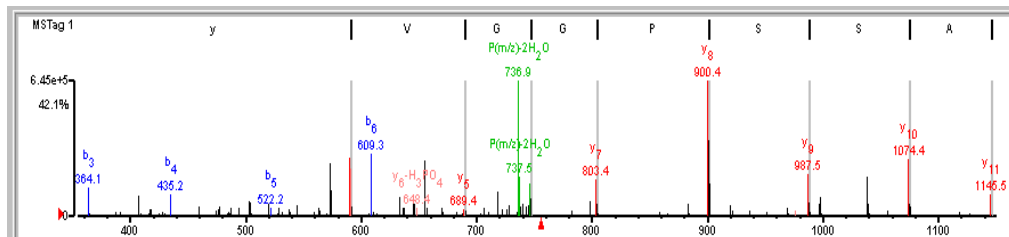
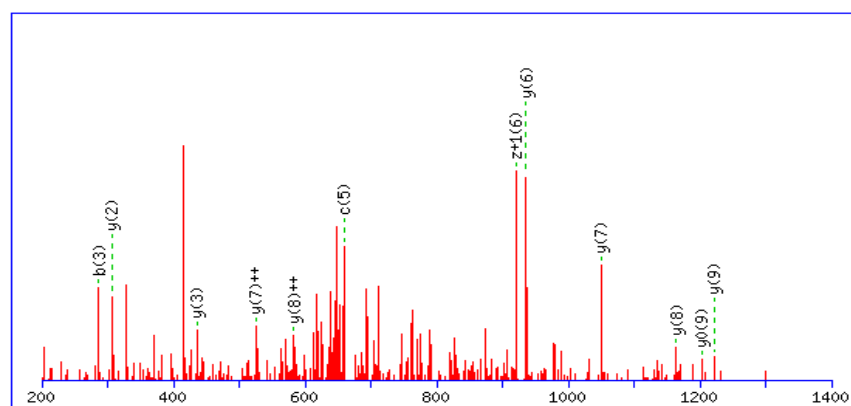


**Figure 28-19.** Mass spectrum of the vimentin (VIME) (VIM) Y61 peptide. This spectrum shows Y61 phosphorylation [(R)SLYASSPGGVyATR(S)]. Peptide Index: 906.



#	b	b <sup>++</sup>	b <sup>0</sup>	b <sup>0++</sup>	c	c <sup>++</sup>	Seq.	w	y	y <sup>++</sup>	y <sup>+</sup>	y <sup>+++</sup>	y <sup>0</sup>	y <sup>0++</sup>	z+1	z+1 <sup>++</sup>	z+2	z+2 <sup>++</sup>	#
1	114.0913	57.5493			131.1179	66.0626	L												10
2	171.1128	86.0600			188.1394	94.5733	G		1221.4493	611.2283	1204.4228	602.7150	1203.4388	602.2230	1205.4306	603.2189	1206.4384	603.7229	9
3	286.1397	143.5735	268.1292	134.5682	303.1663	152.0868	D	1103.4115	1164.4279	582.7176	1147.4013	574.2043	1146.4173	573.7123	1148.4092	574.7082	1149.4170	575.2121	8
4	399.2238	200.1155	381.2132	191.1103	416.2504	208.6288	L	990.3274	1049.4009	525.2041	1032.3744	516.6908	1031.3904	516.1988	1033.3822	517.1947	1034.3900	517.6987	7
5	642.2535	321.6304	624.2429	312.6251	659.2800	330.1436	Y		936.3169	468.6621	919.2903	460.1488	918.3063	459.6568	920.2982	460.6527	921.3060	461.1566	6
6	771.2961	386.1517	753.2855	377.1464	788.3226	394.6649	E	618.2552	693.2872	347.1472	676.2607	338.6340	675.2767	338.1420	677.2685	339.1379	678.2763	339.6418	5
7	900.3387	450.6730	882.3281	441.6677	917.3652	459.1862	E	489.2126	564.2446	282.6259	547.2181	274.1127	546.2341	273.6207	548.2259	274.6166	549.2337	275.1205	4
8	1029.3813	515.1943	1011.3707	506.1890	1046.4078	523.7075	E	360.1700	435.2020	218.1047	418.1755	209.5914	417.1915	209.0994	419.1833	210.0953	420.1911	210.5992	3
9	1160.4217	580.7145	1142.4112	571.7092	1177.4483	589.2278	M	229.1295	306.1594	153.5834	289.1329	145.0701			290.1407	145.5740	291.1485	146.0779	2
10							R	73.0284	175.1190	88.0631	158.0924	79.5498			159.1002	80.0538	160.1081	80.5577	1

**Figure 28-20.** Mass spectrum of the Vimentin (VIME) (VIM) Y150 peptide. This spectrum and table provides information that shows Y150 phosphorylation [(R)LGDLyEEEMR(E)]. Peptide Index: 947.

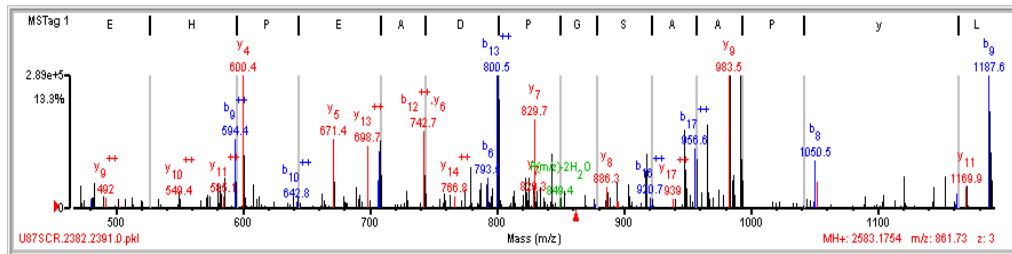
We used Ingenuity Pathway Analysis (IPA; <http://www.ingenuity.com>) to determine which c-Met-dependent signaling pathways are responsible for decreased HGF expression. To do this, we used IPA software to connect known

modulators of HGF expression (Ingenuity Knowledge Base) with all of the peptides that were identified in Table 7 to decrease significantly with c-Met knockdown in U87 sh-control and U87 sh-control  $\Delta$ EGFR cells (Figure 29). Ten out of the possible sixteen proteins that were listed in Table 7 formed biological relationships with proteins found within Ingenuity Knowledge Base's database that would lead to HGF expression. The majority of the proposed signaling pathways converged on STAT3. Therefore, our data suggested that STAT3 signaling may play a key role in regulating HGF expression in a c-Met-dependent manner.



**Figure 29.** Ingenuity pathway analysis of c-Met-dependent phosphopeptides identified by mass spectrometry that may modulate HGF expression. Biological relationships that lead to HGF expression were explored in Ingenuity Knowledge Base's database from peptides that were identified by PhosphoScan analysis as being responsive to the c-Met signal in U87 cells (Dr. Vaibhav Chumbalkar, Dr. Oliver Bögl's former post-doctoral fellow, assisted with IPA analysis).

Although STAT3 did not surface in our mass spectrometry-based screen as a significantly changed phosphopeptide with c-Met knockdown, it was identified in all of the cell lines that were processed for mass spectrometry analysis (Figure 30), and confirmed to decrease with c-Met knockdown in U87 and U87  $\Delta$ EGFR cells (Figure 31A). This finding was confirmed in cell lysates from the cell lines that were processed for Phosphoscan analysis (Figure 31B).



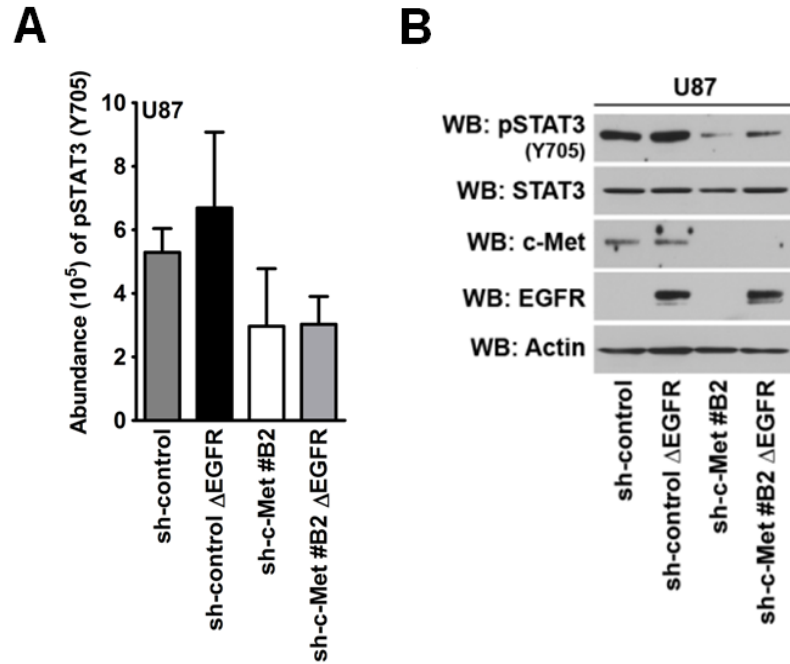


**Figure 31.** STAT3 Y705 phosphorylation decreases with c-Met knockdown in U87 and U87  $\Delta$ EGFR cells. (A) PhosphoScan mean intensity values ( $10^5$ ) of STAT3 Y705 phosphorylation in U87 sh-control cells with or without c-Met knockdown and / or  $\Delta$ EGFR expression (n = 2; duplicate samples per experiment; mean abundance  $\pm$  SEM). (B) Western blot validation of pSTAT3 Y705 phosphorylation in cells that were analyzed by mass spectrometry.

Inhibition of the c-Met and  $\Delta$ EGFR signal in U87  $\Delta$ EGFR cells with AG1478 and SU11274 treatment, respectively, effectively decreased the phosphorylation of STAT3 (Y705) and of Src (Y416) (Figure 32), a known non-receptor tyrosine kinase that activates STAT3 by phosphorylation at Y705 (Wojcik et al., 2006). Even though Src (Y416) phosphorylation was attenuated with EGFR and c-Met inhibition in U87 parental cells, STAT3 (Y705) phosphorylation was not as strongly attenuated. We also observed that STAT3 (Y705) phosphorylation did not increase in intensity with  $\Delta$ EGFR expression in U87 cells, consistent with findings in previous reports (Huang et al., 2009).

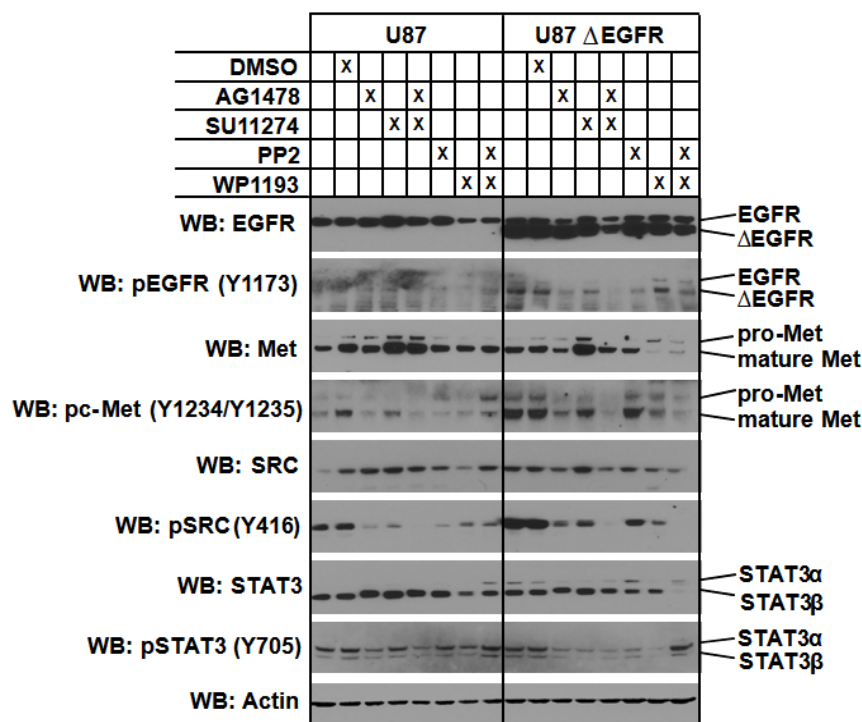


**Figure 32.** STAT3 activity decreases with c-Met and  $\Delta$ EGFR inhibition in U87  $\Delta$ EGFR cells. Western blot analysis of U87 and U87  $\Delta$ EGFR cells that were treated for 20 h with either 0.1% DMSO, 10  $\mu$ M AG1478 (EGFR and  $\Delta$ EGFR antagonist), 10 $\mu$ M SU11274 (c-Met antagonist), a combination of 10  $\mu$ M AG1478 and 10 $\mu$ M SU11274, 10  $\mu$ M PP2 (Src antagonist), 2.5  $\mu$ M WP1193 (STAT3 antagonist), or a combination of 10  $\mu$ M PP2 and 2.5  $\mu$ M WP1193. Src and STAT3 inhibition with PP2 and WP1193, respectively, served as positive controls. Cells were cultured in 10% FBS-containing media.

Taken together, these data suggest that the phosphorylation of STAT3 at Y705 is modulated by c-Met in U87 cells, and that STAT3 may be an important signaling effector necessary for HGF production in these cells.

## STAT3 Partially Rescues Attenuated HGF and Anchorage-independent Growth of c-Met Silenced U87 $\Delta$ EGFR Cells

Given that STAT3 most likely regulates HGF expression in response to the c-Met signal in GBM cells, we tested if inhibition of STAT3 activity could modulate HGF expression. We treated U87  $\Delta$ EGFR cells with WP1193, a phosphorylation inhibitor of STAT3 Y705 (Kong et al., 2010), and analyzed HGF mRNA expression by qRT-PCR in these cells. We found that with STAT3 Y705 inhibition that HGF mRNA levels were attenuated (Figure 33A). The inhibition of STAT3 Y705 phosphorylation following the treatment of U87  $\Delta$ EGFR cells with WP1193 was confirmed by western blot (Figure 33B).

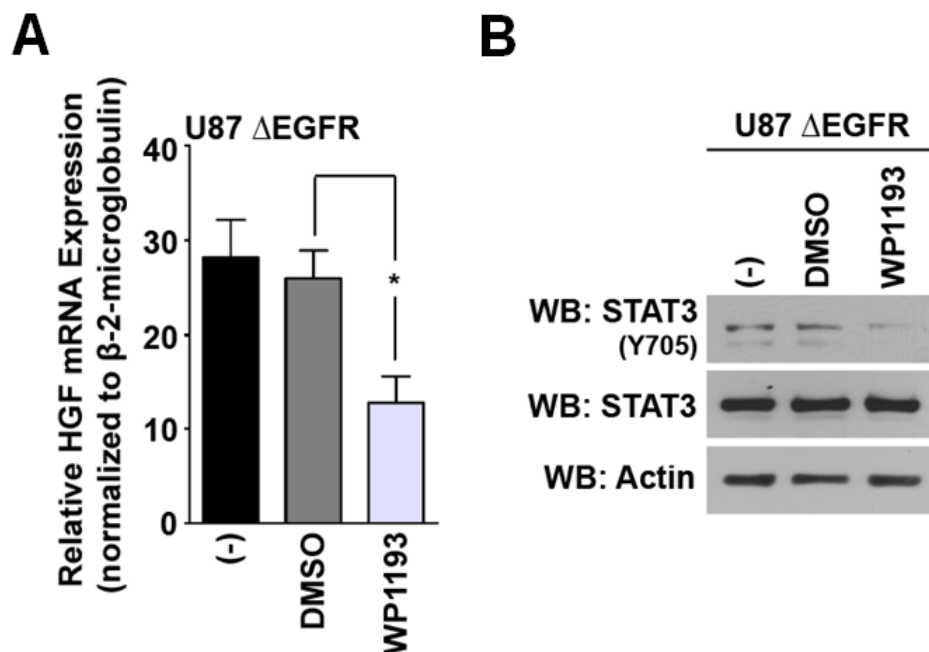


**Figure 33.** STAT3 Y705 inhibition attenuates HGF mRNA expression in U87  $\Delta$ EGFR cells. (A) HGF mRNA amounts were quantified in U87  $\Delta$ EGFR cells by qRT-PCR after 16 h of being untreated (-), or after they were treated with vehicle (0.1% DMSO) or with 2.5  $\mu$ M WP1193 (STAT3 phosphorylation inhibitor). Cells were cultured in media containing 10% FBS (\* =  $P < 0.05$ ; Student's t-test compared with DMSO-treated cells;  $n = 3 \pm \text{SEM}$ ; samples were analyzed at least in duplicate per experiment). (B) Aliquots of the cells that were treated in (A) were analyzed using western blotting techniques to ensure that WP1193 had decreased STAT3 Y705 phosphorylation.



Constitutively activate STAT3, produced by substitution of two SH2 domain cysteine residues with Ala661 and Asn664 (Bromberg et al., 1999; Ning et al., 2001), spontaneously dimerizes to enhance STAT3's function as a transcription factor (Bromberg et al., 1999). We tested whether the expression of constitutively active STAT3 (STAT3-CA) would be able to rescue the HGF production deficit found in U87 sh-control  $\Delta$ EGFR cells with c-Met knockdown. We overexpressed an empty vector control or STAT3-CA in U87 sh-control  $\Delta$ EGFR and in U87 sh-c-Met #B2  $\Delta$ EGFR cells, and analyzed their HGF mRNA abundance by q-RT-PCR and by western blot. We found that STAT3-CA partially rescued HGF mRNA (Figure 34A) and protein (Figure 34B) amounts in  $\Delta$ EGFR-expressing GBM cells with c-Met knockdown.

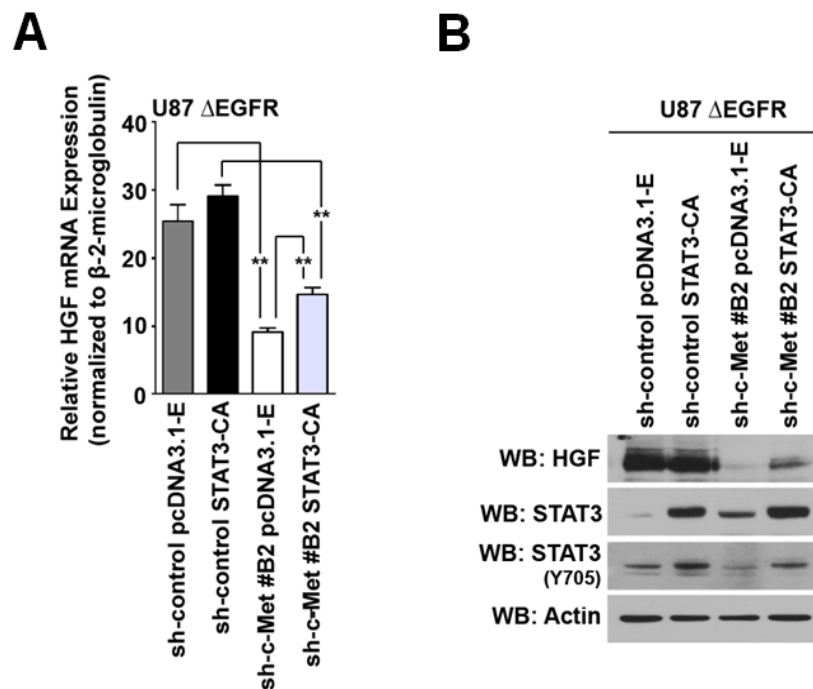


**Figure 34.** Constitutively active STAT3 partially rescues HGF expression in c-Met silenced U87  $\Delta$ EGFR cells. (A) qRT-PCR quantified HGF mRNA amounts in U87 sh-control  $\Delta$ EGFR pcDNA3.1-E cells, U87 sh-control  $\Delta$ EGFR STAT3-CA cells, U87 sh-c-Met #B2  $\Delta$ EGFR pcDNA3.1-E cells, and in U87 sh-c-Met #B2  $\Delta$ EGFR STAT3-CA cells. Cells were cultured in media containing 10% FBS

( $P < 0.01$ ; Student's t-test;  $n = 3 \pm \text{SEM}$ ; samples were analyzed at least in duplicate per experiment). (B) All cells detailed in (A) were analyzed for their HGF expression and STAT3 Y705 phosphorylation by western blot.

In an effort to determine whether the promoter activity of HGF, which contains a STAT3 consensus binding site in the proximal promoter at -99/-91 (TTACCGTAA; Tomida and Saito, 2004), would decrease with c-Met knockdown in U87 cells we performed promoter assays. We initially examined if the activity of a HGF-1029-luciferase reporter (Figure 35A) would increase compared with a pGL2-basic construct in U87 cells. By doing this, we determined that the HGF-1029-luciferase construct was functional (Figure 35B). Surprisingly, we found that HGF promoter activity with the first -1029 bp did not decrease with silencing of c-Met in U87 cells (Figure 35C). These data suggested that the HGF gene may be regulated transcriptionally beyond the first -1029 base pairs, or that HGF expression may be modulated at the RNA level.

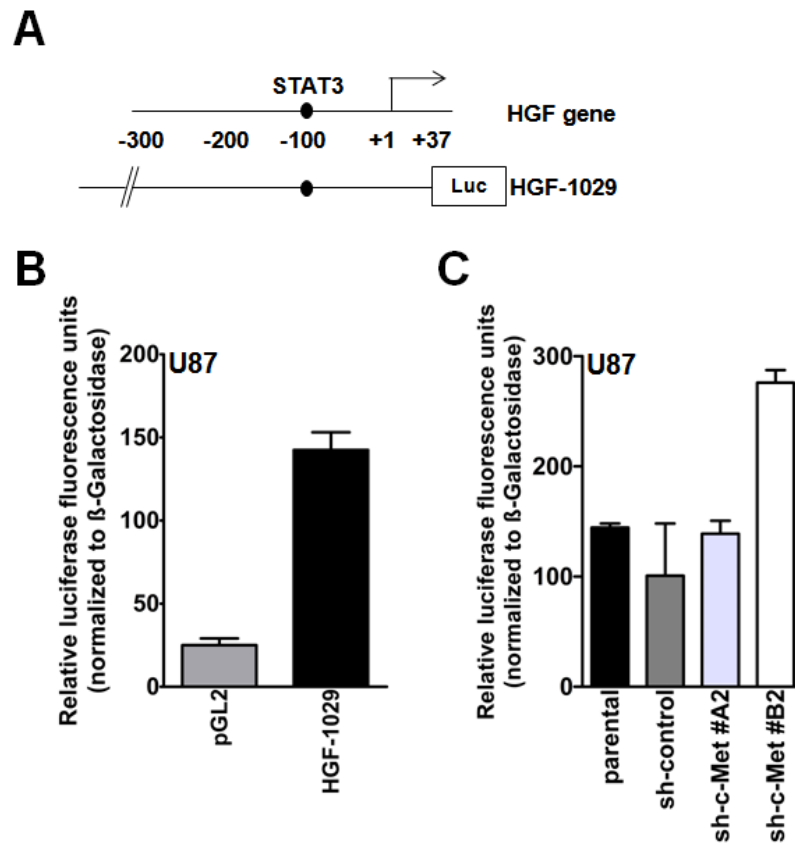


**Figure 35.** HGF promoter activity is unresponsive to c-Met knockdown in U87 cells. (A) Schematic of the pGL2-HGF-luciferase (-1029 bp) reporter construct used to examine HGF promoter activity in (B) and (C). The STAT3 consensus binding site at circa -100 bp is depicted. (B) U87 cells were transfected with a HGF-1029-luciferase reporter construct or a pGL2-basic-luciferase reporter construct along with a pSV- $\beta$ -galactosidase construct and then harvested for measurement of luciferase and  $\beta$ -galactosidase activity ( $\pm$  SEM). (C). Luciferase assays measured the activity of the HGF-1029 promoter construct when transfected into U87, U87 sh-control, U87 sh-c-Met #A2 and U87 sh-c-Met #B2 cells (normalized to  $\beta$ -galactosidase activity;  $n=2 \pm$  SEM).

To determine if the stability of HGF mRNA was affected with c-Met knockdown in U87 cells, we pretreated U87, U87 sh-control, U87 sh-c-Met #A2, and U87 sh-c-Met #B2 cells with actinomycin D, a transcription inhibitor, for 1 h and then quantified HGF mRNA levels at 0 h and 8 h by qRT-PCR. HGF did not decay at a faster rate in U87 cells with c-Met knockdown than in U87 parental or

U87 sh-control cells within 8 h (Figure 36). c-Myc was used as a positive control, due to its rapid turnover rate in U87 cells (Marderosian et al., 2006). These results fail to show a profound impact on HGF mRNA stability, and so indicate that c-Met-dependent HGF regulation was most likely not due to post-transcriptional instability of mRNA.

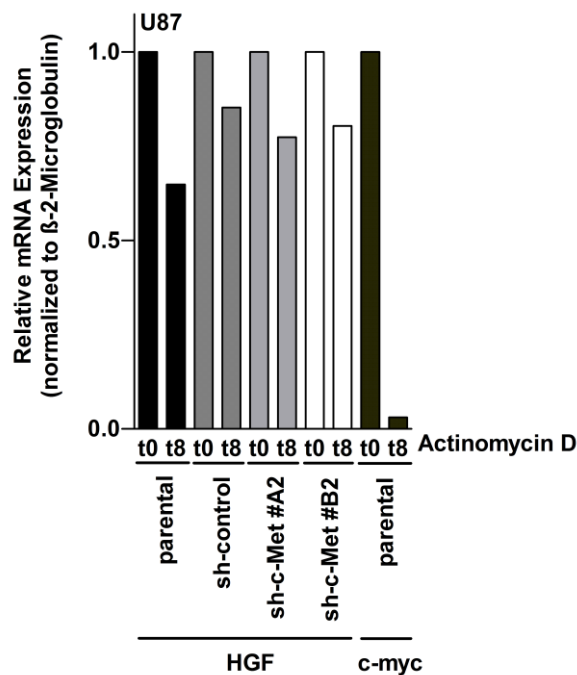


**Figure 36.** c-Met knockdown does not affect HGF mRNA stability. Q-RT-PCR measured HGF mRNA amounts at 0 h and 8 h following the exposure of U87 cells to 5 ug / mL Actinomycin D (samples were analyzed in triplicate and compared relative to cells analyzed at t0; c-myc mRNA instability served as a positive control).

We determined if STAT3-CA could restore the loss in anchorage-independent growth that we had observed with c-Met knockdown in U87  $\Delta$ EGFR

cells (Figure 23). By performing *in vitro* colony formation assays, we found that STAT3-CA was capable of partially restoring deficits in anchorage-independent growth found with c-Met knockdown in these cells (Figure 37). This effect was comparable to its capability of rescuing HGF expression in c-Met knockdown cells (Figure 34).

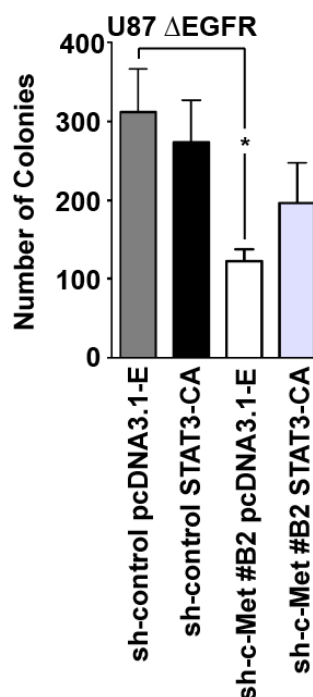


**Figure 37.** STAT3 partially rescues colony formation associated with c-Met knockdown in U87  $\Delta$ EGFR cells. Anchorage-independent growth was assessed using U87 sh-control  $\Delta$ EGFR pcDNA3.1-E cells, U87 sh-control  $\Delta$ EGFR STAT3-CA cells, U87 sh-c-Met #B2  $\Delta$ EGFR pcDNA3.1-E cells, and U87 sh-c-Met #B2  $\Delta$ EGFR STAT3-CA cells after 14 days in culture (\* =  $P < 0.05$ ; Student's t-test;  $n = 3 \pm \text{SEM}$ ; samples were analyzed at least in duplicate per experiment).

Our results therefore suggest that STAT3 is a key signaling effector that regulates HGF expression in response to c-Met signaling in  $\Delta$ EGFR-expressing

GBM cells, although it does not appear to be the only regulator. Other pathways are therefore most likely required for maximal HGF expression in this model (Figure 38). Taken together, our data suggest that the ligand-dependent and ligand-independent activation of c-Met drives HGF expression partly via STAT3.

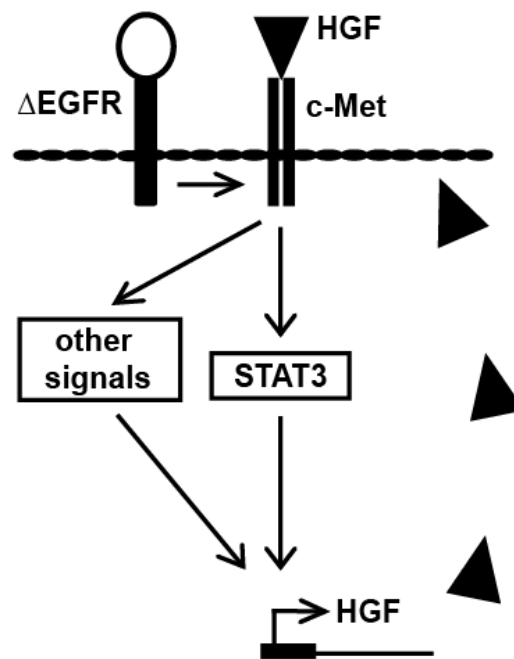


**Figure 38.** Proposed model of enhanced HGF expression via c-Met activation in GBM cells.

## **CHAPTER 6**

### **RESULTS**

#### **THE C-MET / HGF AXIS IS UPREGULATED IN MESENCHYMAL GBM TUMORS**

Using IPA, we showed that STAT3 activity is necessary, but still requires additional signaling pathways, for HGF expression in response to the c-Met signal in GBM cells (Figure 29); a finding subsequently validated *in vitro* (Figure 34). The IPA bioinformatic analysis identified that C/EBP $\beta$  and STAT3 are dependent on the same upstream signaling effectors that are required for c-Met-dependent HGF expression, suggesting that they may work in concert to maximally upregulate HGF expression.

STAT3 and C/EBP $\beta$  are master regulators of the mesenchymal GBM subtype (Carro et al., 2010). This subclass of GBM tumors is associated with a poorer prognosis compared with proneural tumors (Phillips et al., 2006). YKL-40, a mesenchymal signature gene, confers resistance to radiotherapy (Pellowski et al., 2005) and is upregulated in recurrent tumors (Phillips et al., 2006). This was consistent with an observation that many recurrent tumors tend to shift their gene expression signature to that of the mesenchymal GBM subtype (Phillips et al. 2006). Based on our prior bioinformatic data that processed c-Met dependent phosphopeptides in the context of HGF regulation, we were interested in determining whether the c-Met / HGF axis is upregulated in mesenchymal GBM tumors. TCGA GBM tumors have been classified into four subtypes by Verhaak and colleagues (2010) based on specific signature gene sets for each GBM subtype; with those subtypes being mesenchymal, proneural, neural, and classical. We extracted c-Met and HGF gene expression values (Agilent platform; TCGA's GBM level 3 gene expression data) for each tumor that had already been classified as one of the four GBM subclasses by Verhaak et al., 2010. Elevated c-Met (Figure 39) and HGF (Figure 40) mRNA expression associated significantly



with the mesenchymal GBM subtype when compared with tumors having a proneural, neural, or classical assignment.

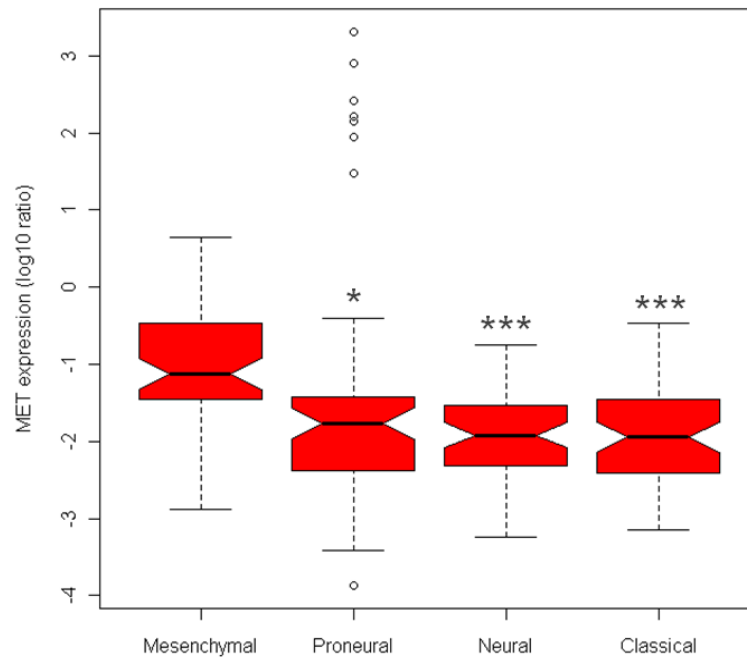


**Figure 39.** c-Met mRNA expression is upregulated in the mesenchymal GBM subtype (Verhaak determined). c-Met mRNA abundance was determined in tumors that were assigned as one of four GBM subtypes (mesenchymal, proneural, neural, and classical) by Verhaak and colleagues (2010). Level 3 mRNA expression data was downloaded from TCGA, which was represented as a  $\text{Log}_{10}$  ratio to a reference RNA (\* =  $P < 0.05$ ; \*\*\* =  $P < 0.001$ ; Welch's t-test compared with the mesenchymal GBM subtype;  $n = 200$ ; Dr. Brian Vaillant, Dr. Howard Colman's former post-doctoral fellow, performed this analysis).

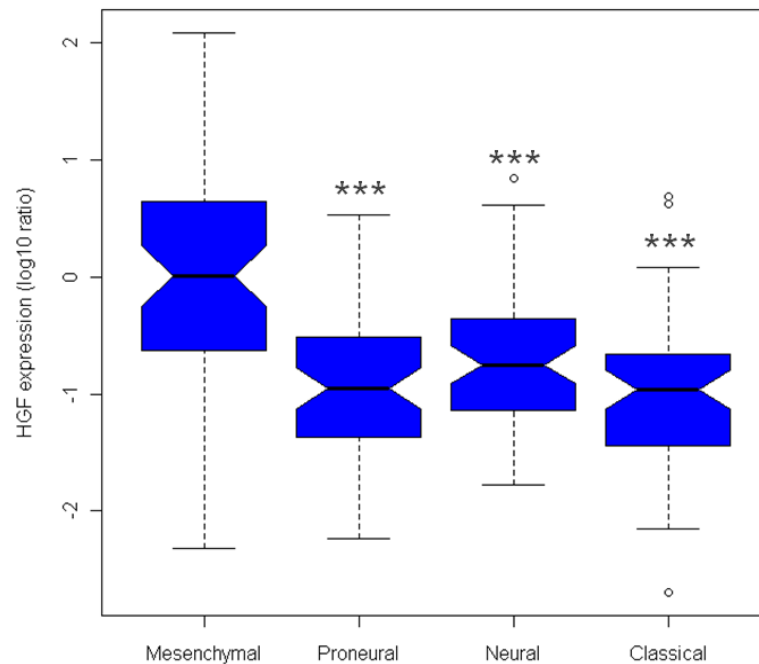


**Figure 40.** Enhanced HGF mRNA expression associates with the mesenchymal GBM subtype (Verhaak determined). HGF mRNA expression was determined in tumors that were assigned a GBM subtype (mesenchymal, proneural, neural, and classical; Verhaak et al., 2010). TCGA levels 3 mRNA expression data were represented as a Log<sub>10</sub> ratio to a reference RNA (\*\*\*) =  $P < 0.001$ ; Welch's t-test compared with the mesenchymal GBM subtype;  $n = 200$ ; Dr. Brian Vaillant, Dr. Howard Colman's former post-doctoral fellow, performed this analysis).

At the time when Verhaak and colleagues (2010) classified TCGA GBM tumors into either mesenchymal, proneural, neural, or classical subtypes, there were only 200 GBM tumors in the database with gene expression profiles. Since then, the TCGA database has included gene expression data for an additional 295 tumors. Therefore, we wanted to examine whether our initial findings, which showed that enhanced c-Met and HGF expression correlated with mesenchymal GBM tumors, would remain robust in an analysis that made use of a larger 495

tumor dataset. Verhaak and colleagues (2010) defined specific lists of gene sets for the various GBM subtypes, which we used to calculate average metagene expression values for each tumor. Tumors were then assigned to a GBM subtype based on the highest average metagene score. We then analyzed each tumor for their c-Met and HGF mRNA expression. In agreement with our previous data, we found that their higher expression levels correlated with the mesenchymal GBM subtype (Figure 41 and Figure 42, respectively).

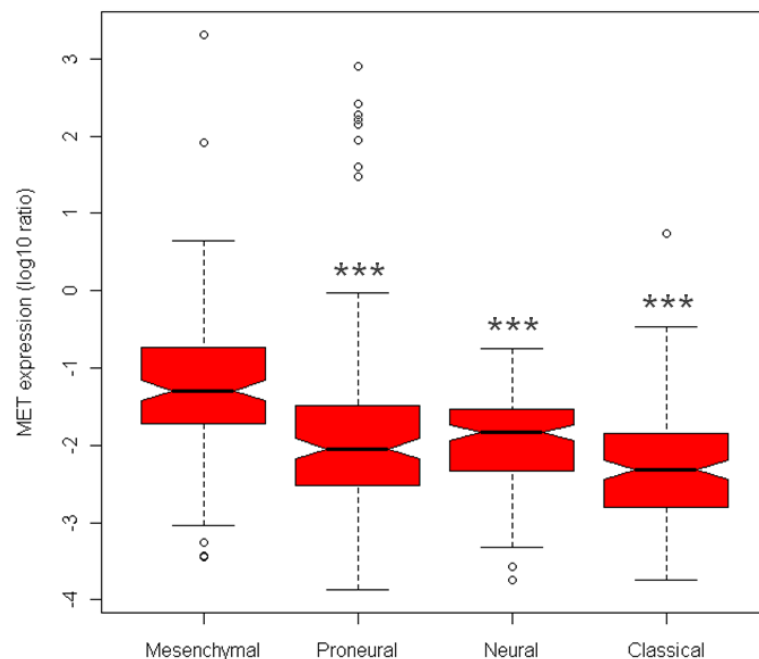


**Figure 41.** c-Met mRNA expression is elevated in mesenchymal GBM tumors (Verhaak calculated). Tumors were assigned a GBM classifier (mesenchymal, proneural, neural, classical) according to the highest metagene score for each GBM subtype, from lists previously defined by Verhaak et al. (2010). c-Met mRNA expression ( $\log_{10}$  ratios to reference RNA) levels were then documented per tumor (\*\*\*) =  $P < 0.001$ ; Welch's t-test compared with the mesenchymal GBM subtype;  $n = 495$ ; Dr. Brian Vaillant, Dr. Howard Colman's former post-doctoral fellow, performed this analysis).

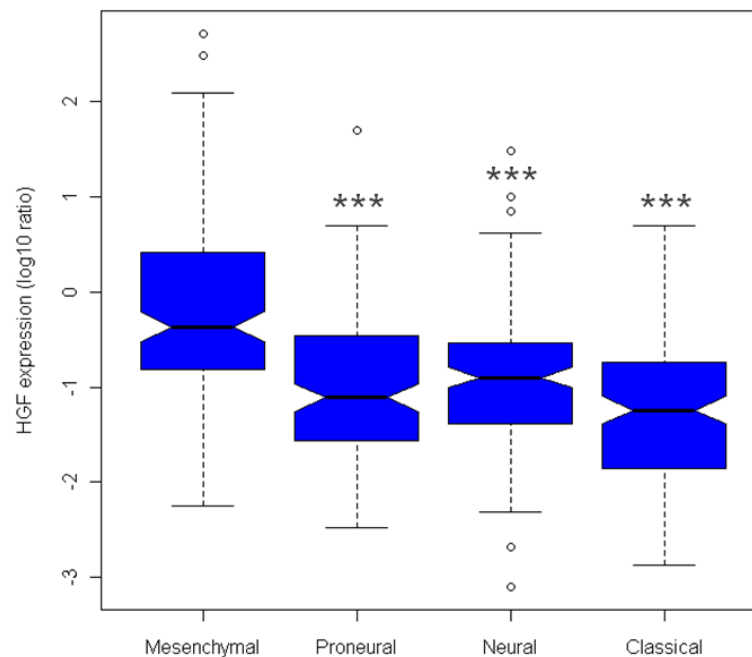


**Figure 42.** Mesenchymal GBM tumors express increased levels of HGF mRNA (Verhaak calculated). GBM tumors (495) were designated as mesenchymal, proneural, neural or classical as defined by gene lists reported by Verhaak et al., 2010. TCGA HGF mRNA expression, expressed as  $\log_{10}$  ratios to a reference RNA, were then documented per tumor (\*\* =  $P < 0.001$ ; Welch's t-test compared with the mesenchymal GBM subtype;  $n = 495$ ; Dr. Brian Vaillant, Dr. Howard Colman's former post-doctoral fellow, performed this analysis).

Phillips and colleagues (2006) were the first authors to describe a set of genes that classified mesenchymal, proneural, and proliferative GBM tumors. They clearly showed that patient survival was significantly impacted if GBMs were either mesenchymal or proliferative, compared with those patients having proneural tumors; mesenchymal tumors had the worst prognosis. Both Phillips et al., 2006 and Verhaak et al., 2010 identified the mesenchymal and proneural GBM subclasses, assigning them with similar functional definitions, however their gene lists for each of these subtypes differed. We used the gene lists described by

Phillips et al., 2006 for mesenchymal, proneural, or proliferative GBM tumors in the TCGA dataset to determine which subclass had the highest c-Met and HGF expression. We found that increased levels of c-Met and HGF mRNA expression associated most with the mesenchymal class of GBM tumors that were defined by Phillips et al. (2006), although there was no significant difference in expression between the mesenchymal and proliferative GBM subclasses (Figure 43 and Figure 44, respectively). Significantly, the proneural GBMs expressed much less c-Met and HGF than mesenchymal tumors, suggesting that survival may be impacted with greater abundance of the c-Met / HGF axis, which is consistent with a previous report (Kong et al., 2009).

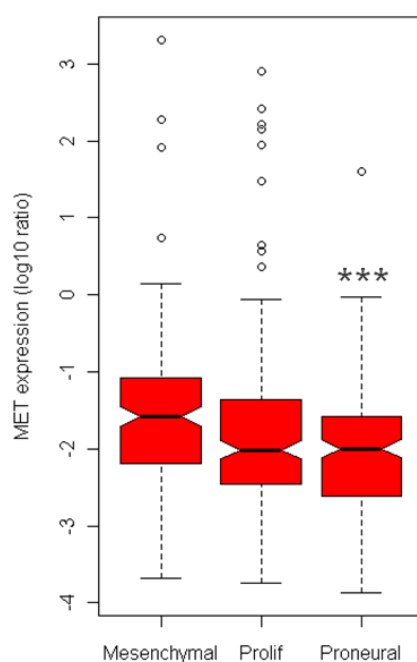


**Figure 43.** Mesenchymal and proliferative GBM tumors express elevated c-Met mRNA levels (Phillips calculated). c-Met mRNA expression ( $\log_{10}$  ratios to reference RNA) for 495 GBM tumors was downloaded from the TCGA database. Each GBM tumor was subclassified as a GBM subtype (mesenchymal, proliferative, or proneural). This was based on the highest average gene list score per GBM subtype, as defined by Phillips et al., 2006 (\*\*\*) =  $P < 0.001$ ; Welch's t-test compared with the mesenchymal GBM subtype;  $n = 495$ ;  $P < 0.01$  when c-Met expression was compared in proliferative versus proneural GBMs using Welch's t-test; Dr. Brian Vaillant, Dr. Howard Colman's former post-doctoral fellow, performed this analysis).

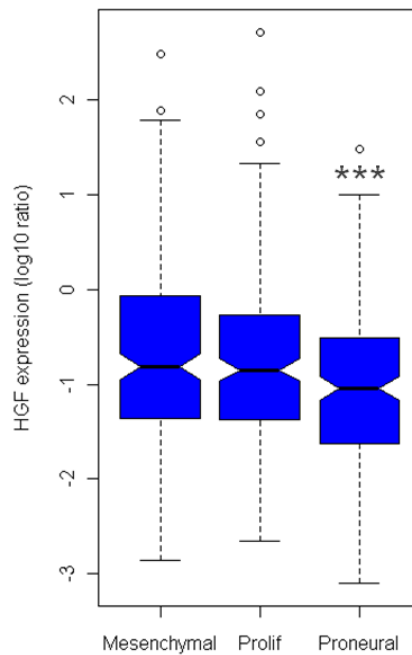


**Figure 44.** Increased HGF mRNA expression associates most with the mesenchymal and proliferative GBM subtypes (Phillips calculated). HGF gene expression values were extracted from the TCGA database for 495 GBM tumors. Each tumor was assigned to either the mesenchymal, proliferative, or proneural GBM subtype, according to the highest average metagene score. Gene lists per GBM subtype were described by Phillips et al., 2006 (\*\*\*) =  $P < 0.001$ ; Welsh's t-test compared with the mesenchymal GBM subtype;  $n = 495$ ;  $P < 0.05$  when HGF expression was compared in proliferative versus proneural GBMs using Welsh's t-test; Dr. Brian Vaillant, Dr. Howard Colman's former post-doctoral fellow, performed this analysis).

False-discovery rates in microarray studies are high if only single datasets are evaluated; data interpretation would need to be performed with caution (Colman et al., 2010). Therefore, we validated our findings in an independent sample set of GBM tumors, available in the REMBRANDT database, that were processed on a different platform (Affymetrix gene expression platform) to that of our previous dataset (Agilent gene expression platform). Average metagene scores were calculated per GBM subtype for each tumor, which was based on

Verhaak et al., 2010- determined gene lists for the four GBM subtypes. Then, tumors were binned to a GBM subtype, and their c-Met and HGF expression levels extracted. We found higher c-Met (Figure 45) and HGF (Figure 46) expression levels in the mesenchymal-angiogenic GBM subclass compared with all others. Proneural and neural tumors did not differ significantly from mesenchymal tumors in terms of their overall c-Met expression, which was possibly due to the presence of a few outliers in those GBM subtypes and an inferior c-Met probe set on the Affymetrix gene expression platform.

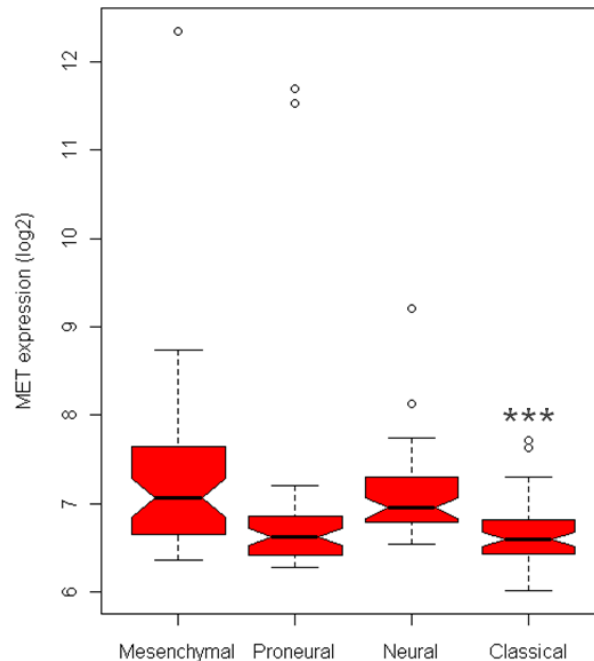


**Figure 45.** Validation that higher c-Met expression levels associates with the mesenchymal GBM subtype in an independent sample set (Verhaak calculated). Expression data for GBM tumors were obtained from the REMBRANDT database, which were represented as log2 transformed data after they had been normalized to pooled normal brain. Tumors were assigned to a GBM subtype according to their highest average metagene value per Verhaak determined GBM subtype. Gene lists per GBM subtype were described by Verhaak et al., 2010 (\*\*\*) =  $P < 0.001$ ; Welch's t-test compared with the mesenchymal GBM subtype;  $n = 180$ ; Dr. Brian Vaillant, Dr. Howard Colman's former post-doctoral fellow, performed this analysis).

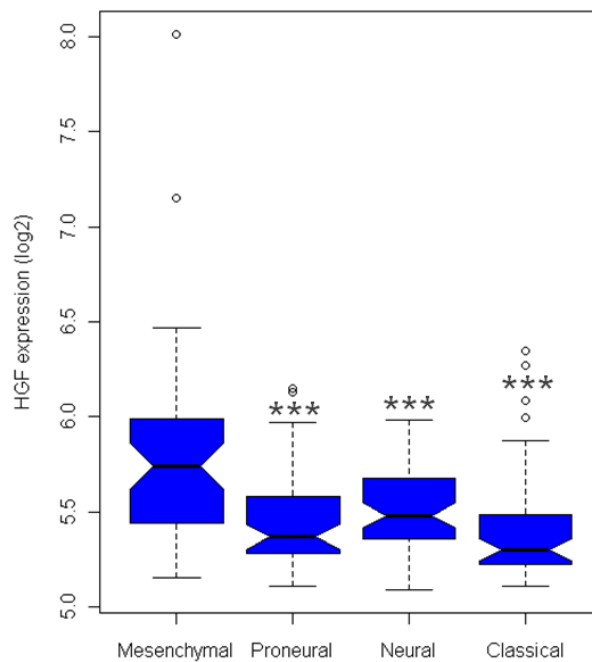


**Figure 46.** Independent dataset validation that elevated HGF expression levels associate with the mesenchymal GBM subtype (Verhaak calculated). mRNA expression data for 180 GBM tumors was obtained from the REMBRANDT database. These data were normalized to pooled normal brain expression data, and then log2 transformed. Verhaak et al., 2010 determined which genes defined each GBM subtype, and accordingly this list was used to calculate an average expression score per tumor. Tumors were assigned to a GBM subtype based on the highest average expression score, and their HGF expression levels reported (\*\*\*) =  $P < 0.001$ ; Welch's t-test compared with the mesenchymal GBM subtype;  $n = 180$ ; Dr. Brian Vaillant, Dr. Howard Colman's former post-doctoral fellow, performed this analysis).

In summary, our results suggest that upregulation of the c-Met / HGF axis is strongly associated with the mesenchymal GBM subtype. Since antagonists of this receptor ligand pair are available, our data may be developed further by performing additional basic and pre-clinical studies with an eventual goal of being able to treat patients according to the molecular subtype of their tumor.



## **CHAPTER 7**

### **DISCUSSION**

GBM is a relentless and cruel disease. Not only is it invariably lethal, but patients suffer loss of higher neurocognition within a very short amount of time (Bosma et al., 2007). Conventional therapies have only slightly improved upon patient prognosis over the past few decades, making the expedited identification of effective targets necessary (Lassman and Holland, 2007). For these reasons, GBM has often been given priority status. For example, GBM was the first cancer genome analyzed by the TCGA for important genetic changes that lead to dysregulated signaling pathways, even though it is not a very prevalent cancer (The Cancer Genome Atlas Research Network, 2008). One such pathway is the c-Met / HGF signaling axis, which has been found to be a key determinant of brain tumor malignancy (Abounader and Lattera, 2009). In studies with a limited number of samples, it has been shown that c-Met and HGF coexpression increases with glioma grade (Koochekpour et al., 1997; Moriyama et al., 1998). We showed for the first time that c-Met and HGF expression are positively correlated in a large dataset of 495 GBMs. Importantly, our data revealed that the highest expression levels of HGF and c-Met were found in mesenchymal GBM tumors; the most aggressive GBM subtype that is associated with the worst prognosis (Phillips et al., 2005). Interestingly, HGF appeared to have a stronger differentiation for the mesenchymal GBM subgroup than c-Met. This may be due to an inferior c-Met probe set, which will not correctly reflect the underlying biology. Undeniably however, c-Met and HGF expression are upregulated in mesenchymal GBMs compared with proneural, or less aggressive, GBMs. Theoretically it would be ideal to have a unified gene set for the mesenchymal GBM subtype, however this is limited and complicated by the fact that there are

various gene expression platforms containing different gene-specific probe sets, and by the statistical tests that were employed to analyze the data. Phillips et al. (2006) and Verhaak et al. (2010) identified different gene sets that defined the mesenchymal and proneural GBM subtypes. In agreement however, they found a subset of GBMs with an aggressive mesenchymal-angiogenic molecular profile, which they termed mesenchymal GBMs, and a list of genes known to modulate normal neural development, which they named the proneural GBM subtype. Both authors' mesenchymal gene list included YKL-40, a mesenchymal marker protein (Carro et al., 2010) associated with a poor outcome for GBM patients (Colman et al., 2010; Pellowski et al., 2005). Recurrent GBMs, whether proneural or proliferative, tend to shift their molecular profile to that of a mesenchymal signature (Phillips et al., 2005). These data suggest that the c-Met / HGF signaling axis might be a good target for the treatment of primary mesenchymal GBMs, and for recurring GBMs. With additional preclinical studies into the applicability of these findings, we may be a step closer to adding another element of personalized patient care for individuals with GBM.

The mesenchymal or aggressive behavior of GBM usually includes local invasion and neo-angiogenesis, which are phenotypic hallmarks of glioma malignancy (Carro et al., 2010). Interestingly, we found that the gross morphology of U87 cells changed from a mesenchymal-like to an epithelial-like shape following knockdown of c-Met, and also with the expression of kinase-deficient c-Met mutants. These data indicate that the expression and activity of c-Met may be important components necessary for preservation of the mesenchymal-like appearance, and possibly even mesenchymal behavior, of GBM cells.

Another important novel finding of our study is that c-Met signaling regulates the expression of HGF in GBM cells. In a complementary study, Abounader and colleagues (2001) showed that c-Met expression is transcriptionally induced by HGF-mediated c-Met activation in GBM cells. Together these findings emphasize the importance of the autocrine c-Met / HGF signaling axis in GBM. Perpetuation of an autocrine signal has also been found in many other ligand-receptor systems, including EGFR signaling, as EGFR auto-induces its own expression in various cancer cell lines (Clark et al., 1985; McCulloch et al., 1998; Seth et al., 1999), and of its ligands, HB-EGF, epiregulin, and amphiregulin (Chu et al., 2005). Our finding that c-Met signaling modulates the expression of its own ligand in GBM cells, suggests that c-Met-dependent biological programs, such as cellular proliferation, mobility, invasion, angiogenesis, and tumorigenicity (Abounader and Lattera, 2009) may be amplified in GBM as a consequence of this regulation.

That these interconnections at the level of signaling and expression are relevant to the biology of the disease is supported by our findings in culture and animal models. We found that c-Met expression was necessary for U87 cells to form colonies in three-dimensional cultures, and to maintain the tumorigenic potential of orthotopic U87 xenografts. HGF expression was attenuated with c-Met knockdown *in vitro* to the same extent that tumorigenicity decreased *in vivo*. It is therefore possible that the two findings are mechanistically connected, and that regulation of the c-Met / HGF autocrine signal plays a key role in the tumorigenicity of c-Met-dependent U87 cells. In agreement with what we found, others have shown that the tumorigenicity of intracranial U87 xenografts was

attenuated with c-Met (Martens et al., 2006) or HGF (Pillay et al., 2009) antagonism. That this pathway may not be present in all GBM cells is suggested by the work of Martens and colleagues (2006), who showed that a non-c-Met-dependent GBM cell line, meaning that it did not coexpress c-Met and HGF (Beroukhi et al., 2007), did not respond to anti-c-Met therapy *in vivo*. This finding was further explored *in vitro* by Beroukhi and colleagues (2007). They provided data to suggest that enhanced cytotoxicity could only be achieved with a c-Met TKI in GBM cells that coexpressed c-Met and HGF. Strikingly, when Lal and colleagues (2005) cotargeted c-Met and HGF with U1/ribozymes in preestablished intracranial U87 xenografts, and then subjected the mice to hypofractionated  $\gamma$ -radiation, 80% of the mice survived long-term. The efficacy of non-targeted standard chemotherapeutic agents similarly enhanced the survival of mice when used in conjunction with an anti-HGF neutralizing antibody in U87 cells and xenografts (Jun et al., 2007). Taken together, these data suggest that targeting the c-Met signaling axis in GBMs that are dependent upon the autocrine HGF signal for their anchorage-independent growth and tumorigenicity, either before or after standard care treatment regimens, may be a powerful strategy for therapy of these tumors. However, we would also like to point out the limitation that not all GBMs, or even all cells in any one GBM, are likely to be susceptible to this approach, and that careful analysis of the expression of both c-Met and HGF needs to precede application of such therapies.

In cancer cell lines, such as thyroid carcinoma, GBM (Reznik et al., 2008), NSCLC (Xu et al., 2010), bladder carcinoma (Yamamoto et al., 2006), and breast carcinoma (Bonine-Summers et al., 2007; Mueller et al., 2010), a significant

amount of pathway crosstalk occurs between the EGFR and c-Met signaling axes. Not only does the EGFR transactivate the c-Met receptor in various cancer cell lines (Bergström et al., 2000; Fischer et al., 2004), but c-Met signaling also modulates the activity of the EGFR in c-Met-dependent gastric cancer cells (Bachleitner-Hofmann et al., 2008). Oncogene switching also takes place between c-Met and EGFR, where alternate receptor activation is a mechanism employed by cancer cells to compensate for loss of function of the other receptor (Mueller et al., 2008; Bachleitner-Hofmann et al., 2008). As a result, the activity of c-Met has been reported to be a key factor circumventing the effectiveness of EGFR TKIs (Tang et al., 2008). Therefore, greater therapeutic efficacies have been accomplished by cotargeting c-Met and EGFR in tumors that have become resistant to EGFR TKIs (Tang et al., 2008). Our laboratory has shown that Y1235 of c-Met is activated by EGF-stimulated EGFR in GBM cells (Chumbalkar et al., 2011), which suggests that crosstalk between c-Met and EGFR may play an important role in GBM, which may ultimately be targetable.

We have shown that many GBMs contain a robust HGF autocrine loop that is inducible through c-Met signaling, and Abounader et al. (2001) provided evidence that HGF-mediated c-Met activation induces the expression of the c-Met gene. As a result of enhanced HGF expression, dysregulated HGF / c-Met signaling most likely leads to c-Met overexpression. Once overexpressed, receptors may be activated in a ligand-independent manner due to their closer proximity with other RTKs (Mineo et al., 1999). This occurs especially when a receptor is a preferential target of those nearby receptors, such as is the case with c-Met activation being a preferred downstream signaling pathway for the  $\Delta$ EGFR

(Chumbalkar et al., 2011; Huang et al., 2007; Pillay et al., 2009). It is still unclear whether  $\Delta$ EGFR transactivates c-Met directly, or whether intermediary signaling effectors are necessary for  $\Delta$ EGFR-mediated c-Met activation in GBM cells, but we do know that they associate in a complex (data not shown). We showed that c-Met activation by  $\Delta$ -EGFR enhances HGF expression, which provides a rationale for targeting HGF in GBMs that express the  $\Delta$ EGFR. However, Pillay et al. (2009) showed that HGF antagonism of U87  $\Delta$ EGFR-expressing intracranial xenografts was ineffective. This was contrary to what they found when they treated U87 cells, and U87 cells that expressed the WT EGFR, with the same anti-HGF monoclonal antibody. We propose that HGF neutralizing antibody treatment of GBMs expressing  $\Delta$ EGFR may not reach therapeutic efficacy levels, due to incomplete neutralization of the higher amounts of HGF that are most likely being produced in these tumors. This idea is supported by a remarkable reduction in tumorigenicity when  $\Delta$ EGFR-driven GBM xenografts are treated with anti-HGF and anti-EGFR therapies in combination, compared with either agent alone (Lal et al., 2009; Pillay et al., 2009).

Depending on the cellular context, the c-Met / HGF signaling axis can promote either survival or apoptosis (Trusolino et al., 2010). Interestingly, HGF has been called 'tumor cytotoxic factor', because excessive amounts of this cytokine may induce apoptosis in various cancer cell lines (Trusolino et al., 2010). It has been suggested that higher levels of HGF may titrate out the available ligand-binding domains of c-Met on the cell surface, thereby liberating bound FAS, a death receptor that often associates with c-Met as a survival mechanism, and hence promote apoptosis (Trusolino et al., 2010). However, we and others have

shown that  $\Delta$ EGFR-expressing GBM cells express high levels of BCL-XL (Nagane et al., 1996), which may likely serve to promote cell survival while still maintaining constitutive ligand-dependent and ligand-independent c-Met activity.

We found that c-Met was required by  $\Delta$ EGFR to maintain its elevated production of HGF in U87 cells. We also showed that when c-Met's expression was silenced in U87 cells expressing  $\Delta$ EGFR, the tumorigenicity of intracranial xenografts was significantly compromised. In fact,  $\Delta$ EGFR lost all oncogenic potency with c-Met knockdown. These findings suggest that targeting c-Met in c-Met-addicted GBMs that express the  $\Delta$ EGFR, such as in a subset of tumors belonging to the mesenchymal GBM subgroup, may be an effective treatment strategy. However, very few mesenchymal GBMs were detected by Verhaak and colleagues (2010) to express the  $\Delta$ EGFR. We predict that a large number of  $\Delta$ EGFR-expressing GBMs were not discovered in their study, due to the scanty expression of  $\Delta$ EGFR in the bulk of a tumor that limits its detectability (Jungbluth et al., 2003; Wiesner et al., 2009), and due to TCGA's sample exclusion criteria (Verhaak et al., 2010). Therefore, it is possible that the subset of mesenchymal GBMs that express  $\Delta$ EGFR may be larger than reported by Verhaak et al. (2010). Using different techniques, other investigators have found that approximately 30% of GBMs contain the  $\Delta$ EGFR mutation (Hwang et al., 2011), compared with the 7% of GBMs reported by Verhaak et al. (2010).

c-Met-dependent effectors of HGF expression that were identified in our phosphotyrosine-based mass spectrometry screen, mostly merged on STAT3. Others have found that HGF promoter activity is upregulated via STAT3 signaling in a variety of cancer cell lines (Tomida and Saito, 2004; Wojcik et al., 2006).



Interestingly, STAT3 expression is critical for maintenance of the mesenchymal gene expression signature, and of the associated aggressive phenotype of GBM (Carro et al., 2010). In agreement, aberrant STAT3 activity correlates with a poor survival prognosis for GBM patients (Birner et al., 2010). Zhang et al. (2002) provided evidence to suggest that STAT3 is a crucial component of the c-Met signal in cancer cells, which is required for anchorage-independent colony formation and tumor growth. We found that STAT3 activity was attenuated with c-Met knockdown in U87  $\Delta$ EGFR cells, and that the loss in anchorage-independent growth of these cells could partially be restored via constitutively active STAT3 expression. These data suggested that c-Met-mediated STAT3 signaling plays a key role in maintaining anchorage-independent growth of U87 cells expressing  $\Delta$ EGFR.

It has been suggested that STAT3 Y705 phosphorylation is not significantly enhanced by  $\Delta$ EGFR in GBM cells (Huang et al., 2009). However, the STAT3 signal is recruited by  $\Delta$ EGFR to induce the transformation of astrocytes (de la Iglesia et al., 2008). Additionally, proliferation and survival mechanisms associated with  $\Delta$ EGFR expression in GBM cells are strengthened by STAT3 signaling (Huang et al., 2009). We found that activated STAT3 partially modulates HGF expression in U87  $\Delta$ EGFR-expressing cells. It is possible that HGF-stimulated c-Met activates STAT3 within the perinuclear compartment of U87 and U87  $\Delta$ EGFR cells, as this mechanism of compartmentalization of c-Met-dependent STAT3 activation has been employed by other cancer cells (Kermorgant et al., 2008). Taken together, these data suggest that  $\Delta$ EGFR usurps

the c-Met-dependent STAT3 signal in U87 cells, to partly promote oncogenicity via increased HGF expression.

STAT3 signaling was necessary, yet insufficient, to modulate HGF expression in U87 cells, and in U87 cells expressing  $\Delta$ EGFR. Using IPA, we showed that C/EBP $\beta$  and STAT3 share upstream signaling molecules that regulate HGF expression in U87 and U87  $\Delta$ EGFR-expressing cells in a c-Met-dependent manner. Similarly to STAT3, C/EBP $\beta$  is a master regulator of the mesenchymal GBM subtype (Carro et al., 2010). These data suggest that activation of the C/EBP $\beta$  pathway will most likely be required, in addition to STAT3 signaling, in order to maximally upregulate the expression of HGF in c-Met-dependent GBM cells.

In summary, our data have highlighted the significant contribution of dysregulated c-Met pathway signaling, and of c-Met and  $\Delta$ EGFR crosstalk, to GBM tumorigenesis. We have identified a new element in this network, the positive feedback on HGF expression by c-Met signaling, and connected it to the already known signal coming from  $\Delta$ EGFR to c-Met. Our data show that this is an important component of the network for tumorigenesis, and by implication may represent an opportunity for therapy of tumors where these signals are important, the mesenchymal GBMs.

## BIBLIOGRAPHY

- Abella, J.V., P. Peschard, M.A. Naujokas, T. Lin, C. Saucier, S. Urbe, and M. Park, *Met/Hepatocyte growth factor receptor ubiquitination suppresses transformation and is required for Hrs phosphorylation*. Mol Cell Biol, 2005. **25**(21): p. 9632-45.
- Abounader, R., S. Ranganathan, B. Lal, K. Fielding, A. Book, H. Dietz, P. Burger, and J. Laterra, *Reversion of human GBM malignancy by U1 small nuclear RNA/ribozyme targeting of scatter factor/hepatocyte growth factor and c-Met expression*. J National Cancer Inst, 1999. **91**(18): p. 1548-56.
- Abounader, R., S. Ranganathan, B.Y. Kim, C. Nichols, and J. Laterra, *Signaling pathways in the induction of c-Met receptor expression by its ligand scatter factor/hepatocyte growth factor in human glioblastoma*. J Neurochem, 2001. **76**(5): p. 1497-508.
- Abounader, R., B. Lal, C. Luddy, G. Koe, B. Davidson, E.M. Rosen, and J. Laterra. *In vivo targeting of SF/HGF and c-Met expression via U1snRNA/ribozymes inhibits GBM growth and angiogenesis and promotes apoptosis*. FASEB J, 2002. **16**(1): p. 108-10.
- Abounader, R., and J. Laterra, *Scatter factor/hepatocyte growth factor in brain tumor growth and angiogenesis*. Neuro-Oncology, 2005. **7**(4): p. 436-51.
- Abounader, R., and J. Laterra, *Chapter 39, C-Met / HGF Signaling and Targeted Therapeutics in Brain Tumors*. In: E.G. Van Meir (ed.) CNS cancer: Cancer

- drug discovery and development. Illustrated ed. New York: Humana Press, 2009. p. 933-52.
- Agarwal, S., C. Zerillo, J. Kolmakova, J.G. Christensen, L.N. Harris, D.L. Rimm, M.P. Digiovanna, and D.F. Stern, *Association of constitutively activated hepatocyte growth factor receptor (Met) with resistance to a dual EGFR/Her2 inhibitor in non-small-cell lung cancer cells*. British J Cancer, 2009. **100**(6): p. 941-9.
- Bachleitner-Hofmann, T., M.Y. Sun, C.T. Chen, L. Tang, L. Song, Z. Zeng, M. Shah, J.G. Christensen, N. Rosen, D.B. Solit, and M.R. Weiser, *HER kinase activation confers resistance to MET tyrosine kinase inhibition in MET oncogene–addicted gastric cancer cells*. Mol Cancer Ther, 2008. **7**: p. 3499–508.
- Bachoo, R.M., E.A. Maher, K.L. Ligon, N.E. Sharpless, S.S. Chan, M.J. You, Y. Tang, J. DeFrances, E. Stover, R. Weissleder, D.H. Rowitch, D.N. Louis, and R.A. DePinho, *Epidermal growth factor receptor and Ink4a/Arf: convergent mechanisms governing terminal differentiation and transformation along the neural stem cell to astrocyte axis*. Cancer Cell, 2002. **1**: p. 269-77.
- Bardelli, A., L. Pugliese, and P.M. Comoglio, *“Invasive-growth” signaling by the Met / HGF receptor: The hereditary renal carcinoma connection*. Biochem Biophys Acta, 1997. **1333**: M41- 51.
- Beau-Faller, M., A.M. Ruppert, A.C. Voegeli, A. Neuville, N. Meyer, E. Guerin, M. Legrain, B. Mennezier, J.M. Wihlm, G. Massard, E. Quoix, P. Oudet, and M.P. Gaub, *MET gene copy number in non-small cell lung cancer:*

- molecular analysis in a targeted tyrosine kinase inhibitor naïve cohort.* J Thorac Oncol, 2008. **3**(4): p. 331-9.
- Bergström, J.D., B. Westermarck, and N.E. Heldin, *Epidermal growth factor receptor signaling activates met in human anaplastic thyroid carcinoma cells.* Exp Cell Res, 2000. **259**: p. 293-99.
- Beroukhi, R., G. Getz, L. Nghiemphu, J. Barretina, T. Hsueh, D. Linhart, I. Vivanco, J.C. Lee, J.H. Huang, S. Alexander, J. Du, T. Kau, R.K. Thomas, K. Shah, H. Soto, S. Perner, J. Prensner, R.M. DeBiasi, F. Demichelis, C. Hatton, M.A. Rubin, L.A. Garraway, S.F. Nelson, L. Liao, P.S. Mischel, T.F. Cloughesy, M. Meyerson, T.A. Golub, E.S. Lander, I.K. Mellinghoff, and W.R. Sellers. *Assessing the significance of chromosomal aberrations in cancer: methodology and application to glioma.* PNAS, 2007. **104**(50): p. 20007-12.
- Bertotti, A., P. M. Comoglio, and L. Trusolino,  *$\beta 4$  integrin activates a Shp2-Src signaling pathway that sustains HGF-induced anchorage-independent growth.* J Cell Biol, 2006. **175**: p. 993-1003.
- Bertotti, A., M.F. Burbridge, S. Gastaldi, F. Galimi, D. Torti, E. Medico, S. Giordano, S. Corso, G. Rolland-Valognes, B.P. Lockhart, J.A. Hickman, P.M. Comoglio, and L. Trusolino, *Only a subset of Met-activated pathways are required to sustain oncogene addiction.* Science Signaling, 2009. **2**(100): ra80: p. 1-15.
- Birchmeier, C., W. Birchmeier, E. Gherardi, and G.F. Vande Woude, *Met, metastasis, motility and more.* Mol Cell Biol, 2003. **4**: p. 915-25.

- Birner, P., K. Toumangelova-Uzeir, S. Natchev, and M. Guentchev, *STAT3 tyrosine phosphorylation influences survival in glioblastoma*. J Neuro-oncology, 2010. **100**: p. 339-43.
- Boccaccio, C., G. Gaudino, G. Gambarotta, F. Galimi, and P.M. Comoglio, *Hepatocyte growth factor (HGF) receptor expression is inducible and is part of the delayed-early response to HGF*. J Biol Chem, 1994. **269**(17): p. 12846-51.
- Boise, L. H., M. Gonzalez-Garcia, C. E. Postema, L. Ding, T. Lindsten, L. A. Turka, X. Mao, G. Nunez, and C. B. Thompson, *bcl-x. a bcl-2-related gene that functions as a dominant regulator of apoptotic cell death*. Cell, 1993. **74**: p. 597-608.
- Bonine-Summers, A.R., M.E. Aakre, K.A. Brown, C.L. Arteaga, J.A. Pietenpol, H.L. Moses, and N. Cheng, *Epidermal growth factor receptor plays a significant role in hepatocyte growth factor mediated biological responses in mammary epithelial cells*. Cancer Biol Therapy, 2007. **6**(4): e1-e10.
- Bosma, I., M.J. Vos, J.J. Heimans, M.J.B. Taphoorn, N.K. Aaronson, T.J. Postma, H.M. van der Ploeg, M. Muller, W. P. Vandertop, B.J. Slotman, and M. Klein, *The course of neurocognitive functioning in high-grade glioma patients*. Neuro-oncol, 2007. **9**(1): p. 53-62.
- Bromberg, J.F., M.H. Wrzeszczynska, G. Devgan, Y. Zhao, R.G. Pestell, C. Albanese, and J.E. Darnell, *Stat3 as an oncogene*. Cell, 1999. **98**(3): p. 295-303.
- Buchanan, S.G., J. Hendle, P.S. Lee, C.R. Smith, P-Y. Bounaud, K. Jessen, C.M. Tang, H.H. Huser, J.D. Felce, K.J. Froning, M.C. Peterman, B.E. Aubol,

- S.F. Gessert, J.M. Sauder, K.D. Schwinn, M. Russell, I. Rooney, J. Adams, B.C. Leon, T.H. Do, J.M. Blaney, P. Sprengeler, D. Thompson, L. Smyth, L. Pelletier, S. Atwell, K. Holme, S.R. Wasserman, S. Emtage, S.K. Burley, and S.H. Reich, *SGX523 is an exquisitely selective, ATP-competitive inhibitor of the MET receptor tyrosine kinase with antitumor activity in vivo*. Mol Cancer Ther, 2009. **8**: p. 3181-90.
- Camp, E.R., J. Summy, T.W. Bauer, W. Liu, G.E. Gallick, and L.M. Ellis, *Molecular mechanisms of resistance to therapies targeting the epidermal growth factor receptor*. Clin Cancer Res, 2005. **11**: p. 397-405.
- Cao, B., Y. Su, M. Oskarsson, P. Zhao, E.J. Kort, R.J. Fisher, L.M. Wang, and G.F. Vande Woude, *Neutralizing monoclonal antibodies to hepatocyte growth factor/scatter factor (HGF/SF) display antitumor activity in animal models*. Proc Natl Acad Sci USA, 2001. **98**(13): p. 7443-8.
- Caolo, V., N.M. van den Akker, S. Verbruggen, M.M. Donners, G. Swennen, H. Schulten, J. Waltenberger, M.J. Post, and D.G. Molin, *Feed-forward signaling by membrane-bound ligand receptor circuit: the case of NOTCH DELTA-like 4 ligand in endothelial cells*. J Biol Chem, 2010. **285**(52): p. 40681-9.
- Carro, M.S., W.K. Lim, M.J. Alvarez, R.J. Bollo, X. Zhao, E.Y. Snyder, E.P. Sulman, S.L. Anne, F. Doetsch, H. Colman, A. Lasorella, K. Aldape, A. Califano, and A. Lavarone, *The transcriptional network for mesenchymal transformation of brain tumours*. Nature, 2010. **463**(7279): p. 318-25.
- Cavenee, W.K., *Genetics and new approaches to cancer therapy*. Carcinogenesis, 2002. **23**: p. 683-6.

- Chakravarti, A., M.A. Delaney, E. Noll, P.M. Black, J.S. Loeffler, A. Muzikansky, and N.J. Dyson, *Prognostic and pathologic significance of quantitative protein expression profiling in human gliomas*. Clin Cancer Res, 2001. **7**(8): p. 2387-95.
- Chen, X., A. Stoeck, S.J. Lee, L. Shih, M.M. Wang, and T.L. Wang, *Jagged1 expression regulated by Notch3 and Wnt/ $\beta$ -catenin signaling pathways in ovarian cancer*. Oncotarget, 2010. **1**(3): p. 210-8.
- Chiara, F., P. Michieli, L. Pugliese, and P.M. Comoglio, *Mutations in the met oncogene unveil a "dual switch" mechanism controlling tyrosine kinase activity*. J Biol Chem, 2003. **278**(31): p. 29352-8.
- Clark, A.J., S. Ishii, N. Richert, G.T. Merlino, and I. Pastan, *Epidermal growth factor regulates the expression of its own receptor*. Proc Natl Acad Sci U S A, 1985. **82**(24): 8374-8.
- Christensen, J.G., R. Schreck, J. Burrows, P. Kuruganti, E. Chan, P. Le, J. Chen, X. Wang, L. Ruslim, R. Blake, K.E. Lipson, J. Ramphal, S. Do, J.J. Cui, J.M. Cherrington, and D.B. Mendel, *A selective small molecule inhibitor of c-Met kinase inhibits c-Met-dependent phenotypes in vitro and exhibits cytoreductive antitumor activity in vivo*. Cancer Res, 2003. **63**: p. 7345-55.
- Chu, E.K., J.S. Foley, J. Cheng, A.S. Patel, J.M. Drazen, and D.J. Tschumperlin, *Bronchial epithelial compression regulates epidermal growth factor receptor family ligand expression in an autocrine manner*. Am J Respir Cell Mol Biol, 2005. **32**: p. 373-80.
- Chumbalkar, V., K. Latha, Y. Hwang, R. Maywald, L. Hawley, R. Sawaya, L. Diao, K. Baggerly, W.K. Cavenee, F.B. Furnari, and O. Bogler, *Analysis of*



- Phosphotyrosine Signaling in glioblastoma Identifies STAT5 as a Novel Downstream Target of  $\Delta$ EGFR*. J Proteome Res, 2011. **10**: p. 1343-52.
- Colman, H., L. Zhang, E.P. Sulman, J.M. McDonald, N.L. Shooshtari, A. Rivera, S. Popoff, C.L. Nutt, D.N. Louis, J.G. Cairncross, M.R. Gilbert, H.S. Phillips, M.P. Mehta, A. Chakravarti, C.E. Pelloso, K. Bhat, B.G. Feuerstein, R.B. Jenkins, and K. Aldape, *A multigene predictor of outcome in glioblastoma*. Neuro-Oncology, 2010. **12**(1): p. 49-57.
- Crepaldi, T., M. Prat, S. Giordano, E. Medico, and P.M. Comoglio, *Generation of a truncated hepatocyte growth factor receptor in the endoplasmic reticulum*. J Biol Chem, 1994. **269**(3): p. 1750-5.
- D'Atri, S., L. Tentori, P.M. Lacal, G. Graziani, E. Pagani, E. Benincasa, G. Zambruno, E. Bonmassar, and J. Jiricny, *Involvement of the mismatch repair system in temozolomide-induced apoptosis*. Mol Pharmacol, 1998. **54**(2): p. 334-41.
- de la Iglesia, N., G. Konopka, S.V. Puram, J.A. Chan, R.M. Bachoo, M.J. You, D.E. Levy, R.A. Depinho, and A. Bonni, *Identification of a PTEN-regulated STAT3 brain tumor suppressor pathway*. Genes Dev, 2008. **22**(4): p. 449-62.
- Eder, J.P., G.F. Vande Woude, S.A. Boerner, and P.M. LoRusso, *Novel therapeutic inhibitors of the c-Met signaling pathway in cancer*. Clin Cancer Res, 2009. **15**(7): p. 2207-14.
- Engelman, J.A., K. Zejnullahu, T. Mitsudomi, Y. Song, C. Hyland, J.O. Park, N. Lindeman, C.M. Gale, X. Zhao, J. Christensen, T. Kosaka, A.J. Holmes, A.M. Rogers, F. Cappuzzo, T. Mok, C. Lee, B.E. Johnson, L.C. Cantley,

- and P.A. Jänne, *MET amplification leads to gefitinib resistance in lung cancer by activating ERBB3 signaling*. Science, 2007. **316**: p. 1039-43.
- Fischer, O.M., S. Giordano, P.M. Comoglio, and A. Ullrich, *Reactive oxygen species mediate met receptor transactivation by g protein-coupled receptors and the epidermal growth factor receptor in human carcinoma cells*. J Bio Chem, 2004. **279**: p. 28970-8.
- Fletcher, J.I., M. Haber, M.J. Henderson, and M.D. Norris, *ABC transporters in cancer: more than just drug efflux pumps*. Nat Rev Cancer, 2010. **10**: p. 147-56.
- Foveau, B., F. Ancot, C. Leroy, A. Petrelli, K. Reiss, V. Vingtdoux, S. Giordano, V. Fafeur, and D. Tulasne, *Down-regulation of the met receptor tyrosine kinase by presenilin-dependent regulated intramembrane proteolysis*. Mol Biol Cell, 2009. **20**: p. 2495-507.
- Frederick, L., G. Eley, X.Y. Wang, and C.D. James, *Analysis of genomic rearrangements associated with EGFRvIII expression suggests involvement of Alu repeat elements*. Neuro-Oncology, 2000. **2**: p. 159-63.
- Furnari, F.B., T. Fenton, R.M. Bachoo, A. Mukasa, J.M. Stommel, A. Stegh, W.C. Hahn, K.L. Ligon, D.N. Louis, C. Brennan, L. Chin, R.A. DePinho, and W.K. Cavenee, *Malignant astrocytic glioma: genetics, biology, and paths to treatment*. Genes Dev, 2007. **21**: p. 2683-710.
- Gentile, A., L. Trusolino, and P.M. Comoglio, *The Met tyrosine kinase receptor in development and cancer*. Cancer Metastasis Rev, 2008. **27**: p. 85-94.
- Gentleman, R.C., V.J. Carey, D.M. Bates, B. Bolstad, M. Dettling, S. Dudoit, B. Ellis, L. Gautier, Y. Ge, J. Gentry, K. Hornik, T. Hothorn, W. Huber, S.

- Lacus, R. Irizarry, F. Leisch, C. Li, M. Maechler, A.J. Rossini, G. Sawitzki, C. Smith, G. Smyth, L. Tierney, J.Y. Yang, and J. Zhang, *Bioconductor: open software development for computational biology and bioinformatics*. Genome Biol, 2004. **5**(10): R80.
- Gherardi, E., M.E. Youles, R.N. Miguel, T.L. Blundell, L. Lamelle, J. Gough, A. Bandyopadhyay, G. Hartmann, and P.J. Butler, *Functional map and domain structure of the MET (HGF/SF) receptor*. Proc Natl Acad Sci USA, 2003. **100**: p. 12039-44.
- Goldoni, S., A. Humphries, A. Nyström, S. Sattar, R.T. Owens, D.J. McQuillan, K. Ireton, and R.V. Iozzo, *Decorin is a novel antagonistic ligand of the Met receptor*. J Cell Biol, 2009. **185**(4): p. 743-54.
- Gonzalez, J. and M.R. Gilbert, *Treatment of astrocytomas*. Curr Opin Neurol, 2005. **18**(6): p. 632-8.
- Görke, R., A. Meyer-Bäse, D. Wagner, H. He, M.R. Emmett and C.A. Conrad, *Determining and interpreting correlations in lipidomic networks found in glioblastoma cells*. BMC Syst Biol, 2010. **4**: 126.
- Grovdal, L. M., E. Stang, A. Sorkin, and I. H. Madshus, *Direct interaction of Cbl with pTyr 1045 of the EGF receptor (EGFR) is required to sort the EGFR to lysosomes for degradation*. Exp Cell Res, 2004. **300**: p. 388-95.
- Halatsch, M-E., U. Schmidt, J. Behnke-Mursch, A. Unterberg, and C.R. Wirtz, *Epidermal growth factor receptor inhibition for the treatment of glioblastoma multiforme and other malignant brain tumours*. Cancer Treat Rev, 2006. **32**(2): p. 74-89.

- Heimberger, A.B., R. Hlatky, D. Suki, D. Yang, J. Weinberg, M. Gilbert, R. Sawaya, and K. Aldape, *Prognostic Effect of Epidermal Growth Factor Receptor and EGFRvIII in Glioblastoma Multiforme Patients*. Clin Cancer Res, 2005. **11**: 1462-66.
- Hov, H., R.U. Holt, T.B. Rø, U-M. Fagerli, H. Hjorth-Hansen, V. Baykov, J.G. Christensen, A. Waage, A. Sundan, and M. Børset, *A selective c-Met inhibitor blocks an autocrine hepatocyte growth factor growth loop in ANBL-6 cells and prevents migration and adhesion of myeloma cells*. Clin Cancer Res, 2004. **10**(19): p. 6686-94.
- Huang, H.S., M. Nagane, C.K. Klingbeil, H. Lin, R. Nishikawa, X.D. Ji, C.M. Huang, G.N. Gill, H.S. Wiley, and W.K. Cavenee, *The enhanced tumorigenic activity of a mutant epidermal growth factor receptor common in human cancers is mediated by threshold levels of constitutive tyrosine phosphorylation and unattenuated signaling*. J Biol Chem, 1997. **272**(5): p. 2927-35.
- Huang, P.H., A. Mukasa, R. Bonavia, R.A. Flynn, Z.E. Brewer, W.K. Cavenee, F.B. Furnari, and F.M. White, *Quantitative analysis of EGFRvIII cellular signaling networks reveals a combinatorial therapeutic strategy for glioblastoma*. Proc. Natl. Acad. Sci. USA, 2007. **104**: p. 12867-72.
- Huang, P.H., A.M. Xu, and F.M. White, *Oncogenic EGFR signaling networks in glioma*. Science Signaling, 2009. **2**(87) re6: p. 1-13.
- Hung, W., and B. Elliott, *Co-operative effect of c-Src tyrosine kinase and Stat3 in activation of hepatocyte growth factor expression in mammary carcinoma cells*. J Biol Chem, 2001. **276**(15): p. 12395-403.

- Hwang, Y., V. Chumbalkar, K. Latha, and O. Bogler. *Forced dimerization increases the activity of  $\Delta$ EGFR/EGFRvIII and enhances its oncogenicity*. Mol Cancer Res, 2011. [Epub ahead of print]
- Jiang, J.G., Q. Chen, A. Bell, and R. Zarnegar, *Transcriptional regulation of the hepatocyte growth factor (HGF) gene by the Sp family of transcription factors*. Oncogene, 1997. **14**(25): p. 3039-49.
- Jiang, J.G., and R. Zarnegar, *A novel transcriptional regulatory region within the core promoter of the hepatocyte growth factor gene is responsible for its inducibility by cytokines via the C/EBP family of transcription factors*. Mol Cell Biol, 1997. **17**(10): p. 5758-70.
- Jiang, J.G., C. Johnson, and R. Zarnegar, *Peroxisome proliferator-activated receptor gamma-mediated transcriptional up-regulation of the hepatocyte growth factor gene promoter via a novel composite cis-acting element*. J Biol Chem, 2001. **276**(27): p. 25049-56.
- Jo, M., D.B. Stolz, J.E. Esplen, K. Dorko, G.K. Michalopoulos, and S.C. Strom, *Cross-talk between epidermal growth factor receptor and c-Met signal pathways in transformed cells*. J Biol Chem, 2000. **275**: p. 8806-11.
- Joffre, C., R. Barrow, L. Ménard, V. Calleja, I.R. Hart, and S. Kermorgant, *A direct role for Met endocytosis in tumorigenesis*. Nat Cell Biol, 2011. **13**(7): p. 827-37.
- Jun, H.T., J. Sun, K. Rex, R. Radinsky, R. Kendall, A. Coxon, and T.L. Burgess, *AMG 102, a fully human anti-hepatocyte growth factor/scatter factor neutralizing antibody, enhances the efficacy of temozolomide or docetaxel*

- in U-87 MG cells and xenografts*. Clin Cancer Res, 2007. **13**(22): p. 6735-42.
- Jungbluth, A.A., E. Stockert, H.J. Huang, V.P. Collins, K. Coplan, K. Iversen, D. Kolb, T.J. Johns, A.M. Scott, W.J. Gullick, G. Ritter , L. Cohen , M.J. Scanlan , W.K. Cavenee , and L.J. Old, *A monoclonal antibody recognizing human cancers with amplification/overexpression of the human epidermal growth factor receptor*. Proc Natl Acad Sci USA, 2003. **100**: p. 639-44.
- Kajiwarra, Y., S. Panchabhai, and V.A. Levin, *A new preclinical 3-dimensional agarose colony formation assay*. Technol Cancer Res Treat, 2008. **7**: p. 329-34.
- Kermorgant, S., D. Zicha, and P.J. Parker, *PKC controls HGF-dependent c-Met traffic, signalling and cell migration*. EMBO J, 2004. **23**: p. 3721-34.
- Kermorgant, S., and P.J. Parker, *Receptor trafficking controls weak signal delivery: a strategy used by c-Met for STAT3 nuclear accumulation*. J Cell Biol, 2008. **182**: p. 855-63.
- Knudsen, B.S., and G. Vande Woude, *Showering c-Met dependent cancers with drugs*. Curr Opinion Genet Develop, 2008. **18**(1): p. 87-96.
- Kong, D-S., S-Y. Song, D-H. Kim, K.M. Joo, J-S. Yoo, J.S. Koh, S.M. Dong, Y-L. Suh, J-I. Lee, K. Park, J.H. Kim, and D-H. Nam, *Prognostic significance of c-Met expression in glioblastomas*. Cancer, 2009. **115**(1): p. 140-8.
- Kong, L-Y., A. Gelbard, J. Wei, C. Reina-Ortiz, Y. Wang, E.C. Yang, Y. Hailemichael, I. Fokt, A. Jayakumar, W. Qiao, G.N. Fuller, W.W. Overwijk, W. Priebe, and A.B. Heimberger, *Inhibition of p-STAT3 Enhances IFN- $\alpha$*

- Efficacy against Metastatic Melanoma in a Murine Model*. Clin Cancer Res, 2010. **16**: p. 2550-61.
- Kong-Beltran, J. Stamos, and D. Wickramasinghe, *The Sema domain of Met is necessary for receptor dimerization and activation*. Cancer Cell, 2004. **6**(1): p. 75-84.
- Koochekpour, S., M. Jeffers, S. Rulong, G. Taylor, E. Klineberg, E.A. Hudson, J.H. Resau, and G.F. Vande Woude, *Met and hepatocyte growth factor/scatter factor expression in human gliomas*. Cancer Res, 1997. **57**(23): p. 5391-8.
- Krakstad, C., and M. Chekenya, *Survival signalling and apoptosis resistance in glioblastomas: opportunities for targeted therapeutics*. Mol Cancer, 2010. **9**: 135.
- Kunkel, P., S. Müller, P. Schirmacher, D. Stavrou, R. Fillbrandt, M. Westphal, and K. Lamszus, *Expression and localization of scatter factor/hepatocyte growth factor in human astrocytomas*. Neuro-oncology, 2001. **3**(2): p. 82-8.
- Lal, B., S. Xia, R. Abounader, and J. Laterra, *Targeting the c-Met pathway potentiates glioblastoma responses to  $\gamma$ -radiation*. Clin Cancer Res, 2005. **11**(12): p. 4479-86.
- Lal, B., C.R. Goodwin, Y. Sang, C.A. Foss, K. Cornet, S. Muzamil, M.G. Pomper, J. Kim, and J. Laterra, *EGFRvIII and c-Met pathway inhibitors synergize against PTEN-null/EGFRvIII+ glioblastoma xenografts*. Mol Cancer Ther, 2009. **8**(7): p. 1751-60.

- Lammering, G., K. Valerie, P.S. Lin, T.H. Hewit, and R.K. Schmidt-Ullrich, *Radiation-induced activation of a common variant of EGFR confers enhanced radioresistance*. *Radiother Oncol*, 2004. **72**: p. 267-73.
- Lassman, A.B., and E.C. Holland, *Incorporating molecular tools into clinical trials and treatment for gliomas?* *Curr Opin Neurol*, 2007. **20**(6): p. 708-11.
- Laterra, J., E. Rosen, M. Nam, S. Ranganathan, K. Fielding, and P. Johnston, *Scatter factor/hepatocyte growth factor expression enhances human glioblastoma tumorigenicity and growth*. *Biochem Biophys Res Com*, 1997. **235**(3): p. 743-7.
- Lee, J.H., S.U. Han, H. Cho, B. Jennings, B. Gerrard, M. Dean, L. Schmidt, B. Zbar, and G.F. Vande Woude, *A novel germ line juxtamembrane Met mutation in human gastric cancer*. *Oncogene*, 2000. **19**(43): p. 4947-53.
- Lee, J.C., I. Vivanco, R. Beroukhim, J.H. Huang, W.L. Feng, R.M. DeBiasi, K. Yoshimoto, J.C. King, P. Nghiemphu, Y. Yuza, Q. Xu, H. Greulich, R.K. Thomas, J.G. Paez, T.C. Peck, D.J. Linhart, K.A. Glatt, G. Getz, R. Onofrio, L. Ziaugra, R.L. Levine, S. Gabriel, T. Kawaguchi, K. O'Neill, H. Khan, L.M. Liao, S.F. Nelson, P.N. Rao, P. Mischel, R.O. Pieper, T. Cloughesy, D.J. Leahy, W.R. Sellers, C.L. Sawyers, M. Meyerson, and I.K. Mellinghoff, *Epidermal growth factor receptor activation in glioblastoma through novel missense mutations in the extracellular domain*. *PLoS Med*, 2006. **3**, e485.
- Li, N., M. Lorinczi, K. Ireton, and L.A. Elferink, *Specific Grb2-mediated interactions regulate clathrin-dependent endocytosis of the cMet-tyrosine kinase*. *J Biol Chem*, 2007. **282**: p. 16764-75.



- Li, L., A. Dutra, E. Pak, J.E. Labrie III, R.M. Gerstein, P.P. Pandolfi, L.D. Recht, and A.H. Ross, *EGFRvIII expression and PTEN loss synergistically induce chromosomal instability and glial tumors*. Neuro-oncol, 2009. **11**(1): p. 9-21.
- Lopez-Gines, C., M. Cerda-Nicolas, R. Gil-Benso, A. Pellin, J.A. Lopez-Guerrero, R. Callaghan, R. Benito, P. Roldan, J. Piquer, J. Llacer, and J. Barbera, *Association of chromosome 7, chromosome 10 and EGFR gene amplification in glioblastoma multiforme*. Clin Neuropathol, 2005. **24**(5): p. 209-18.
- Louis, D.N., H. Ohgaki, O.D. Wiesler, W.K. Cavenee, P.C. Burger, A. Jouvet, B.W. Scheithauer and P. Kleihues, *The 2007 WHO classification of tumours of the central nervous system*. Acta Neuropathol, 2007. **114**(2): p. 97-109.
- Ma, P.C., G. Maulik, J. Christensen, and R. Salgia, *c-Met: structure, functions and potential for therapeutic inhibition*. Cancer Metastasis Rev, 2003. **22**(4): p. 309-25.
- Macek, B., M. Mann, and J.V. Olsen, *Global and site-specific quantitative phosphoproteomics: principles and applications*. Annu Rev Pharmacol Toxicol 2009. **49**: p. 199-221.
- Marderosian, M., A. Sharma, A.P. Funk, R. Vartanian, J. Masri, O.D. Jo, and J.F. Gera, *Tristetraprolin regulates Cyclin D1 and c-Myc mRNA stability in response to rapamycin in an Akt-dependent manner via p38 MAPK signaling*. Oncogene, 2006. **25**: p. 6277–90.
- Martens, T., N-O. Schmidt, C. Eckerich, R. Fillbrandt, M. Merchant, R. Schwall, M. Westphal, and K. Lamszus, *A novel one-armed anti-c-Met antibody inhibits glioblastoma growth in vivo*. Clin Cancer Res, 2006. **12**: p. 6144-52.

- Maulik, G., P. Madhiwala, S. Brooks, P.C. Ma, T. Kijima, E.V. Tibaldi, E. Schaefer, K. Parmar, and R. Salgia, *Activated c-Met signals through PI3K with dramatic effects on cytoskeletal functions in small cell lung cancer*. J Cell Mol Med, 2002. **6**(4): p. 539-53.
- McCulloch, R.K., C.E. Walker, A. Chakera, J. Jazayeri, and P.J. Leedman, *Regulation of EGF-receptor expression by EGF and TGF alpha in epidermoid cancer cells is cell type-specific*. Int J Biochem Cell Biol, 1998. **30**(11): p. 1265-78.
- Mineo, C., G.N. Gill, and R.G. Anderson, *Regulated migration of epidermal growth factor receptor from caveolae*. J Biol Chem, 1999. **274**(43): p. 30636-43.
- Moon, Y-W., R.J. Weil, S.D. Pack, W-S. Park, E. Pak, T. Pham, J.D. Karkera, H-K. Kim, A.O. Vortmeyer, B.G. Fuller, and Z. Zhuang, *Missense mutation of the MET gene detected in human glioma*. Mod Pathol, 2000. **13**(9): p. 973-77.
- Moriyama, T., H. Kataoka, H. Kawano, K. Yokogami, S. Nakano, T. Goya, H. Uchino, M. Koono, and S. Wakisaka, *Comparative analysis of expression of hepatocyte growth factor and its receptor, c-Met, in gliomas, meningiomas and schwannomas in humans*. Cancer letters, 1998. **124**(2): p. 149-55.
- Mueller, H.W., A. Michel, D. Heckel, U. Fischer, M. Tönnies, L.C. Tsui, S. Scherer, K.D. Zang, and E. Meese, *Identification of an amplified gene cluster in glioma including two novel amplified genes isolated by exon trapping*. Hum Genet, 1997. **101**(2): p. 190-7.

- Nabeshima, K., Y. Shimao, S. Sato, H. Kataoka, T. Moriyama, H. Kawano, S. Wakisaka, and M. Koono, *Expression of c-Met correlates with grade of malignancy in human astrocytic tumours: an immunohistochemical study*. Histopathology, 1997. **31**(5): p. 436-43.
- Nagane, M., F. Coufal, H. Lin, O. Bögl, W.K. Cavenee, and H-J. S. Huang, *A common mutant epidermal growth factor receptor confers enhanced tumorigenicity on human glioblastoma cells by increasing proliferation and reducing apoptosis*. Cancer Res, 1996. **10**(2): p. 5079-86.
- Nagane, M., A. Levitzki, A. Gazit, W.K. Cavenee, and H.J. Huang, *Drug resistance of human glioblastoma cells conferred by a tumor-specific mutant epidermal growth factor receptor through modulation of Bcl-XL and caspase-3-like proteases*. Proc Natl Acad Sci USA, 1998. **95**: p. 5724-9.
- Ning, Z.Q., J. Li, and R.J. Arceci, *Signal transducer and activator of transcription 3 activation is required for Asp(816) mutant c-Kit-mediated cytokine-independent survival and proliferation in human leukemia cells*. Blood, 2001. **97**(11): p. 3559-67.
- Nishikawa, R., X-D. Ji, R.C. Harmon, C.S. Lazar, G.N. Gill, W.K. Cavenee, and H-J.S. Huang, *A mutant epidermal growth factor receptor common in human GBM confers enhanced tumorigenicity*. Proc Natl Acad Sci USA, 1994. **91**: p. 7727-31.
- Nobusawa, S., T. Watanabe, P. Kleihues, and H. Ohgaki, *IDH1 mutations as molecular signature and predictive factor of secondary glioblastomas*. Clin Cancer Res, 2009. **15**: p. 6002-7.

- Ohgaki, H. and P. Kleihues, *Genetic pathways to primary and secondary glioblastoma*. Am J Pathol, 2007. **170**(5): p. 1445-53.
- Ohgaki, H. and P. Kleihues, *Genetic alterations and signaling pathways in the evolution of gliomas*, Cancer Sci, 2009. **100**(12): p. 2235-41.
- Ohgaki, H. and P. Kleihues, *Genetic profile of astrocytic and oligodendroglial gliomas*. Brain Tumor Pathol, 2011. [Epub ahead of print]
- Pai, R., T. Nakamura, W.S. Moon, and A.S. Tarnawski, *Prostaglandins promote colon cancer cell invasion; signaling by cross-talk between two distinct growth factor receptors*. FASEB J, 2003. **17**(12): p. 1640-7.
- Pedersen, M.W., M. Meltorn, L. Damstrup, and H.S. Poulsen, *The type III epidermal growth factor receptor mutation. Biological significance and potential target for anti-cancer therapy*. Ann Oncol, 2001. **12**: p. 745-60.
- Pelloski, C.E., A. Mahajan, M. Maor, E.L.Chang, S. Woo, M. Gilbert, H. Colman, H. Yang, A. Ledoux, H. Blair, S. Passe, R.B. Jenkins , and K.D. Aldape, *YKL-40 expression is associated with poorer response to radiation and shorter overall survival in glioblastoma*. Clin Cancer Res, 2005. **11**: p. 3326-34.
- Pelloski, C.E., K.V. Ballman, A.F. Furth, L. Zhang, E. Lin, E.P. Sulman, K. Bhat, J.M. McDonald, W.K.A. Yung, H. Colman, S.Y. Woo, A.B. Heimberger, D. Suki, M.D. Prados, S.M. Chang, F.G. Barker, J.C. Buckner, C.D. James, and K. Aldape, *Epidermal growth factor receptor variant III status defines clinically distinct subtypes of glioblastoma*. J Clin Onc, 2007. **25**(16): p. 2288-94.

- Peruzzi, B., and D.P. Bottaro, *Targeting the c-Met signaling pathway in cancer*. Clin Cancer Res, 2006. **12**(12): p. 3657-60.
- Phillips, H.S., S. Kharbanda, R. Chen, W.F. Forrest, R.H. Soriano, T.D. Wu, A. Misra, J.M. Nigro, H. Colman, L. Soroceanu, P.M. Williams, Z. Modrusan, B.G. Feuerstein, and K. Aldape, *Molecular sub-classes of high-grade glioma predict prognosis, delineate a pattern of disease progression, and resemble stages in neurogenesis*. Cancer Cell, 2006. **9**: p. 157-73.
- Piccirillo, S.G., R. Combi, L. Cajola, A. Patrizi, S. Redaelli, A. Bentivegna, S. Baronchelli, G. Maira, B. Pollo, A. Mangiola, F. DiMeco, L. Dalprà, and A.L. Vescovi, *Distinct pools of cancer stem-like cells coexist within human glioblastomas and display different tumorigenicity and independent genomic evolution*. Oncogene, 2009. **28**(15): p. 1807-11.
- Pillay, V., L. Allaf, A.L. Wilding, J.F. Donoghue, N.W. Court, S.A. Greenall, A.M. Scott, and T.G. Johns. *The Plasticity of Oncogene Addiction: Implications for targeted therapies directed to receptor tyrosine kinases*. Neoplasia, 2009. **11**(5): p. 448-58.
- R Development Core Team (2009). *R: A language and environment for statistical computing*. Vienna, Austria: R Foundation for Statistical Computing. 1-409.
- Rahaman, S.O., P.C. Harbor, O. Chernova, G.H. Barnett, M. Vogelbaum, and S.J. Haque, *Inhibition of constitutively active Stat3 suppresses proliferation and induces apoptosis in glioblastoma multiforme cells*. Oncogene, 2002. **21**(55): p. 8404-13.

- Rahimi, N., E. Tremblay, L. Mcadam, M. Park, R. Schwall, and B. Elliott, *Identification of a hepatocyte growth factor autocrine loop in a murine mammary carcinoma*. Cell Growth Differ, 1996. **7**: p. 263-70.
- Ramnarain, D.B., S. Park, D.Y. Lee, K.J. Hatanpaa, S.O. Scoggin, H. Otu, T.A. Libermann, J.M. Raisanen, R. Ashfaq, E.T.Wong, J. Wu, R. Elliott, and A.A. Habib, *Differential gene expression analysis reveals generation of an autocrine loop by a mutant epidermal growth factor receptor in glioma cells*. Cancer Res, 2006. **66**: p. 867-74.
- Reem, G.H., and N.H. Yeh, *Interleukin 2 regulates expression of its receptor and synthesis of gamma interferon by human T lymphocytes*. Science, 1984. **27**(4660): p. 429-30.
- Reardon, D.A. and P.Y. Wen, *Therapeutic advances in the treatment of glioblastoma: rationale and potential role of targeted agents*. Oncologist, 2006. **11**(2): p. 152-64.
- Reznik, T.E., Y. Sang, Y. Ma, R. Abounader, E.M. Rosen, S. Xia, and J. Laterra, *Transcription-dependent epidermal growth factor receptor activation by hepatocyte growth factor*. Mol Cancer Res, 2008. **6**: p. 139-50.
- Sandberg, R., and O. Larsson, *Improved precision and accuracy for microarrays using updated probe set definitions*. BMC Bioinformatics, 2007. **8**: 48.
- Sathornsumetee, S., D.A. Reardon, A. Desjardins, J.A. Quinn, J.J. Vredenburgh and J.N. Rich, *Molecularly targeted therapy for malignant glioma*. Cancer, 2007. **110**(1): p. 13-24.
- Schmidt M.H.H., F.B. Furnari, W.K. Cavenee, and O. Böglér, *Epidermal growth factor receptor signaling intensity determines intracellular protein*

- interactions, ubiquitination, and internalization*. Proc Natl Acad Sci USA, 2003. **100**(11): p. 6505-10.
- Schneider, M.R., and E. Wolf, *The epidermal growth factor receptor ligands at a glance*. J Cell Physiol, 2009. **218**(3): 460-6.
- Seol, D.W., Q. Chen, M.L. Smith, and R. Zarnegar, *Regulation of the c-Met proto-oncogene promoter by p53*. J Biol Chem, 1999. **274**: p. 3565-72.
- Seth, D., K. Shaw, J. Jazayeri, and P.J. Leedman, *Complex post-transcriptional regulation of EGF-receptor expression by EGF and TGF- $\alpha$  in human prostate cancer cells*. Br J Cancer, 1999. **80**: 657-69.
- Sheth, P.R., J.L. Hays , L.A. Elferink, and S.J. Watowich , *Biochemical basis for the functional switch that regulates hepatocyte growth factor receptor tyrosine kinase activation*. Biochem, 2008. **47**(13): p. 4028-38.
- Shinomiya, N., C.F. Gao, Q. Xie, M. Gustafson, D.J. Waters, Y-W. Zhang, and G.F. Vande Woude, *RNA interference reveals that ligand-independent met activity is required for tumor cell signaling and survival*. Cancer Res, 2004. **64**(21): p. 7962-70.
- Shinojima, N., K. Tada, S. Shiraishi, T. Kamiryo, M. Kochi, H. Nakamura, K. Makino, H. Saya, H. Hirano, J-I. Kuratsu, K. Oka, Y. Ishimaru, and Y. Ushio, *Prognostic value of epidermal growth factor receptor in patients with glioblastoma multiforme*. Cancer Res, 2003. **63**(20): p. 6962-70.
- Singh, A.B., and R.C. Harris, *Autocrine, paracrine and juxtacrine signaling by EGFR ligands*. Cell Signal, 2005. **17**(10): p. 1183-93.

- Song, L., J. Turkson, J.G. Karras, R. Jove, and E.B. Haura, *Activation of Stat3 by receptor tyrosine kinases and cytokines regulates survival in human non-small cell carcinoma cells*. *Oncogene*, 2003. **22**(27): p. 4150-65.
- Stupp R., W.P. Mason, M.J. van den Bent, M. Weller, B. Fisher, M.J.B. Taphoorn, K. Belanger, A.A. Brandes, C. Marosi, U. Bogdahn, J. Curschmann, R.C. Janzer, S.K. Ludwin, T. Gorlia, A. Allgeier, D. Lacombe, J.G. Cairncross, E. Eisenhauer, and R.O. Mirimanoff, for the European Organisation for Research and Treatment of Cancer Brain Tumor and Radiotherapy Groups and the National Cancer Institute of Canada Clinical Trials Group, *Radiotherapy plus concomitant and adjuvant temozolomide for glioblastoma*. *N Engl J Med*, 2005. **352**(10): p. 987-96.
- Sulman E.P., and K. Aldape, *The use of global profiling in biomarker development for gliomas*, *Brain Pathol*, 2011. **21**(1): p. 88-95.
- The Cancer Genome Atlas Network, *Comprehensive genomic characterization defines human glioblastoma genes and core pathways*. *Nature*, 2008. **455**: p. 1061-8.
- Tomida, M., and T. Saito, *The human hepatocyte growth factor (HGF) gene is transcriptionally activated by leukemia inhibitory factor through the Stat binding element*. *Oncogene*, 2004. **23**(3): p. 679-86.
- Trusolino, L., A. Bertotti, and P.M. Comoglio, *MET signalling: principles and functions in development, organ regeneration and cancer*. *Nat Rev Mol Cell Biol*, 2010. **11**(12): p. 834-48.
- Tseng, J.R. K.W. Kang, M. Dandekar, S. Yaghoubi, J.H. Lee, J.G. Christensen, S. Muir, P.W. Vincent, N.R. Michaud, and S.S. Gambhir, *Preclinical efficacy of*



- the c-Met inhibitor CE-355621 in a U87 MG mouse xenograft model evaluated by 18F-FDG small-animal PET. J Nucl Med, 2008. 49(1): p. 129-34.*
- Tsou, C.C., C.F. Tsai, Y.H. Tsui, P.R. Sudhir, Y.T. Wang, Y.J. Chen, J-Y. Chen, T-Y Sung, and W-L Hsu, *IDEAL-Q, an automated tool for label-free quantitation analysis using an efficient peptide alignment approach and spectral data validation. Mol Cell Proteomics, 2010. 9: p. 131-44.*
- Verhaak R.G., K.A. Hoadley, E. Purdom, V. Wang, Y. Qi, M.D. Wilkerson, C.R. Miller, L. Ding, T. Golub, J.P. Mesirov, G. Alexe, M. Lawrence, M. O'Kelly, P. Tamayo, B.A. Weir, S. Gabriel, W. Winckler, S. Gupta, L. Jakkula, H.S. Feiler, J.G. Hodgson, C.D. James, J.N. Sarkaria, C. Brennan, A. Kahn, P.T. Spellman, R.K. Wilson, T.P. Speed, J.W. Gray, M. Meyerson, G. Getz, C.M. Perou, and D.N. Hayes, *Integrated genomic analysis identifies clinically relevant subtypes of glioblastoma characterized by abnormalities in PDGFRA, IDH1, EGFR, and NF1. Cancer Cell, 2010. 17: p. 98-110.*
- Villares, G.J., M. Zigler, K. Blehm, C. Bogdan, D. McConkey, D. Colin, and M. Bar-Eli, *Targeting EGFR in bladder cancer. World J Urol, 2007. 25(6): p. 573-9.*
- Weller, M., R. Stupp, G. Reifenberger, A.A. Brandes, M.J. van den Bent, W. Wick, and M.E. Hegi, *MGMT promoter methylation in malignant gliomas: ready for personalized medicine? Nat Rev Neurol, 2010. 6: p. 39-51.*
- Wiesner, S.M., S.A. Decker, J.D. Larson, K. Ericson, C. Forster, J.L. Gallardo, C. Long , Z.L. Demorest, E.A. Zamora, W.C. Low, K. SantaCruz, D.A. Largaespada, and J.R. Ohlfest, *De novo induction of genetically*

- engineered brain tumors in mice using plasmid DNA*. Cancer Res, 2009. **69**(2): p. 431-9.
- Wikstrand, C.J., C. Reist, G.E. Archer, M.R. Zalutsky, and D.D. Bigner, *The class III variant of the epidermal growth factor receptor (EGFRvIII): characterization and utilization as an immunotherapeutic target*. J Neurovirol, 1998. **4**: p. 148-58.
- Wojcik, E.J., S. Sharifpoor, N.A. Miller, T.G. Wright, R. Watering, E.A. Tremblay, K. Swan, C.R. Mueller, and B.E. Elliott. *A novel activating function of c-Src and Stat3 on HGF transcription in mammary carcinoma cells*. Oncogene, 2006. **25**(19): p. 2773-84.
- Wong, A.J., J.M. Ruppert, S.H. Bigner, C.H. Grzeschik, P.A. Humphrey, D.S. Bigner, and B. Vogelstein, *Structural alterations of the epidermal growth factor receptor gene in human gliomas*. Proc Natl Acad Sci USA, 1992. **89**(7): p. 2965-9.
- Xu, L., M.B. Nilsson, P. Saintigny, T. Cascone, M.H. Herynk, Z. Du, P.G. Nikolinakos, Y. Yang, L. Prudkin, D. Liu, J.J. Lee, F.M. Johnson, K-K. Wong, L. Girard, A.F. Gazdar, J.D. Minna, J.M. Kurie, I.I. Wistuba, and J.V. Heymach, *Epidermal growth factor receptor regulates MET levels and invasiveness through hypoxia-inducible factor-1alpha in non-small cell lung cancer cells*. Oncogene, 2010. **29**(18): p. 2616-27.
- Yamamoto, N., Mammadova, G., R.X-D. Song, Y. Fukami, and K-I. Sato, *Tyrosine phosphorylation of p145met mediated by EGFR and Src is required for serum-independent survival of human bladder carcinoma cells*. J Cell Sci, 2006. **119**(22): p. 4623-33.

- Yan, H., D.W. Parsons, G. Jin, R. McLendon, B.A. Rasheed, W. Yuan, I. Kos, I. Batinic-Haberle, S. Jones, G.J. Riggins, H. Friedman, A. Friedman, D. Reardon, J. Herndon, K.W. Kinzler, V.E. Velculescu, B. Vogelstein and D.D. Bigner, *IDH1 and IDH2 mutations in gliomas*. N Engl J Med, 2009. **360**(8): p. 765-73.
- Yarden, Y., and M.X. Sliwkowski, *Untangling the ErbB signalling network*. Nat Rev Mol Cell Biol, 2001. **2**(2): p. 127-37.
- Ymer, S.I., S.A. Greenall, A. Cvrljevic, D.X. Cao, J.F. Donoghue, V.C. Epa, A.M. Scott, T.E. Adams, and T.G. Johns, *Glioma specific extracellular missense mutations in the first cysteine rich region of epidermal growth factor receptor (EGFR) initiate ligand independent activation*. Cancers, 2011. **3**: p. 2032-49.
- Zhang, Y-W., L-M. Wang, R. Jove, and G.F. Vande Woude, *Requirement of Stat3 signaling for HGF / SF-Met mediated tumorigenesis*. Oncogene, 2002. **21**: p. 217-26.

## Vita

Jeannine Garnett was born in Pietermaritzburg, South Africa. After receiving her Bachelor's degree in 2002 from the Durban Institute of Technology, Durban, South Africa, she moved to San Francisco and then later to Tucson where she worked in industry and academia performing research. In August of 2005, Jeannine enrolled in the PhD program at the University of Texas Health Science Center at Houston Graduate School of Biomedical Sciences. Jeannine joined Dr. Oliver Bögler's laboratory in January of 2009 at the University of Texas MD Anderson Cancer Center, where she examined the regulation of HGF expression by  $\Delta$ EGFR-mediated c-Met activation in GBM cells.